siam

2nd Annual Meeting of the Bulgarian Section of SIAM
December 20-21, 2007
Sofia

BGSIAM'07

PROCEEDINGS

HOSTED BY THE INSTITUTE OF MATHEMATICS AND INFORMATICS
BULGARIAN ACADEMY OF SCIENCES

2nd Annual Meeting of the Bulgarian Section of SIAM
December 20-21, 2007, Sofia

BGSIAM'07 Proceedings

ISSN: 1313-3357

Printed in Sofia, Bulgaria
Cover design: Boris Staikov
Printing and binding: Demetra Ltd.

PREFACE

The Bulgarian Section of SIAM (BGSIAM) was founded on January 18, 2007 and the accepted Rules of Procedure were officially approved by the SIAM Board of Trustees on July 15, 2007. The activities of BGSIAM follow the general objectives of SIAM, as established in its Certificate of Incorporation.

Realizing the importance of interdisciplinary collaboration and the role that applied mathematics plays in advancing science and technology in industry, we solicit the support of SIAM as the major international organization for Industrial and Applied Mathematics in order to promote the application of mathematics to science, engineering and technology in Republic of Bulgaria.

The 2nd Annual Meeting of BGSIAM (BGSIAM'07) was hosted by the Institute of Mathematics and Informatics, Bulgarian Academy of Sciences, Sofia. It took part on December 20 and 21, 2007. The conference support provided by SIAM is very highly appreciated.

During BGSIAM'07 conference a wide range of problems concerning recent achievements in the field of industrial and applied mathematics were presented and discussed. The meeting provided a forum for exchange of ideas between scientists, who develop and study mathematical methods and algorithms, and researchers, who apply them for solving real life problems.

More than 50 participants from four universities, two institutes of the Bulgarian Academy of Sciences and also from outside the traditional academic departments took part in BGSIAM'07. They represent most of the strongest Bulgarian research groups in the field of industrial and applied mathematics. The involvement of younger researchers was especially encouraged and we are glad to report that 7 from the presented 23 talks were given by Ph.D. students.

LIST OF INVITED LECTURES:

- OLEG ILIEV
  ITWM - Fraunhofer Institute for Industrial Mathematics, Kaiserslautern, Germany
  MODELLING AND SIMULATION OF MULTISCALE PROBLEMS IN INDUSTRIAL FILTRATION PROCESSES

- VLADIMIR VELIOV
  Institute for Econometrics, Operations Research and Systems Theory, Vienna University of Technology, Austria
  ON THE NUMERICAL INTEGRATION OF SYSTEMS WITH DETERMINISTIC UNCERTAINTIES

- VLADIMIR GEORGIEV
  University of Pisa, Italy
  STABILITY OF SOLITARY WAVES FOR HARTREE TYPE EQUATIONS
- STEFAN DODUNEKOV
  Institute of Mathematics and Informatics, Bulgarian Academy of Sciences, Bulgaria
  MATHEMATICS IN DATA PROTECTION

LIST OF SPECIAL SESSIONS:

- Numerical Methods and Algorithms
- Control Systems and Applications
- Neural Networks
- Industrial Mathematics

The present volume contains the Rules of Procedure for BGSIAM (Part A), the scientific program of BGSIAM'07 (Part B), extended abstracts of the conference talks (Part C), and the list of participants (Part D). The extended abstracts are ordered alphabetically according to the family names of the speakers.

Svetozar Margenov
Chair of BGSIAM Section

Stefka Dimova
Vice-Chair of BGSIAM Section

Angela Slavova
Secretary of BGSIAM Section

Sofia, January 2008

Part A

Rules of Procedure for BGSIAM

Rules of Procedure for BGSIAM Section

This Section Rules of Procedure (hereinafter called "Rules") applies to the Bulgarian SIAM Section called "BGSIAM".

BGSIAM to which these Section Rules apply is formed under the aegis of SIAM, and shall operate within its bylaws. This Section shall not affiliate with any other organization without first obtaining the written approval of the SIAM Board of Trustees or its designee. No provisions of these Section Rules shall be construed so as to contradict the SIAM Bylaws.

These Section Rules may be modified by the Board with due notice to the Section.

Article I: Purpose

The objectives of SIAM, as established in its Certificate of Incorporation, are

- To further the application of mathematics to industry and science.
- To promote basic research in mathematics leading to new methods and techniques useful to industry and science.
- To provide media for the exchange of information and ideas between mathematicians and other technical and scientific personnel.

Purposes of the proposed BGSIAM shall be consistent with these objectives. Realizing the importance of interdisciplinary collaboration and the role that applied mathematics plays in advancing science and technology in industry, we solicit the support of SIAM as the major international organization for Industrial and Applied Mathematics in order to promote the application of mathematics to science, engineering and technology in Republic of Bulgaria. We hope that under the leadership of SIAM, as a vibrant and effective professional society, we will find the best way to ensure that applied mathematics receives the recognition and resources it needs to meet the educational, scientific and industrial challenges that lie ahead in the developing of our country.

Article II: Activities

The Bulgarian Section of SIAM will (co-)organize seminars, workshops and conferences on advanced topics in applied mathematics and computational sciences. BGSIAM will stimulate the enhanced collaboration between universities' research groups and the related institutes of Bulgarian Academy of Sciences. The Section will work to strengthen of the connection between research groups from the academic departments and the industrial partners. The joint projects with Bulgarian Small and Medium Enterprises (SMEs) will be strongly encouraged and supported. The participation of the Bulgarian mathematicians into SIAM activities will further expand the international collaboration of the local community. The participation of

mathematicians from the neighboring countries into activities of BGSIAM is among the priorities of the Section.

The organization of related scientific meetings, workshops and conferences in Bulgaria will be encouraged to apply for in cooperation with BGSIAM status. For such events, if there is a discounted registration fee offered to members of any sponsoring or cosponsoring organization, the same discounted fee must also be offered to the members of BGSIAM.

Article III: Territory

The Bulgarian SIAM Section (BGSIAM) will operate on the territory of Republic of Bulgaria and will draw membership from Bulgarian Universities, Bulgarian Academy of Sciences and also from outside the traditional academic departments. By doing so, we would like to enrich our community and increase the role, influence and the impact of mathematics on science, education, technology and the society as a whole.

Article IV: Membership

Any member of SIAM engaged or interested in mathematics and its applications and who is a Bulgarian resident shall be eligible for membership in the Section. A written application to the Chair of the BGSIAM is required. Any member of SIAM who does not live in Bulgaria may join the Section and participate in its activities, except that that member will not be a voting member nor will that member be eligible for officer in the Section. A candidate for nonresident membership shall be advised of these rules at the time of that member's application for membership. Section members will be designated as nonresident members if they reside outside Bulgaria.

Article V: Officers

Section 1. The Bulgarian Section of SIAM shall have a Chair, Vice Chair, and Secretary. The Secretary combines the duties of the Treasurer. The officers shall be regular members of SIAM in good standing.

Section 2. The Chair of the Section shall preside at the meetings of the Section. In the absence of the Chair, the Vice Chair shall assume the duties of the Chair.

Section 3. The Secretary shall keep a record of the affairs of the Section, handle correspondence, and submit an annual report of Section activities to the Secretary of SIAM, which report shall be suitable for publication in SIAM News or its equivalent.

Section 4. The Secretary shall receive and take custody of Section funds, and shall submit an annual Treasurer's Report and other financial reports, as requested, to the Treasurer of SIAM. The annual Treasurer's Report shall be prepared as of December 31 and shall be transmitted to the Treasurer of SIAM by no later than January 15 of the year following.

Section 5. The BGSIAM officers are elected for a period of two years. Re-election of an officer for an additional term is permissible.

Article VI: Meetings

Section 1. There shall be at least one technical meeting per year.

Article VII: Elections

Section 1. Section elections shall be secret ballot at the annual Section business meeting, or by mail ballot. The winners of the election shall be determined by the plurality of the votes cast for each officer. Mail ballots must be submitted to the Section members at least 20 days in advance of the date of the annual Section business meeting.

Section 2. A Nominating Committee shall be appointed by the Chair. Nominees must be eligible as stated in Article V. The nominations made by the Section members are to be send to the Nominating Committee atmost 30 days in advance of the date of the annual Section business meeting.

Article VIII: Annual Business Meeting

Section 1. The Section shall conduct an annual Section business meeting once per year in the period November 5 December 20. Other business meetings may be called by the Chair on four weeks' notice.

Article IX: Section Funds

Section 1. The Section can accept donations.

Section 2. The Section shall deposit all unused o which it has legal title in excess of $200 in an insured savings account, unless current operating commitments are in excess of that amount or unless the Section Treasurer obtains a written authorization from the SIAM Treasurer.

Section 3. The Section Treasurer shall maintain books of account that show income and expense items for all activities and balances for all accounts of the Section.

Section 4. Requests for funds in support of Section activities shall be made in writing to the Treasurer of SIAM who will forward it to the SIAM Committee on Section/Chapter Funds. Grants to Sections may be made by the SIAM Treasurer acting on behalf of the Committee on Section/Chapter Funds. Only one such grant may be made to any given Section during any fiscal year. Other requests for funds shall be substantiated by a proposed budget for expenditures and a current statement of accumulated revenue and expenses.

Section 5. No officer or member of the Section may apply for a grant to support Section activities or enter into any contract to support such activities or provide services, or have authority to contract debts for, pledge the credit of, or in any way bind SIAM, except to the extent that Section funds exist.

Section 6. All Society dues of Section members shall be payable to SIAM.

Article X: Amendments

Section 1. These Rules may be altered or amended with the approval of the SIAM Board of Trustees. Submission to the Board of proposed alterations or amendments shall be made only after approval by the majority vote of members of the Section present (or represented by proxy) at a scheduled meeting.

Article XI: Termination of the Section

Section 1. BGSIAM may terminate itself by the unanimous vote of the members of the Section present (or represented by proxy) at a scheduled meeting, provided that notice of the proposed termination and the meeting at which it is to be considered has been given to all Section members at least 30 days in advance and to the Board at least 90 days in advance.

Section 2. A Section may be terminated by the Board if there has been no Section activity for one year.

Section 3. In the event a Section is terminated, the funds to which it has legal title shall revert to the account of SIAM.

Approved:
SIAM Board of Trustees, Regular Session, July 15, 2007, Agenda Item 9

Part B

Scientific program

Thursday, December 20	
09:30 - 11:10	**Plenary Session**
09:30 - 09:50	Svetozar Margenov, *Opening: One Year BGSIAM*
Chairman	Svetozar Margenov
09:50 - 10:30	Stefan Dodunekov, *Mathematics in Data Protection*
10:30 - 11:10	Vladimir Georgiev, George Venkov, *Stability of Solitary Waves for the Maxwell-Schrödinger System*
	Coffee Break
11:30 - 12:30	**Special Session: Numerical Methods and Algorithms**
Chairman	Natalia Kolkovska
11:30 - 11:50	Geno Nikolov, Vesselin Gushev, *Modified Product Cubature Formulae*
11:50 - 12:10	Andrey Andreev, Milena Racheva, *Optimal Order FEM for Coupled Eigenvalue Problems on Overlapping Domains*
12:10 - 12:30	Boško S. Jovanović, Lubin G. Vulkov, etc., *Formulation, Analysis and Numerical Solution of Parabolic Interface Problems on Disjoint Intervals*
	Lunch Break
14:00 - 15:20	**Special Session: Numerical Methods and Algorithms**
Chairman	Stefka Dimova
14:00 - 14:20	Natalia Kolkovska, *On the Numerical Solution of a Stationary Two-Phase Venttsel Problem*
14:20 - 14:40	Daniela Vasileva, *On a Local Semirefinement Multigrid Algorithm for Convection-Diffusion Problems*
14:40 - 15:00	Nikola Kosturski, Svetozar Margenov, *MIC(0) Preconditioning of 3D FEM Problems on Unstructured Grids: Conforming and Nonconforming Elements*
15:00 - 15:20	Ivan Hristov, *Bifurcation of the Magnetic Flux Static Distributions in Multilayered Josephson Junctions*
	Coffee Break
15:40 - 18:00	**Special Session: Control Systems and Applications**
Chairman	Tsvetomir Tsachev
15:40 - 16:20	Vladimir Veliov, *On the Numerical Integration of Systems with Deterministic Uncertainties*
16:20 - 16:40	Mikhail Krastanov, *On the Local Attainability of a Closed Set*
16:40 - 17:00	Tsvetomir Tsachev, Dimitar Vassilev, *Age Structured Model for Optimal Fiscal Policy*
17:00 - 17:20	Iordan Iordanov, Stoyan Stoyanov, Andrey Vassilev, *Price Dynamics in a Strategic Model of Trade between Two Regions*
17:20 - 17:40	Mikhail Krastanov, Rossen Rozenov, *On Chamley's Problem of Optimal Taxation*
17:40 - 18:00	Tzanko Donchev, Vinicio Ríos, Peter Wolenski, *Approximate Semi-Solutions to Hamilton-Jacobi Equations and Minimal Time Function*
	RECEPTION

Friday, December 21	
09:30 - 10:50	**Special Session: Neural Networks**
Chairman	Angela Slavova
09:30 - 09:50	Valéry Covachev, Zlatinka Covacheva, Haydar Akça, Sannay Mohamad, *Global Exponential Periodicity for Discrete Hopfield Neural Networks with Delays and Impulses*
09:50 - 10:10	Angela Slavova, Maya Markova, *Polynomial Lotka-Volterra CNN Model: Dynamics and Complexity*
10:10 - 10:30	Valeri Mladenov, *Neural Networks for Solving Sudoku Problems*
10:30 - 10:50	Angela Slavova, Victoria Ivanova, *Applications of Cellular Neural Networks for Image Processing*
Coffee Break	
11:10 - 13:10	**Special Session: Industrial Mathematics**
Chairman	Ivan Dimov
11:10 - 11:50	Oleg Iliev, Zahra Lakdawala, Arnulf Latz, Peter Popov, Stefan Rief, Konrad Steiner, Andreas Wiegmann, *Modelling and Simulation of Multiscale Problems in Industrial Filtration Processes*
11:50 - 12:30	Emanoul Atanassov, Todor Gurov, Aneta Karaivanova, Mihail Nedjalkov, Sofiya Ivanovska, Rayna Georgieva, *SALUTE - Grid Application for Quatum Transport*
12:30 - 12:50	Krassimir Georgiev, Nikola Kosturski, Svetozar Margenov, Jiří Starý, *On the Adaptive Time-Stepping for Large Scale Parabolic Problems: Computer Simulation of Heat and Mass Transfer in Vacuum Freeze-Drying*
12:50 - 13:10	Svetozar Margenov, Yavor Vutov, *Parallel PCG Algorithms for Voxel Elasticity Problems*
CLOSING	

Part C

Extended abstracts*

*Arranged alphabetically according to the speaker's name.

Global Exponential Periodicity for Discrete Hopfield Neural Networks with Delays and Impulses

Valéry Covachev, Zlatinka Covacheva,
Haydar Akça, Sannay Mohamad

1 Introduction

In the present paper we introduce the discrete counterpart of a class of Hopfield neural networks with periodic integral impulsive conditions and finite distributed delays. We apply the continuation theorem of coincidence degree theory [3] to obtain a sufficient condition for the existence of a periodic solution of the discrete system considered. By introducing an appropriate Lyapunov functional we derive a sufficient condition for the uniqueness and global exponential stability of the periodic solution.

2 Statement of the problem. Main results

We consider a class of Hopfield neural networks with periodic integral impulsive conditions and finite distributed delays, which are formulated in the form of a system of impulsive delay differential equations

$$\begin{gathered}\frac{dx_i}{dt} = -a_i(t)x_i(t) + \sum_{j=1}^{m} b_{ij}(t) f_j\left(\int_0^{\omega} g_{ij}(s)x_j(t-s)\,ds\right) + I_i(t), \\ t \neq t_k, \\ \Delta x_i(t_k) \equiv x_i(t_k+0) - x_i(t_k) \\ = -\gamma_{ik}x_i(t_k) + \sum_{j=1}^{m} B_{ijk}\Phi_j\left(\int_0^{\omega} c_{ij}(s)x_j(t_k-s)\,ds\right) + \alpha_{ik}, \\ i = \overline{1,m}, \quad k \in \mathbb{Z},\end{gathered} \tag{1}$$

where m is the number of neurons in the network, $x_i(t)$ is the state of the i-th neuron at time t, $a_i(t) > 0$ is the rate at which the i-th neuron resets its state when isolated from the system, $b_{ij}(t)$ is the synaptic connection weight from the j-th neuron to the i-th one, $f_j(\cdot)$ are signal transmission functions of the j-th neuron, ω is the maximum transmission delay from one neuron to another, $g_{ij}(\cdot)$ and $c_{ij}(\cdot)$ are nonnegative delay kernels, $I_i(t)$ is the external input to the i-th neuron, t_k ($k \in \mathbb{Z}$) are the instants of impulse effect which form a strictly increasing sequence, γ_{ik} ($i = \overline{1,m}$, $k \in \mathbb{Z}$) are positive constants.

We assume that the above system (1) satisfies the following periodicity conditions: $a_i(t)$, $b_{ij}(t)$, $I_i(t)$ are ω-periodic in t; $t_{k+p} = t_k + \omega$, $\gamma_{i,k+p} = \gamma_{ik}$, $B_{ij,k+p} = B_{ijk}$, $\alpha_{i,k+p} = \alpha_{ik}$.

As in [5, 1] we formulate the discrete counterpart of system (1). For a positive integer N we choose the discretization step $h = \omega/N$. For the moment we assume N so large that $h < \min_{k=\overline{1,p}}(t_{k+1} - t_k)$. Then each interval $[nh, (n+1)h]$ contains at most one instant of impulse effect t_k.
For convenience we denote $n = [t/h]$, the greatest integer in t/h, and $n_k = [t_k/h]$. Clearly, we will have $n_{k+p} = n_k + N$ for all $k \in \mathbb{Z}$.
Let $n \in \mathbb{Z}$, $n \neq n_k$. This means that the interval $[nh, (n+1)h]$ contains no instant of impulse effect t_k. First we approximate the integral term in (1) by a sum and then we approximate the differential equation (1) on the interval $[nh, (n+1)h]$ by

$$\frac{dx_i}{dt} + a_i(nh)x_i(t) = I_i(nh) + \sum_{j=1}^{m} b_{ij}(nh) f_j \left(\sum_{\ell=1}^{N} g_{ij}(\ell h) x_j\left((n-\ell)h\right) \varphi(h) \right).$$

We multiply both sides of this equation by $\exp\left(a_i(nh)t\right)$ and integrate over the interval $[nh, (n+1)h]$. Thus we obtain

$$\begin{aligned} x_i\left((n+1)h\right) - x_i(nh) &= -\left(1 - e^{-a_i(nh)h}\right) x_i(nh) \qquad (2) \\ + \quad \frac{1 - e^{-a_i(nh)h}}{a_i(nh)} &\left\{ I_i(nh) + \sum_{j=1}^{m} b_{ij}(nh) f_j \left(\sum_{\ell=1}^{N} g_{ij}(\ell h) x_j\left((n-\ell)h\right) \varphi(h) \right) \right\}. \end{aligned}$$

Henceforth by abuse of notation we write $x_i(n) = x_i(nh)$ and define $\Delta x_i(n) = x_i(n+1) - x_i(n)$ $(i = \overline{1,m},\ n \in \mathbb{Z})$.
Next, for $n = n_k$ the interval $[nh, (n+1)h]$ contains the instant of impulse effect t_k. On this interval we approximate the impulse condition in (1) by

$$\begin{aligned} \Delta x_i(n_k) \quad = \quad & -\gamma_{ik} x_i(n_k) + \alpha_{ik} + \sum_{j=1}^{m} B_{ijk} \Phi_j \left(\sum_{\ell=1}^{N} c_{ij}(\ell) x_j(n_k - \ell) \right), \qquad (3) \\ & i = \overline{1,m}, \quad k \in \mathbb{Z}. \end{aligned}$$

Introducing some notations, we can write the difference system (2), (3) in operator form as

$$\Delta x = Hx, \qquad (4)$$

where

$$\begin{aligned} (Hx)_i(n) &= -A_i(n)x_i(n) + I_i(n) \\ + \quad & \begin{cases} \sum\limits_{j=1}^{m} b_{ij}(n) f_j \left(\sum\limits_{\ell=1}^{N} g_{ij}(\ell) x_j(n-\ell) \right), & n \neq n_k, \\ \sum\limits_{j=1}^{m} B_{ijk} \Phi_j \left(\sum\limits_{\ell=1}^{N} c_{ij}(\ell) x_j(n_k - \ell) \right), & n = n_k. \end{cases} \end{aligned}$$

In order to formulate our assumptions, we need some more notation:

$$I_N = \{0, 1, \ldots, N-1\},$$

$$\underline{A}_i = \min_{n\in I_N} A_i(n), \quad \overline{A}_i = \sum_{n=0}^{N-1} A_i(n), \qquad i = \overline{1,m}.$$

Now we introduce the following conditions:

H1. $A_i(n+N) = A_i(n)$, $I_i(n+N) = I_i(n)$ for $i = \overline{1,m}$, $n \in \mathbb{Z}$;
$n_k \in \mathbb{Z}$ for all $k \in \mathbb{Z}$ and $n_{k+p} = n_k + N$; $b_{ij}(n+N) = b_{ij}(n)$ $(n \neq n_k)$, $B_{ij,k+p} = B_{ijk}$ $(k \in \mathbb{Z})$ for $i,j = \overline{1,m}$.

H2. $\underline{A}_i > 0$, $\overline{A}_i < 1$ for $i = \overline{1,m}$.

H3. The functions $f_j(\cdot)$, $\Phi_j(\cdot)$ $(j = \overline{1,m})$ are bounded on $\mathbb{R}$ and there exist positive constants M_j and L_j such that

$$|f_j(x) - f_j(y)| \le M_j|x-y|, \quad |\Phi_j(x) - \Phi_j(y)| \le L_j|x-y|$$

for all $x, y \in \mathbb{R}$.

H4. $g_{ij}(\ell) \ge 0$, $c_{ij}(\ell) \ge 0$ for $i,j = \overline{1,m}$, $\ell = \overline{1,N}$.

We again introduce some notation:

$$\overline{I}_i = \max_{n\in I_N} |I_i(n)|, \qquad i = \overline{1,m},$$

$$\overline{b}_{ij} = \sup_{n\neq n_k} |b_{ij}(n)|, \quad \overline{B}_{ij} = \max_{k=\overline{1,p}} |B_{ijk}|, \qquad i,j = \overline{1,m}.$$

For an N-periodic sequence $v(n)$ we denote $\tilde{v} = \frac{1}{N}\sum\limits_{n=0}^{N-1} v(n)$; for $i = \overline{1,m}$

$$\rho_i = \overline{I}_i + \frac{1}{N}\sum_{j=1}^{m} \left[(N-p)\overline{b}_{ij}|f_j(0)| + p\overline{B}_{ij}|\Phi_j(0)|\right].$$

Next we denote

$$\mathcal{M}_j = \max\{L_j,\ M_j\}, \qquad j = \overline{1,m},$$

$$G_{ij} = \sum_{\ell=1}^{N} g_{ij}(\ell), \quad C_{ij} = \sum_{\ell=1}^{N} c_{ij}(\ell), \qquad i,j = \overline{1,m},$$

$$\mathcal{B}_{ij} = \max\{\overline{b}_{ij},\ \overline{B}_{ij}\}, \quad \mathcal{G}_{ij} = \max\{G_{ij},\ C_{ij}\}, \qquad i,j = \overline{1,m}.$$

We introduce the $m \times m$ matrices

$$A = \operatorname{diag}\left(\frac{\underline{A}_i\left(1-\overline{A}_i\right)}{1+N\underline{A}_i},\ i = \overline{1,m}\right), \qquad B = \left(\mathcal{B}_{ij}\mathcal{M}_j\mathcal{G}_{ij}\right)_{i,j=1}^{m}.$$

Then we introduce the conditions

H5. $\min\limits_{i=\overline{1,m}} \left(\tilde{A}_i - \mathcal{M}_i \sum\limits_{j=1}^{m} \mathcal{B}_{ji}\mathcal{G}_{ji} \right) > 0.$

H6. $\underline{A}_i > \mathcal{M}_i \sum\limits_{j=1}^{m} \mathcal{B}_{ji}\mathcal{G}_{ji}$ for $i = \overline{1,m}$.

H7. The matrix $A - B$ is an M-matrix [2, 4].

Clearly, condition **H6** implies **H5** but the converse is not true. Condition **H7** means that the matrix $A - B$ is nonsingular and its inverse has positive entries only.
Our results are formulated as follows:

Theorem 1 *Suppose that conditions* **H1**–**H5**, **H7** *hold. Then the equation* (4) *has at least one N-periodic solution.*

Theorem 1 is proved using Mawhin's continuation theorem [3, p. 40].

Theorem 2 *Suppose that conditions* **H1**–**H4**, **H6**, **H7** *hold. Then the N-periodic solution of* (4) *is unique and globally exponentially stable.*

In fact, let us suppose that $x^*(n) = (x_1^*(n), x_2^*(n), \ldots, x_m^*(n))^T$ is an N-periodic solution of equation (4), and $x(n) = (x_1(n), x_2(n), \ldots, x_m(n))^T$ is any solution of (4) for $n \geq 0$, defined at least for $n \geq -N$. Then by introducing an appropriate Lyapunov functional we derive the estimate

$$\sum_{i=1}^{m} |x_i(n) - x_i^*(n)| \leq C\lambda^{-n} \sum_{i=1}^{m} \max_{s \in I_{-N}} |x_i(s) - x_i^*(s)|, \quad n \in \mathbb{Z}_0^+,$$

where $C > 0$ and $\lambda > 1$.

References

[1] H. Akça, R. Alassar, V. Covachev, Z. Covacheva, *Discrete counterparts of continuous-time additive Hopfield-type neural networks with impulses*, Dyn. Syst. Appl., **13** (2004), 77–92.

[2] M. Fiedler, *Special Matrices and Their Applications in Numerical Mathematics*, Martinus Nijhoff, Dordrecht, 1986.

[3] R. E. Gaines, J. L. Mawhin, *Coincidence Degree and Nonlinear Differential Equations*, Springer-Verlag, Berlin, 1977.

[4] R. A. Horn, C. R. Johnson, *Topics in Matrix Analysis*, Cambridge University Press, Cambridge, 1991.

[5] S. Mohamad, K. Gopalsamy, *Dynamics of a class of discrete-time neural networks and their continuous-time counterparts*, Math. Comput. Simul., **53** (2000), 1–39.

Mathematics in Data Protection

Stefan Dodunekov

Data protection is an important issue in the global information society. The growth in the types and number of services on Internet leads to new challenges and new practical and theoretical problems.
The main idea of the lecture is to demonstrate that almost all branches of mathematics are involved in data protection.
In Part 1, as an introduction the two aspects of data protection are outlined, namely reliability and security of data. The basic practical problems, terminology and general approaches are explained through simple examples.
In Part 2, to support the main idea examples of data protection techniques based on classical mathematical areas are given. The list includes Arithmetic (Classical Ciphers), Number Theory (RSA Cryptosystem), Combinatorics (Finite Geometries, Designs, Hadamard matrices and codes), Linear Algebra (Linear codes), Commutative Algebra (Cyclic Codes and their generalizations), Algebraic Geometry (Elliptic Curve Cryptosystem), Probability Theory (Tests for primality), Group Theory (Classification of Codes), Complexity Theory (Decoding and Cryptanalysis).
As a conclusion we point out two things. First in order to work on Data Protection problems a solid mathematical background is required. Second, many classical branches of mathematics which had been considered as a core of the so called pure mathematics, today are directly applied to solve practical data protection problems.
We end up with two "open" questions: 1) Find a mathematical subject which is not connected to Data Protection; 2) What is "pure mathematics"?

Approximate Semi-Solutions to Hamilton-Jacobi Equations and Minimal Time Function

Tzanko Donchev, Vinicio Ríos, Peter Wolenski

This paper studies the minimal time function associated with a given closed target set $S \subseteq \mathbb{R}^n$ and a dynamical system governed by a differential inclusion

$$\dot{x}(t) \in F(x(t)) \text{ a.e. } t \in [0, \hat{T}),\ x(0) = x, \tag{1}$$

where $\hat{T} > 0$ ($\hat{T} = \infty$ is possible). The multifunction $F : \mathbb{R}^n \rightrightarrows \mathbb{R}^n$ is assumed throughout to satisfy the following standing hypotheses (SH):

- $F(\cdot)$ is upper semicontinuous with nonempty convex compact values.

The minimal time function $T_S(\cdot) : \mathbb{R}^n \to [0, \infty]$, defined by

$$T_S(x) := \inf \{T : \exists\, x(\cdot) \text{ satisfying (1) with } x(T) \in S\}. \tag{2}$$

By convention, $T_S(x) = \infty$ when no trajectory with initial point x reaches the set S, and $T_S(x) = 0$ when $x \in S$. The main purpose of this paper is to show that the minimal time function is the unique proximal semi-solution of a limiting version of the Hamilton-Jacobi (HJ) equation satisfying an appropriate boundary condition. Including discontinuous data precludes the possibility that $T_S(\cdot)$ will satisfy the exact Hamilton-Jacobi inequalities that are associated to certain invariant augmentation of the original data.
The novelty of the results in this paper lies in the very mild structural assumptions placed on F that lead to a characterization of the minimal time function. Indeed we replace the locally Lipschitz condition on $F(\cdot)$ by locally backward sided Lipschitz condition and upper semi-continuity.
Let

$$h_F(x, \zeta) := \inf\{\langle v, \zeta\rangle : v \in F(x)\} \quad \forall\, x, \zeta \in \mathbb{R}^n.$$

We will use the local *other (backward) sided Lipschitz* assumption (BSL) on F: For every compact set K there exists a constant $m = m(K)$ such that

$$h_F(x, x - y) - h_F(y, x - y) \geq m|x - y|^2 \tag{3}$$

for all $x, y \in \mathbb{R}^n$. The multifunction $F(\cdot)$ is said to be one sided Lipschitz (OSL) when $-F(\cdot)$ is BSL.
Consider the following auxiliary control system

$$\dot{x}(t) \in G(t, x(t)) \text{ a.e. } t \in [\tau, \tau + T)\ x(\tau) = x, \tag{4}$$

Suppose $E \subset \mathbb{R}^n$ is nonempty, $U \subset \mathbb{R}^n$ is open, and $G : I \times \mathbb{R}^n \rightrightarrows \mathbb{R}^n$ is a submultifunction of F. A solution $x(\cdot)$ to (4) whose extension $\tilde{x}(\cdot) \in \Upsilon_{(G,U)}(\tau, x)$ satisfies $\tilde{x}(t) \in E$ for all $t \in [\tau, \tau + Esc(\tilde{x}(\cdot); U))$ is called *viable*.

We say that (E, G) is *weakly invariant in* U provided that for all $(\tau, x) \in I \times (E \cap U)$, there exists a *viable* solution. The system (E, G) is called *(strongly) invariant* if all its solutions are viable.
We will call G a *submultifunction of* F if it satisfies $G(t, x) \subset F(x)$ for all $(t, x) \in \mathbb{R}^{n+1}$ and for each $(t, x) \in I \times \mathbb{R}^n$, $G(t, x)$ is nonempty, convex, and compact and it is USC on $I \times \mathbb{R}^n$.
The following theorem devotes the invariance of the system 1 to the weak invariance of all subsystems.

Theorem 1 ***(Invariance principle)*** *Let F be locally OSL and satisfy (SH). The system (E, F) is invariant in U if and only if for every submultifunction G of F $h_G(t, x, \zeta) \leq 0$ $\forall \zeta \in N_E^P(x)$, $\forall x \in E \cap U$, and $\forall t \in I$.*

This condition is, however, practically impossible to be checked. So we present the equivalent form, which is much easy to be verified.
For a given nonzero vector $\zeta \in \mathbb{R}^n$, $y \to_\zeta x$ signifies the limit of y approaching x along the vector ζ; that is, $y \to_\zeta x$ if and only if $y \to x$ and $\dfrac{y - x}{|y - x|} \to \dfrac{\zeta}{|\zeta|}$.

Theorem 2 *Suppose F is locally OSL and satisfies (SH). Then the system (E, F) is invariant in U if and only if*

$$\liminf_{y \to_\zeta x} h_F(y, -\zeta) \geq 0, \tag{5}$$

for all $x \in E \cap U$, and all $\zeta \in N_E^P(x)$.

The following theorem is the main result of the paper.

Theorem 3 *Suppose $F : \mathbb{R}^n \rightrightarrows \mathbb{R}^n$ satisfies (SH) and (3). Then, there exists a unique l.s.c. function $\theta : \mathbb{R}^n \to (-\infty, \infty]$ bounded below on $\mathbb{R}^n$ and satisfying the following.*
(HJI) *For each $x \notin S$ and $\xi \in \partial_P \theta(x)$, we have*

$$1 + h_F(x, \xi) \leq 0, \quad \textit{and} \quad 1 + \liminf_{y \to_\xi x} h_F(y, \xi) \geq 0. \tag{6}$$

(LABC) *Each $x \in S$ satisfies $\theta(x) = 0$ and*

$$1 + \liminf_{y \to_\xi x} h_F(y, \xi) \geq 0, \tag{7}$$

whenever $\xi \in \partial_P \theta(x)$. The unique such function is $\theta(\cdot) = T_S(\cdot)$.

Here the notation $\partial_P \theta(x)$ refers to the set of proximal subgradients of the lower semicontinuous function $\theta(\cdot)$; that is, $\zeta \in \partial_P \theta(x)$ if and only if there exists $\sigma > 0$ and $\eta > 0$ so that

$$\theta(y) \geq \theta(x) + \langle \zeta, y - x \rangle - \sigma |y - x|^2 \quad \forall\, y \in x + \eta B.$$

On the Adaptive Time-Stepping for Large Scale Parabolic Problems: Computer Simulation of Heat and Mass Transfer in Vacuum Freeze-Drying

Krassimir Georgiev, Nikola Kosturski, Svetozar Margenov, Jiří Starý

The work concerns the mathematical modelling and computer simulation of the heat and mass transfer with the core in solving the time-dependent nonlinear partial differential equation of parabolic type.
Instead of an uniform discretization of the considered time interval, an adaptive time stepping procedure is applied in an effort to optimize the whole simulation.

1 Introduction

Freeze-drying is a special technology of dehydrating frozen materials by sublimation under high vacuum [5, 4]. One of its possible applications comes from the food industry, where it can be used for drying certain kinds of food-stuffs, for example carrots, coffee, yogurt, etc.
A possibile devise realizing such a process consists of mainly two interconnected containers. One is the food camera intended for the product to be dried and another is the absorbent camera filled by natural or artificial zeolite granules [1]. The adsorbtion cameras could be one or more. The zeolite is a special type of silica-containing material, with a porous structure, applicable as absorbents and catalysts. Here, they are used for the sorbtion of water molecules comming through the pipe from the food camera.
The whole process of drying has three phases. The first one is a preparation of the source material in the food container, which is then vacuumed. Also during this phase, the absorbent located in the second container is activated, it means warmed up, vacuumed and cooled to a room temperature. The second phase is the self-freezing of the source material surrounded by high vacuum. The last phase is the drying in conditions of an uniform sublimation of water steam from the source material in the food container and its disposal in the absorbent. The sublimation is supported by heaters installed in the food camera.
The mathematical model of the whole process of freeze-drying is described by a system of time-dependent differential equations, but with the possibility to split processes in the food container and in the absorbent camera according to the technological subprocesses involved. Further, we will consider only the process of heat and mass transfer in the absorbent camera.

2 Heat and Mass Transfer Problem and its Numerical Treatment

The process of heat and mass transfer in the absorbent camera is described by the nonlinear partial differential equation of parabolic type,

$$c\rho\frac{\partial T}{\partial t} = \mathcal{L}T \ + \ f(x,t,T), \qquad x \in \Omega, \ t > 0,$$

where

$$\mathcal{L}T = \sum_{i=1}^{d} \frac{\partial}{\partial x_i}\left(k(x,t)\frac{\partial T}{\partial x_i}\right)$$

and $T(x,t)$ denotes the unknown temperature distribution, $k = k(x,t) > 0$ the heat conductivity, $c = c(x,t) > 0$ the heat capacity, $\rho > 0$ the material density. The function $f(x,t,T)$ is responsible for the non-linear process of transfer of water molecules in the absorption container. By default, d is the given dimension of the space ($d = 2$) and $\Omega \in R^d$ denotes the computational domain.
To the parabolic equation, we assign the initial and boundary conditions in the standard form,

$$\begin{aligned} T(x,0) &= T_0(x), \qquad x \in \Omega, \\ T(x,t) &= \mu(x,t), \qquad x \in \Gamma \equiv \partial\Omega, \ t > 0, \end{aligned}$$

where $T_0(x)$ is the initial temperature distribution in the computational domain and $\mu(x,t)$ is the room temperature during the freeze-drying process, which can be controlled by cooling/heating devices.
A discretization by the finite elements in space (Courant linear triangular finite elements) leads to:

$$M\frac{du}{dt} + Ku = F(t), \tag{1}$$

where

$$M = \left[\int_\Omega c\,\rho\,\phi_i\,\phi_j \ dx\right]_{i,j=1}^{N_N}$$

is the corresponding mass matrix,

$$K = \left[\int_\Omega k\,\nabla\phi_i\nabla\phi_j \ dx\right]_{i,j=1}^{N_N}$$

is the corresponding stiffness matrix and

$$F = \left[\int_\Omega f(x,t,u)\,\phi_i \ dx\right]_{i=1}^{N_N}$$

is the right–hand–side.
After that finite differences in time are applied with the time steps $\tau_k = t_k - t_{k-1}$ at the time levels t_k, $k = 1, \ldots, N$. In case of the uniform time discretization with the constant time steps τ the following linear system of equations should be solved

$$(M + \tau\,\vartheta K)\,u^k = \big(M - \tau\,(1-\vartheta)\,K\big)u^{k-1} \;+\; \tau\,\vartheta\,F^k + \tau\,(1-\vartheta)\,F^{k-1}.$$

where $\vartheta \in \langle 0, 1\rangle$ sets the time scheme.
In order to develop fully robust and stable method we restrict our attention to implicit methods with $\vartheta = \frac{1}{2}$ and $\vartheta = 1$, which correspond to the well known *Crank-Nicholson* and *Backward Euler* methods. For the solution of the linear system above, we use the well-known conjugate gradient method with a modified incomplete Cholesky factorization preconditioner [2, 3].

3 Adaptive time steps

To ensure accuracy and not waste the computational effort, it is important to adapt the time steps to the behaviour of the solution. In the simplest case, we can test the time change of the solution and change the time step size, if the variation is too small or too large.
The suitable adaptive time-stepping procedure is based on a local comparison of the backward Euler and Crank-Nicholson time steps and controlled with the aid of the ratio $\eta = \|T_{CN} - T_{BE}\|/\|T_{BE}\|$. To make the procedure cheaper, we solve only the linear system for the backward Eulersteps and can approximate the solution of the corresponding linear system for the Crank-Nicholson steps, $\bar{T}_{CN} \simeq T_{BE} - r$, where

$$r^k = \left(M + \frac{1}{2}\tau^k K\right) T^k_{BE} - \left(M - \frac{1}{2}\tau^k K\right) T^{k-1}_{BE} - \frac{1}{2}\tau^k F^k - \frac{1}{2}\tau^k F^{k-1}.$$

The residual r arises from the substitution of T_{BE} in the linear system for the Crank-Nicholson steps. In other words to obtain $\bar{T}_{CN}$, we perform the only Richardson iteration of the linear system for the Crank-Nicholson steps, whereas the initial approximation of the solution is set to be T_{BE}. And consequently, $\eta^k = \|r^k\|/\|T^k_{BE}\|$.
The described method gives an adaptive time-stepping procedure which was firstly applied to the mathematical modelling of processes in spent nuclear fuel repositories [6].
How often to perform the adaptive time steps ? After a number of numerical tests it was be found that the number of the adaptive time steps should be in the interval [2, 16] with the preference of smaller values and the optimal value of this parameter is 4.

4 Conclusion

The paper concerns the time evolution of the temperature field in the absorbent camera as well as the transfer of the sublimed water molecules and their retention in the zeolite granules. The problem, described by the time-dependent nonlinear partial

differential equation of parabolic type, leads to the repeated solution of linear systems at different time levels.
In an effort to optimize the computation, the adaptive time stepping procedure was implemented in the program code. The procedure is based on the local comparison of Crank-Nicholson and backward Euler time steps.
The described numerical methods were implemented in C^{++} and the resulting program code was tested on a selected real-life problem. The experiments were performed on a standard PC equipped by Pentium IV/1.5 GHz processor, 256 kB of L2 cache, 256 MB of memory, and running the Scientific Linux 4.5 operating system.
The computational domain is discretized by the linear triangular finite elements with the aid of the computer mesh generator Triangle [7].
The tests helped to find the suitable parameters and showed the practical usefulness of the developed solver for such kind of computer simulations.

Acknowledgement:

The presented work is partly supported by the Bulgarian IST Centre of Competence in 21st Century BIS-21^{++} funded by the European Commission within FP6 INCO through the project 016639/2005 as well as by grant I-1402/2004 from the Bulgarian NSF.

References

[1] G. Tsitshvili, T. Andronikashvili, G. Kirov (1992), *Natural zeolites*, Prentice Hall

[2] O. Axelsson (1996), *Iterative Solution Methods*, Cambridge University Press

[3] I. Gustafsson (1996), *An incomplete factorization preconditioning method based on modification of element matrices*, BIT **36, No. 1**, pp. 86–100

[4] A. Mujumdar (1999), *Handbook of Industrial Drying*, Marcel Dekker, Inc.

[5] F. Jafar, M. Farid (2003), *Analysis of heat and mass transfer in freeze–drying*, Drying Technology **21, No. 2**, pp. 249–263

[6] R. Blaheta, P. Byczanski, R. Kohut, J. Starý (2004), *Algorithms for parallel FEM modelling of thermo-mechanical phenomena arising from the disposal of spent nuclear fuel.* In: O. Stephansson, J.B. Hudson, L. Jing (eds.), Coupled Thermo-Hydro-Mechanical-Chemical Processes in Geosystems, Elsevier

[7] Carnegie Mellon University web site (2007), *Triangle: A Two-Dimensional Quality Mesh Generator and Delaunay Triangulator*,
`http://www.cs.cmu.edu/~quake/triangle.html`

Stability of Solitary Waves for the Maxwell-Schrödinger System

Vladimir Georgiev, George Venkov

The classical Maxwell - Schrödinger system (in Lorentz gauge) has the form

$$\partial_{tt}\mathcal{A} - \Delta\mathcal{A} = \mathcal{J}, \tag{1}$$

$$\partial_{t,\mathcal{A}}\psi + \frac{1}{2}\Delta_{\mathcal{A}}\psi - V(x)\psi = 0, \tag{2}$$

$$\partial_t A_0 + \sum_{k=1}^{3} \partial_{x_k} A_k = 0, \tag{3}$$

where $\psi = \psi(x,t)$ is the wave function, $\mathcal{A} = (A_0, A_1, A_2, A_3)$ is the electromagnetic potentials of a charged non- relativistic particle of charge e and

$$\partial_{t,\mathcal{A}} = \partial_t + ieA_0, \quad \Delta_{\mathcal{A}} = \sum_{k=1}^{3} \partial_{k,\mathcal{A}}^2, \tag{4}$$

$$\partial_{k,\mathcal{A}} = \partial_{x_k} + ieA_k, \quad \mathcal{J} = (J_0, J_1, J_2, J_3), \tag{5}$$

$$J_0 = 4\pi e|\psi|^2, \quad J_k = 4\pi e\,\mathrm{Im}(\bar{\psi}\partial_{k,\mathcal{A}}\psi). \tag{6}$$

Moreover, the potential V is defined as follows

$$V(x) = -\frac{\phi(x)e^2 Z}{|x|}, \tag{7}$$

where $\phi(x)$ is smooth function identically 1 for x large enough.
First we consider special solitary type solutions to the system (1), (2), (3) of the form

$$\psi(x,t) = \chi(x)e^{-i\omega t/\hbar}, \quad x \in \mathbf{R}^3, t \in \mathbf{R},$$

and

$$A_0 = \varphi(x), \quad A_j(x) = 0, \quad j = 1,2,3, \quad x \in \mathbf{R}^3,$$

where $\omega \in \mathbf{R}$ and χ is real valued. Then the system (1), (2), (3) takes the simpler form

$$-\frac{1}{2}\Delta\chi + e\varphi\chi + V(x)\chi = \omega\chi, \quad x \in \mathbf{R}^3, \tag{8}$$

$$-\Delta\varphi = 4\pi e\chi^2, \quad x \in \mathbf{R}^3, \tag{9}$$

$$\int_{\mathbf{R}^3} \chi^2 = N, \tag{10}$$

where the last equation is due to the probabilistic interpretation of the wave function. In this note we shall assume the following neutrality relation between N and Z is satisfied

$$N = Z. \tag{11}$$

Our first result guarantees the existence of solitary waves.

Theorem 1 *There exists a sequence of real negative numbers* $\{\omega_k\}_{k\in\mathbf{N}}$ *so that* $\omega_k \to 0$ *and for any* ω_k *there exists a couple* (χ_k, φ_k) *of solutions of (8), (9), (10), such that*

$$\chi_k \in S(\mathbf{R}^3), \quad \int_{\mathbf{R}^3} |\nabla\varphi_k|^2\, dx < \infty.$$

Moreover χ_k, φ_k *are radially symmetric functions.*

A simplified model of Maxwell – Schrödinger system is the Hartree equation

$$i\partial_t\psi(t,x) = -\frac{1}{2}\Delta\psi(t,x) + \left(e^2\int_{\mathbf{R}^3}\frac{|\psi(t,y)|^2}{|x-y|}dy + V(x)\right)\psi(t,x), \tag{12}$$

Turning to the Cauchy problem for the equation (12) , we impose initial data of type

$$\psi(0,x) = \chi(x) + u_0(x), \tag{13}$$

where $\chi(x)$ is such that

$$e^{-i\omega t}\chi(x)$$

is a solitary wave that is $\chi(x)$ is a rapidly decaying smooth function that is a solution of the nonlinear eigenvalue problem (8), (9), (10).
The existence of nontrivial radial solutions to this problem is constructed in Theorem 1 for the case, when the neutrality condition $N = Z$ is satisfied. The function $u_0(x)$ is assumed to be compactly supported in the Sobolev space $H^s(\mathbf{R}^3), s > 3/2$ and its H^s norm is sufficiently small. We shall look for solution of the Cauchy problem (12) of type

$$\psi(t,x) = e^{-i\omega t}\chi(x) + u(t,x). \tag{14}$$

Consider the bilinear form

$$Q(v,w)(t,x) = \int_{\mathbf{R}^3}\frac{v(t,y)\overline{w(t,y)}}{|x-y|}dy \tag{15}$$

for any two complex - valued functions $v(t,x), w(t,x)$. The ansatz (14) and the fact that

$$e^{-i\omega t}\chi(x)$$

is a solitary wave imply that $u(t,x)$ will be a solution to the following perturbed nonlinear Scrödinger problem

$$i\partial_t u(t,x) = -\frac{1}{2}\Delta u(t,x) + L_\chi(u) + N_\chi(u), \tag{16}$$

where

$$L_\chi(u)(t,x) = bW(x)u + b\left(Q(u, e^{-it\omega}\chi) + Q(e^{-it\omega}\chi, u)\right)e^{-it\omega}\chi, \tag{17}$$

is the linear perturbation, while

$$N_\chi(u)(t,x) = bQ(u,u)u + bQ(u,u)e^{-it\omega}\chi + b\left(Q(u, e^{-it\omega}\chi) + Q(e^{-it\omega}\chi, u)\right)u \tag{18}$$

is the nonlinear term. Note that

$$b = e^2, \quad W(x) = Q(\chi, \chi) - \frac{Z\phi(x)}{|x|} = \int_{\mathbf{R^3}} \frac{|u(y)|^2}{|x-y|} dy - \frac{Z\phi(x)}{|x|} \tag{19}$$

in (17).
Our main stability result is the following.

Theorem 2 *Let $\chi(x)$ be a smooth rapidly decaying solution to (8), (9), (10). There exists a small positive number $\delta > 0$ so that for any compactly supported initial data*

$$u_0 \in H^s(\mathbf{R^3}), \ s > 3/2, \quad \|u_0\|_{H^s} \leq \delta$$

the Cauchy problem for (12) has a global solution

$$\psi(t, x) = e^{-i\omega t}\chi(x) + u(t, x),$$

where

$$u(t, x) \in C(\mathbf{R}_t; H^s),$$

and $u(t, x)$ satisfies the dispersive estimate

$$\lim_{t \to +\infty} \|u(t, \cdot)\|_{L^p} = 0 \tag{20}$$

for some $p, 2 < p < 5$.

Bifurcation of the Magnetic Flux Static Distributions in Multileyered Josephson Junctions

Ivan Hristov

In the last decades the propagation of electromagnetic waves in long Josephson Junctions (JJs) has been extensively studied especially in order to develop useful devices for storage and transmission of information. Stacking the junctions may increase the usability of these devices. Such structures make it possible to state and study new physical effects that do not occur in one-layered JJs. A simple scheme of N-layered JJ is shown on Fig.1, where black layers are insulators with thickness D and white layers are superconductors with thickness d.

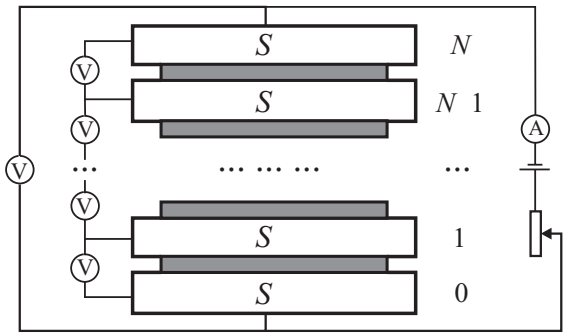

Figure 1: N-layered JJ

In this paper we consider the model of JJs based on inductively coupled layers [1]. The electromagnetic interaction between junctions is represented by a coupling constant s, given by

$$s = -\lambda/(D\sinh(d/\lambda) + 2\lambda\cosh(d/\lambda)),$$

where λ is the London penetration depth.

The simplest generalizable case is the case of three-layered junctions because it takes into account the difference in the behavior of the interior and exterior junctions. The first and the third junctions are coupled only to one neighboring junction while the second junction is coupled to its two neighbor junctions below and above. All of the numerical results, presented below, are for the particular case of three-layered junctions, but the method of investigation and its program realization are for the N-layered case.

The existence of Josephson current generates a specific magnetic flux. When the external current is less then some critical value, the junction layers are in superconductive regime. The transitions from superconductive to resistive regime are mathematically interpreted as bifurcation of the static distributions of the magnetic flux under the change of the parameters.

The vector of static distributions of the magnetic flux $\varphi(x) = (\varphi_1(x), \varphi_2(x), \ldots, \varphi_N(x))^T$ satisfies [1, 2] the nonlinear boundary value problem

$$-\varphi'' + L(J + \Gamma) = 0, \tag{1}$$

$$\varphi'(\pm l) = H, \tag{2}$$

where $J = (\sin\varphi_1, \sin\varphi_2, \ldots, \sin\varphi_N)^T$ is the vector of the Josephson current density, $\Gamma = \gamma(1, 1, \ldots, 1)^T$ is the vector of the external current density, $H = h_e(1, 1, \ldots, 1)^T$ is the vector of the external magnetic field and $2l$ is the length of layers. The matrix L is a matrix of the inductive interaction $(-0.5 < s \leq 0)$:

$$L_{(N\times N)} = \begin{pmatrix} 1 & s & 0 & \ldots & 0 & 0 \\ s & 1 & s & \ldots & 0 & 0 \\ . & . & . & \ldots & . & . \\ 0 & 0 & 0 & \ldots & 1 & s \\ 0 & 0 & 0 & \ldots & s & 1 \end{pmatrix}.$$

We investigate numerically the static distributions of the magnetic flux and seek for the critical values of the parameters h_e and γ where these distributions fail to exist. To solve the nonlinear boundary value problem (1), (2) we use an iterative algorithm, based on the continuous analog of Newton's method (CAMN). As initial approximations for the iteration process we take combinations (for the different layers) of solutions in the one-layered case, $h_e = 0$, $\gamma = 0$:
– Meissner solutions, denoted by M, of the form:

$$\varphi(x) = k\pi, \;\; k = 0, \pm 1, \pm 2, \ldots,$$

– fluxon (antifluxon) solutions, for which there are exact analytical expressions in the case of infinite junctions $(l = \infty)$:

$$\Phi^{\pm 1}(x) \equiv \varphi(x) = 4\arctan(\exp(\pm x)) + 2k\pi.$$

For junctions of finite length objects of type Φ are not fluxons in a strong sense, but by analogy the same terminology is used.
CANM gives a linearized boundary value problem at each iteration step:

$$-v'' + LJ'v = u'' - L(J + \Gamma) \tag{3}$$

$$v'(\pm l) = H - u'(\pm l), \tag{4}$$

where $u = (u_1, u_2, u_3, \ldots, u_N)^T$ is the approximate solution found at the previous iteration step, $v = (v_1, v_2, \ldots, u_N)^T$ is the vector of the iteration corrections and J' is the matrix $\mathrm{diag}(\cos u_1, \cos u_2, \ldots, \cos u_N)$.
The linear boundary value problems (3), (4) are solved by using Galerkin finite element method [3] and quadratic elements. The matrices of the corresponding linear algebraic problems are nonsymmetric. They are stored and used in $sky - line$ form. The linear algebraic problems are solved by using LU-decomposition.

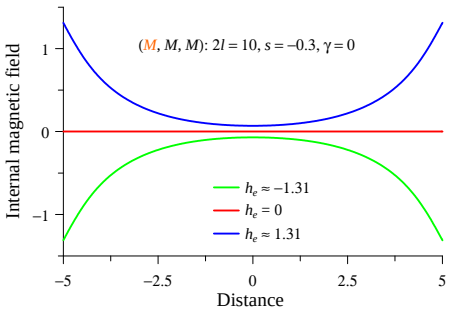

Figure 2: Solution of type MMM

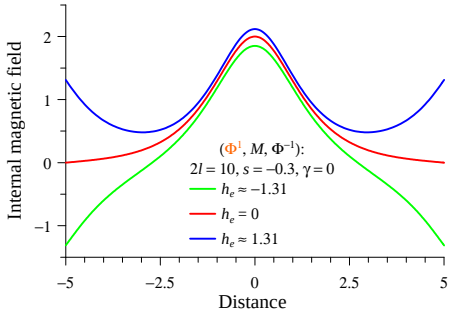

Figure 3: Solution of type $\Phi^1 M \Phi^{-1}$

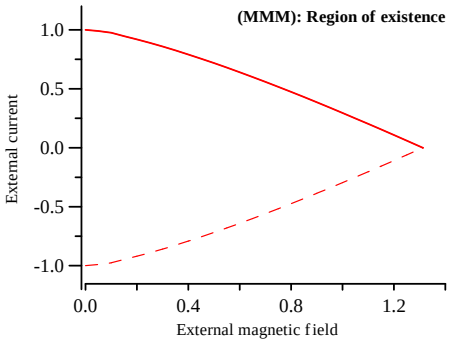

Figure 4: Solution of type MMM

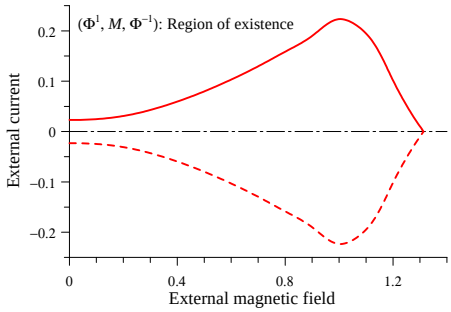

Figure 5: Solution of type $\Phi^1 M \Phi^{-1}$.

To test the accuracy of the realized method we have used the method of Runge by computing the solution on four embedded meshes. The numerous experiments made show a super-convergence of order four.

On Fig.2 and Fig.3 the distribution of the internal magnetic field (the values of $\varphi'(x)$) in the first layer of a three layered junction are graphically shown. The results are for three different values of the external magnetic field (h_e equal to zero and to the two corresponding bifurcation values) when $\gamma = 0$, $l = 5$ and $s = -0.3$.

In Table 1 and Table 2 the critical (bifurcation) values of the external current at fixed external magnetic field for solutions of types MMM and $\Phi^1 M \Phi^{-1}$ are shown. The parameters l and s are fixed. Changing the value of h_e we get the region of existence of the corresponding solution on the plane $P \equiv (h_e, \gamma)$. We expected a symmetry of this region with respect to h_e and γ for solutions of types MMM and $\Phi^1 M \Phi^{-1}$, and this was confirmed by the numerical results. On Fig.3 and Fig.4 the regions of existence ($h_e \geq 0$) in the plane $P \equiv (h_e, \gamma)$ for the same solutions are shown.

Table 1: Critical dependence h_e/γ for solution of type MMM

h_e	γ_{min}	γ_{max}
0.0000000	-1.00000010	1.00000010
0.1000000	-0.97592510	0.97592510
0.2000000	-0.91942270	0.91942270
0.3000000	-0.85865810	0.85865810
0.4000000	-0.79101770	0.79101770
0.5000000	-0.71791390	0.71791390
0.6000000	-0.64025470	0.64025470
0.7000000	-0.55869980	0.55869980
0.8000000	-0.47376610	0.47376610
0.9000000	-0.38588190	0.38588190
1.0000000	-0.29541950	0.29541950
1.1000000	-0.20272030	0.20272030
1.2000000	-0.10812600	0.10812600
1.3000000	-0.01213557	0.01213557
1.3100000	-0.00256270	0.00256270
1.3121000	-0.00059028	0.00059028
1.3127100	-0.00004579	0.00004579
1.3127801	-0.00000230	0.00000230

Table 2: Critical dependence h_e/γ for solution of type $\Phi^1 M \Phi^{-1}$

h_e	γ_{min}	γ_{max}
0.0000000	-0.02309530	0.02309530
0.1000000	-0.02467210	0.02467210
0.2000000	-0.03085960	0.03085960
0.3000000	-0.04285260	0.04285260
0.4000000	-0.05948620	0.05948620
0.5000000	-0.07976990	0.07976990
0.6000000	-0.10322650	0.10322650
0.7000000	-0.12955660	0.12955660
0.8000000	-0.15852090	0.15852090
0.9000000	-0.18988530	0.18988530
1.0000000	-0.22333920	0.22333920
1.1000000	-0.19487790	0.19487790
1.2000000	-0.10172960	0.10172960
1.3000000	-0.01035830	0.01035830
1.3110000	-0.00110260	0.00110260
1.3121000	-0.00025470	0.00025470
1.3125100	-0.00005260	0.00005260
1.3125310	-0.00000980	0.00000980

References

[1] S. Sakai, P. Bodin, N.F. Pedersen, Fluxons in thin-film superconductor-insulator superlattices, J. Appl. Phys., v. **73**, No. 5, 1993, pp. 2411 – 2418.

[2] M. Machida, S. Sakai, Unifed theory for magnetic and electric field coupling in multistacked Josephson junctions, PRB, 70, 144520 (2004).

[3] Thomee V., Galerkin finite element method for parabolic problems.Berlin: Spinger,1997.

Modelling and Simulation of Multiscale Problems in Industrial Filtration Processes

Oleg Iliev, Zahra Lakdawala, Arnulf Latz, Peter Popov,
Stefan Rief, Konrad Steiner, Andreas Wiegmann

Introduction. Filtering out solid particles from fluids is essential for many industrial and environmental applications, such as automotive engines, drinking and waste water purification, air filtration etc. A filter can be described shortly as a filter box (which could be of complicated shape) with inlet/s for dirty fluid, and outlet/s for filtrated fluid. The inlet/s and outlet/s are separated by a filtering medium, which is usually a single layer or a multilayer porous media. The filtering medium itself is a complicated porous medium. In our considerations we deal not only with filter media manufactured from nonwoven technical textiles but also consider a variety of other materials such as ceramics, zeolites, sand, paper, etc. Optimal shape design for the filter housing, achieving optimal pressure drop - flow rate ratio, optimal time performance of a filter etc., require not only the detailed knowledge about the flow field through the filter but also information of the particles being captured by the filtering medium.
Most research on modeling and simulation of filtration processes is done separately on different scales, namely the micro- and the macro-scales. On the microscale, one deals with individual dirt particles and completely resolved geometries of the filter media [1,2]. On the other hand, macroscale considers complete filter elements, concentration of particles, and porous media approximations for the filter media [3,4]. Apparently, the processes on different scales are not independent from each other: the microscale geometry changes due to the deposited particles and therefore changes the macroscopic parameters such as permeability and absorption rate, which further depend on the micro scale equations. Conversely, the macroscopic velocities and pressure influence the filtration processes on the microscale.
Earlier, Fraunhofer ITWM has presented algorithms and softwares for simulations on independent micro- and macro-scales. For microscale, see e.g. [1, 2], and for simulations on macroscale, see e.g. [3, 4]. Following, we shortly discuss the independent macroscale and the microscale models followed by two approaches for multiscale modelling: a subgrid approach, and an approach for coupling continuous macroscale modeling with discrete microscale modeling.

Macroscale model. Stokes-Brinkman model (see equations below), or Navier-Stokes-Brinkman is considered to model macroscale flows in conjunction with filtration of incompressible fluids:

$$-\nabla \cdot (\mu_{eff} \nabla \vec{u}) + \mu K^{-1} \vec{u} = \vec{f}_B - \nabla p \qquad (1)$$
$$\nabla \cdot \vec{u} = 0 \ \text{ in } \Omega_p$$

Here μ_{eff} is some effective viscosity, the permeability tensor is denoted by K. In the pure fluid part $K^{-1} \equiv 0$. Brinkman model differs from the Darcy model due

to the appearing viscous terms in momentum balance (which change the type of the system and number of equations). These viscous terms allow for proper setting of, for example, no-slip conditions on the solid walls. Also, they give a more adequate representation for the flow in cases of high porosity. More details about the algorithms for solving these equations, can be found, for example, in [3,4] and in references therein.

Microscale model. The dynamics of particles is determined by solving the equation of motion for a collection of non interacting particles, which are coupled to the flow, exposed to the thermal fluctuations of fluid molecules and, additionally, can interact with the fibres. All these effects can be described by a stochastic differential equation for the position $\vec{r}(t)$ and the velocity $\vec{u}(t)$ of the particles

$$\frac{d\vec{r}}{dt} = \vec{u}(t) \tag{2}$$

$$d\vec{u} = -\gamma(\vec{u}(t) - \vec{\mathrm{v}}(\vec{r}(t)))dt + \sigma * d\vec{W}(t) \tag{3}$$

$$\langle dW_i(t)dW_j(t)\rangle = \delta_{ij}dt \tag{4}$$

Here γ is the friction coefficient due to the kinematic viscosity ν, fluid mass density ρ_F and particle mass density ρ_p:

$$\gamma = \frac{3}{8}\frac{\rho_F}{\rho_p R_p} c_d \ * |\vec{u}(t) - \vec{\mathrm{v}}(\vec{r}(t))| \tag{5}$$

with the drag coefficient $c_d = f(Re_p)$ being a function of the Reynolds number of the particle Re_p with radius R_p:

$$Re_p = 2R_p \frac{|\vec{u}(t) - \vec{\mathrm{v}}(\vec{r}(t))|}{\nu} \tag{6}$$

For further details on the model and for an algorithm for solving the above equations, we refer to [1,2].

SubGrid approach. A recent development of the numerical solution algorithms for simulation of flow within filter elements include a subgrid approach. The subgrid approach is widely used in modeling turbulent flows, aiming to provide information about finer scale vortices to the current grid discretization where the vortices are unresolved. Based on this idea, we use a similar approach to solve laminar incompressible Navier-Stokes-Brinkman equations in complex domains. When it becomes impossible to solve a problem on a very fine grid due to memory and CPU time constraints, the subgrid approach still allows to capture some of the fine grid details even though the problem is solved on a coarser grid. Numerical upscaling approach is used for this purpose. The domain is resolved by a fine grid, which captures the geometrical details but is too large for solving the problem, and by a coarse grid, where the problem can be solved. A special procedure selects certain coarse cells that contain complicated fine scale geometry. For example, coarse cells that are completely occupied by fine fluid cells are not marked, while coarse cells containing a mixture of fluid, solid, and

porous fine cells, are marked. For all the marked coarse cells, an auxiliary problem on fine grid is solved locally. The formulation of the problem comes from the homogenization theory, where auxiliary cell problems for Stokes problem are solved in order to calculate Darcy permeability at a macroscale. In this way, new permeabilities for all the marked coarse cells are calculated, and the Navier-Stokes-Brinkman system of equations is solved on the coarse scale. The use of such effective permeability tensors allow us to get more precise results compared to the results obtained by the original system solved on the coarse grid. The initial tests on the model problems have met these expectations. A similar approach is used by P.Jenny. However, his approach solves only for the pressure on the coarse grid, while it solves only for the velocity on the fine grid. In our case this is not possible due to the size of the industrial problems we are solving. Moreover, since our main aim is to calculate the pressure drop through the filter accurately, some details of the velocity are not as important. It should be noted that for problems where the details of the solution are important, we plan to modify our approach so that it works as multilevel algorithm with adaptive local refinement. This would mean that the pressure field on the coarse scale will be used to locally recover the velocities, and this will be done iteratively with the use of upscaling procedure.

Coupling continuous macroscale model with discrete microscale model. An idea for coupled modelling and simulation on the micro- and macro-scales is discussed here. The approach is based on a fractional time step discretization, with consecutively solving subproblems on the micro- and macro-scales. The macroscale parameters, permeability and absorption rate, are consecutively upscaled from solutions of microscale problems. The macroscopic solution at each time step is downscaled to provide input velocity and particles distribution for the microscale simulations. The changes in the microstructure are monitored in selected locations of the filter media in order to provide proper information for the upscaling procedure.
In this way, the flow rate-pressure drop ratio, the dirt storage capacity, and the size of the penetrating particles can be analyzed on both: the microscale (the scale at which separate particles flow in the pore space of the filtering medium), and the macroscale (the flow through a filter element).

References

[1] A. Latz and A. Wiegmann, Simulation of fluid particle separation in realistic three dimensional fiber structures. Filtech Europa, Volume I, pp. I-353 - I-361, October 2003.

[2] S. Rief, D. Kehrwald, K. Schmidt, A. Wiegmann, Simulation of ceramic DPF Media, Soot deposition, Filtration efficiency and pressure drop evolution, World Filtration Congress, Leipzig, 2008

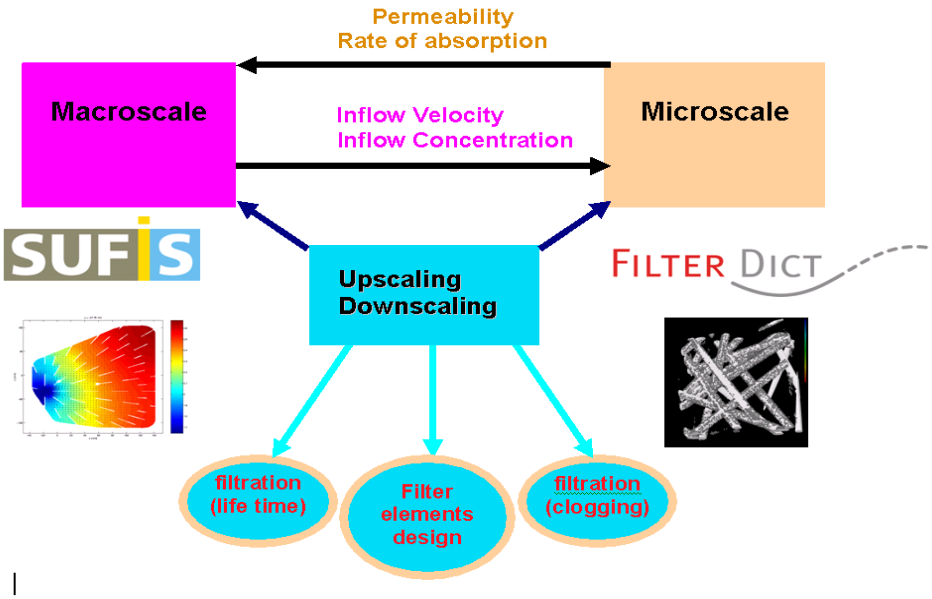

Figure 1: Shifted control volumes: inner and boundary cells

[3] O.Iliev, V.Laptev, D.Vasileva, Algorithms and software for flow through oil filters. Filtech Europa, Volume I, pp. I-327 - I-334, October 2003.

[4] M. Dedering, W. Stausberg, O. Iliev, Z. Lakdawala, R. Ciegis, V. Starikovicius, On new challenges for CFD simulation in filtration, World Filtration Congress, Leipzig, 2008, to appear.

SALUTE - Grid Application for Quantum Transport Problems

Emanoul Atanassov, Todor Gurov, Aneta Karaivanova,
Mihail Nedjalkov, Sofiya Ivanovska, Rayna Georgieva

1 Introduction

The computational Grid (or, shortly, the Grid) proved to be very efficient computing model. Whereas the Web is a service for sharing information over the Internet, the Grid is a service for sharing computer power and data storage capacity over the Internet [1]. The Grid goes well beyond simple communication between computers and aims ultimately to turn the global network of computers into one vast computational resource. Usage of Grid is especially useful for Monte Carlo applications as there the amount of similar calculations that has to be done is huge. Here we present a Grid application developed for solving computationally intensive problems arising from semiconductor physics. The application is called **SALUTE** for simplicity which stands for **S***tochastic* **AL***gorithms for* **U***ltra-fast* **T***ransport in s***E***m***iconductors*.

Let us remind that the **M**onte **C**arlo **M**ethods (MCMs) are based on the simulation of stochastic processes whose expected values are equal to computationally interesting quantities. MCMs form the computational foundation for many fields including transport theory, quantum physics, computational chemistry, finance, etc. Particularly, the MCMs for quantum transport in semiconductors and semiconductor devices have been actively developed during the last decade. These MC calculations need large amount of computational power and the reason is as follows: if temporal or spatial scales become short, the evolution of the semiconductor carriers cannot be described in terms of the Boltzmann transport and therefore a quantum description is needed. As a rule the quantum problems are very computationally intensive and require parallel and Grid implementations. The intrinsically parallel aspect of MC applications makes them an ideal fit for the grid-computing paradigm.

2 Brief Description of SALUTE

SALUTE integrates a set of Monte Carlo algorithms for simulation of ultra-fast carrier transport in semiconductors [2, 3]. The **physical model** describes a femtosecond relaxation process of optically excited electrons which interact with phonons in one-band semiconductor. The interaction with phonons is switched on after a laser pulse creates an initial electron distribution. Experimentally, such processes can be investigated by using ultra-fast spectroscopy, where the relaxation of electrons is explored during the first hundred femtoseconds after the optical excitation. In our model we consider a low-density regime, where the interaction with phonons dominates the carrier-carrier

interaction. Two cases are studied using SALUTE: electron evolution in presence and in absence of electric field. The **mathematical model** is Wigner equation for the nanometer and femtosecond transport regime. In the homogeneous case we solve a version of the Wigner equation called Levinson (with finite lifetime evolution) or Barker-Ferry equation (with infinite lifetime evolution). Another formulation of the Wigner equation considers inhomogeneous case when the electron evolution depends on the energy and space coordinates. At present, SALUTE numerical experiments use GaAs material parameters.

SALUTE includes various advanced MC, quasi-MC, and hybrid MC algorithms which use different variance reduction techniques for the considered versions of the integral operator. The goal is to estimate several important physical quantities. Some numerical results are shown on Figures 1 and 2.

3 Grid Implementation

The SALUTE grid implementation scheme makes heavy use of almost all of the grid services, available in the SEE-GRID* infrastructure for solving important scientific problem. The SEE-GRID infrastructure integrates computational and storage resources, provided by the partners, into a pilot grid infrastructure. Currently there are more than 35 clusters with a total of more than 1500 CPUs and more than 40 TB of storage. The peculiarities of the region are that the network connectivity of many of these clusters is insufficient, which implies the necessity to avoid network-hungry applications and emphasize computationally intensive applications, that make efficient use of the available resources. It also imposes the need of fault-tolerant implementations.

The current grid implementation scheme [4] for SALUTE application provides several important advantages over the older scheme by making use of the newer services and APIs available in the gLite middleware. It leverages the computing and storage resources of the SEE-GRID infrastructure. On the other hand, it enables stress-testing of the infrastructure itself by loading of the computational power, storage and bandwidth capacity of the infrastructure and making efficient use of its core services. We have submitted a total of several thousands of jobs, creating a substantial peak load of the infrastructure. Our grid implementation scheme can provide an example for other grid applications to make use of the SEE-GRID infrastructure.

*SEE-GRID2 (South Eastern European GRid enabled e-Infrastructure Development) initiative is co-funded by the European Commission under the FP6 Research Infrastructures contract # 031775 towards sustainable grid-related activities in the SEE region. More information is available on http://www.see-grid.eu.

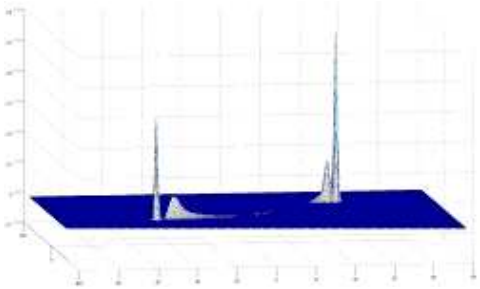

Figure 1: The Wigner function with an applied electric field.

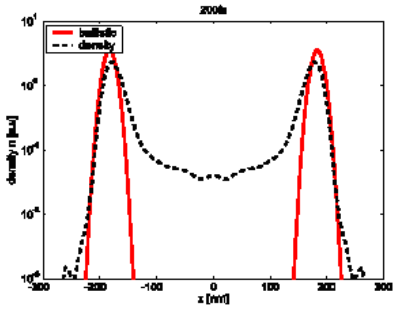

Figure 2: Electron density distribution along the quantum wire after 200 fs evolution time.

References

[1] J. Foster, C. Kesselmann, *The Grid: Blueprint for a New Computing Infrastructure*, Morgan Kaufmann, 1999.

[2] E. Atanassov, T. Gurov, A. Karaivanova, M. Nedjalkov, Monte Carlo Grid Application for Electron Transport, LNCS 3993, Springer, 2006, pp. 616-623.

[3] E. Atanassov, R. Georgieva, T. Gurov, S. Ivanovska, A. Karaivanova, and M. Nedjalkov, New Algorithms in the Grid Application SALUTE, in: Proceedings of the 30 Int. Convention MIPRO: Conference on Hypermedia and Grid Systems, 2007, Opatija, Croatia, ISBN 978-953-233-032-8, pp. 217-222.

[4] E. Atanassov, T. Gurov, A. Karaivanova, SALUTE Application for Quantum Transport - New Grid Implementation Scheme, in: Proceedings of Spanish e-Science Grid Conference, 2007, Madrid, Spain, ISBN 987-84-7834-544-1, NIPO 654-07-015-9, pp. 23-32.

On the Numerical Solution of a Stationary Two-Phase Venttsel Problem

Natalia Kolkovska

Let Ω be the rectangle $(0,1)\times(-1,1)$ in R^2. We divide Ω into two subdomains, $\Omega^1=(0,1)\times(0,1)$ and $\Omega^2=(0,1)\times(-1,0)$, and introduce the notations $\Gamma=(0<x<1)\times(y=0)$, $\Gamma^i=\partial\Omega^i\backslash\Gamma,\ \ i=1,2$ for the parts of their boundaries. We consider the elliptic interface problem

$$-\frac{\partial^2 u^{(i)}}{\partial x^2}-\frac{\partial}{\partial y}k^{(i)}\frac{\partial u^{(i)}}{\partial y}=f^{(i)},\ r\in\Omega^i,\ i=1,2 \tag{1}$$

subjected to the boundary condition

$$u^{(i)}(r)=0,\ r\in\Gamma^i,\ \ i=1,2 \tag{2}$$

and the derivative jump condition on the interface Γ

$$u^{(1)}(r)=u^{(2)}(r)=u(r),\quad r\in\Gamma, \tag{3}$$

$$\alpha\frac{\partial^2 u}{\partial x^2}(r)-\beta u(r)-k^{(1)}\frac{\partial u^{(1)}}{\partial y}(r)+k^{(2)}\frac{\partial u^{(2)}}{\partial y}(r)=g(r),\quad r\in\Gamma. \tag{4}$$

We suppose in the following that α, β and $k^{(i)}$, $i=1,2$ are positive constants.
The model problem (1)-(4) involves a non-standard condition (4) on the interface, which relates the second order tangential derivative and the jump of the normal derivatives. The equation (4) is often referred as 'Venttsel' type condition.
Elliptic problems with Venttsel type conditions set on the outer boundary (one-phase problems) or on the interface (two-phase problems) are encountered in the water wave theory [6], [9], in engineering problems of oil wells [4], in electrostatics [7].
The theoretical analysis of such problems is subject of many papers. A survey of results on the one-phase Venttsel problem can be found in [1] . Results for existence of a solution in Hőlder or Sobolev spaces for the two-phase problem are established in [2]-[3]. The numerical treatment of the one-phase problem with Venttsel type conditions can be found in [5].
In this paper we apply the finite difference method for the numerical solution of (1)-(4). We prove that the difference between the finite difference solution and the exact solution is of optimal order in H^1 mesh-norm.

1 Preliminaries

As usually, by $H^k(\Omega)$ and $H^k(\Gamma)$ we denote the Sobolev spaces on Ω or on Γ. For the two subdomains of Ω we introduce the spaces

$$H^k_{\Gamma^i}(\Omega^i)=\left\{u\in H^k(\Omega^i):u\,|_{\Gamma^{(i)}}=0\right\},\ i=1,2,\ k=1,2.$$

For functions on Ω, whose restrictions on Ω^i belong to the above spaces, we set

$$V^1 = \left\{ u = (u^{(1)}, u^{(2)}) : u^{(1)} \in H^1_{\Gamma^1}(\Omega^1),\ u^{(2)} \in H^1_{\Gamma^2}(\Omega^2),\ u^{(1)}\Big|_\Gamma = u^{(2)}\Big|_\Gamma \in H^1(\Gamma) \right\},$$

$$V^2 = \left\{ u = (u^{(1)}, u^{(2)}) : u^{(1)} \in H^2_{\Gamma^1}(\Omega^1),\ u^{(2)} \in H^2_{\Gamma^2}(\Omega^2),\ u^{(1)}\Big|_\Gamma = u^{(2)}\Big|_\Gamma \in H^2(\Gamma) \right\}.$$

The space V^1 is equipped with the norm

$$\|u\|_{V^1} = \left\|u^{(1)}\right\|_{H^1(\Omega^1)} + \left\|u^{(2)}\right\|_{H^1(\Omega^2)} + \|u\|_{H^1(\Gamma)}.$$

Concerning the boundary problem (1)-(4), we have the following regularity result.

Lemma 1 *Let $f^{(i)} \in L_2(\Omega^i), i = 1, 2$ and $g \in H^{\frac{1}{2}}(\Gamma)$. Then the problem (1)-(4) has a unique solution $u \in V^2$.*

In order to define a weak solution to (1)-(4), we consider the bilinear form

$$a(u,v) = \sum_{i=1,2} \int_{\Omega^i} \left(\frac{\partial u^{(i)}(x,y)}{\partial x} \frac{\partial v^{(i)}(x,y)}{\partial x} + k^{(i)} \frac{\partial u^{(i)}(x,y)}{\partial y} \frac{\partial v^{(i)}(x,y)}{\partial y} \right) dxdy$$

$$+ \int_\Gamma \left(\alpha \frac{\partial u(x,0)}{\partial x} \frac{\partial v(x,0)}{\partial x} + \beta u(x,0) v(x,0) \right) dx, \quad u, v \in V^1.$$

Then the weak form of (1)-(4) is as follows.

Find a function $u \in V^1$ such that

$$a(u,v) = \sum_{i=1,2} \int_{\Omega^i} f^{(i)}(x,y) v^{(i)}(x,y) dxdy + \int_\Gamma g(x) v(x) dx \quad \forall v \in V^1.$$

The averaging operators T_1, T_2, T_2^+, T_2^- are defined for functions v from L_1. At $r = (x,y)$ they are:

$$T_1 v(r) = \int_{-1}^{1} (1 - |s|) v(x + sh_1, y) ds, \quad T_2 v(r) = \int_{-1}^{1} (1 - |s|) v(x, y + sh_2) ds,$$

$$T_2^+ v(r) = \int_{0}^{1} (1 - s) v(x, y + sh_2) ds, \quad T_2^- v(r) = \int_{-1}^{0} (1 + s) v(x, y + sh_2) ds.$$

2 Finite Difference Method

We introduce a uniform mesh $\overline{\omega}_h$ in $\overline{\Omega}$ with mesh sizes $h = (h_1, h_2)$, $h_i = N_i^{-1}, N_i \in N, i = 1, 2$ and set $\omega_h^{(i)} = \overline{\omega}_h \cap \Omega^i$, $\gamma_h^{(i)} = \overline{\omega}_h \bigcap \Gamma^i$, $i = 1, 2$, $\gamma_h = \overline{\omega}_h \bigcap \Gamma$. Thus $\overline{\omega}_h = \omega_h^{(1)} \cup \omega_h^{(2)} \cup \gamma_h^{(1)} \cup \gamma_h^{(2)} \cup \gamma_h$. We denote by $\mathring{\mathrm{H}}_h$ the set of discrete functions, defined on $\overline{\omega}_h$, which vanish on $\gamma_h^{(1)} \cup \gamma_h^{(2)}$.

Let V_h^1 be the discrete analog to the space V^1. The notations in the following operators on discrete functions are taken from [8].
We approximate the problem (1)-(4) with the finite difference scheme

$$\begin{aligned} A_h v \equiv A_1 v(r) + A_2 v(r) &= \varphi(r), \quad r \in \omega_h^{(1)} \cup \omega_h^{(2)} \cup \gamma_h, \\ v(r) &= 0, \quad r \in \gamma_h^{(1)} \cup \gamma_h^{(2)}, \end{aligned}$$

where

$$A_1 v(r) = -\begin{cases} v_{x\bar{x}}(r), & r \in \omega_h^{(1)} \cup \omega_h^{(2)}, \\ (1 + \frac{\alpha}{h_2}) v_{x\bar{x}}(r), & r \in \gamma_h, \end{cases}$$

$$A_2 v(r) = -\begin{cases} (k^{(1)} v_{\bar{y}})_y(r), & r \in \omega_h^{(1)}, \\ (k^{(2)} v_{\bar{y}})_y(r), & r \in \omega_h^{(2)}, \\ \frac{1}{h_2}(k^{(1)} v_y - k^{(2)} v_{\bar{y}}) - \frac{\beta}{h_2} v(r), & r \in \gamma_h, \end{cases}$$

$$\varphi(r) = \begin{cases} T_1 T_2 f^{(1)}(r), & r \in \omega_h^{(1)}, \\ T_1 T_2 f^{(2)}(r), & r \in \omega_h^{(2)}, \\ T_1 T_2^{+} f^{(1)}(r) + T_1 T_2^{-} f^{(2)}(r) - \frac{1}{h_2} T_1 g(r), & r \in \gamma_h. \end{cases}$$

Lemma 2 *The operators A_1, A_2 and A_h are self-adjoint and positive definite on $\mathring{H}_h$.*

As an immediate consequence of the Lemma 2 it follows, that there exists a unique solution to the difference scheme (5).
The main result presented here is the convergence of the finite difference scheme.

Theorem 1 *Let $u \in V^2$ be the solution of (1)-(4) and let v be the solution of the finite difference method (5). There exists a positive constant C (independent on u, v and h) such that*

$$\|v - u\|_{V_h^1} \quad \leq C|h|^1 \ \|u\|_{V^2}.$$

The proof of this theorem is based on a-priori estimates, analysis of the error of approximation and the Bramble-Hilbert Lemma.
The above estimate of the rate of convergence is consistent with the smoothness of the exact solution. Let us note, that the rate of convergence is the same as for the elliptic problem with Dirichlet boundary condition [8].
The result in Theorem 1 can be extended to discontinuous self-adjoint elliptic type equations with 'Venttsel' type condition on the interface.

References

[1] Apushkinskaya, D., Nazarov, A. : A survey of results on nonlinear Venttsel problems. Applications of Mathematics. **45** (2000) 69–80.

[2] Apushkinskaya, D., Nazarov, A. :Linear two-phase Ventssel problems. Ark. Mat. **39** (2001) 201-222.

[3] Apushkinskaya, D., Nazarov, A. :Quasilinear elliptic two-phase Ventssel's problems in the transversal case. J mat. Sci., **112** (2002) 3927-3943

[4] Cannon, J., Meyer, G. : On diffusion in a fractured medium. SIAM J. Appl. Math. **20** (1971) 434–448.

[5] Kolkovska, N. : Numerical Solution of an Elliptic Problem with a Non-classical Boundary Condition. LNCS **4310** (2007) 623-627.

[6] Korman, P. : Existence of periodic solutions for a class of nonlinear problems. Nonlinear Analysis, Theory, Methods, & Applications. **7** (1983) 873–879.

[7] Radoev, B., Boev, T., Avramov, M. : Electrostatics of heterogeneous monolayers. Constitutive equations and mathematical models. Adv. Colloid Intreface Sci. **114-115** (2005) 93-101.

[8] Samarskii,A. : The theory of difference schemes. (2001) (M. Dekker).

[9] Shinbrot M. : Water waves over periodic bottoms in three dimensions. J. Inst. Maths Applics. **25** (1980) 367–385.

MIC(0) Preconditioning of 3D FEM Problems on Unstructured Grids: Conforming and Nonconforming Elements*

Nikola Kosturski, Svetozar Margenov

Mesh generation techniques are now widely employed in various scientific and engineering fields that make use of physical models based on partial differential equations. While there are a lot of works devoted to finite element methods (FEM) and their applications, it appears that the issues of meshing technologies in this context are less investigated. Thus, in the best cases, this aspect is briefly mentioned as a technical point that is possibly non-trivial. In this study, the topics of grid generation and FEM applications are studied together following their natural synergy.
Let $\Omega \subset \mathbb{R}^3$ be a bounded domain with boundary $\partial\Omega = \Gamma = \Gamma_D \cup \Gamma_N$. The following model elliptic problem

$$-\Delta u = f, \qquad \Gamma_D \equiv \partial\Omega, \tag{1}$$

with Dirichlet boundary conditions on the whole boundary corresponding to the exact solution

$$u(x, y, z) = x^3 + y^2 + z^4 + \sin(x - y),$$

and the related parabolic problem

$$\frac{\partial u}{\partial t} - \Delta u = f, \qquad \Gamma_D \equiv \partial\Omega, \tag{2}$$

where $t \in [0, 1]$, the time-step is $\tau = 0.01$, and the Dirichlet boundary conditions on the whole boundary correspond to the exact solution

$$u(x, y, z, t) = x^4 + y^3 + \sin(x - z) + t^2$$

are considered.
FEM discretization on a triangulation $\mathcal{T}_h$ of the domain Ω reduces the elliptic problem (1) to the linear system

$$K\mathbf{u}_h = \mathbf{f}_h, \tag{3}$$

where K stands for the stiffness matrix.
Crank-Nicholson time stepping is used for the solution of the parabolic problem (2). At each time step, the following linear system is to be solved

$$\left(M + \frac{\tau}{2}K\right)\mathbf{u}_h^{n+1} = \left(M - \frac{\tau}{2}K\right)\mathbf{u}_h^{n} + \tau\mathbf{f}_h^{n+\frac{1}{2}}, \tag{4}$$

where the upper index of the unknown vector indicates the number of the current time step, and M stands for the mass matrix.

*This work is partly supported by the Bulgarian Ministry of Science under grant VU-MI 202/2006.

The implementation of two variants of finite elements defined on $\mathcal{T}_h$ is studied, namely, conforming (Courant) and nonconforming (Crouzeix-Raviart) linear finite elements. The modified incomplete Cholesky factorization MIC(0) [2] is used for the preconditioned conjugate gradient (PCG) [1] solution of the systems (3) and (4). Let us remind, that the sufficient conditions for existence of a stable MIC(0) factorization of the symmetric $N \times N$ matrix $A = (a_{ij})$ are

$$L \geq 0, \qquad A\mathbf{e} \geq 0, \qquad A\mathbf{e} + L^T\mathbf{e} > 0, \tag{5}$$

where $\mathbf{e} = (1, \ldots, 1)^T$ and $(-L)$ is the strictly lower triangular part of A. Due to the positive offdiagonal entries of the stiffness matrix K, the MIC(0) factorization is not directly applicable to precondition the FEM system. The diagonal compensation is the simplest procedure to approximate K by an M-matrix $\bar{K}$, to which the MIC(0) factorization is applied. This means that the positive offdiagonal entries of K are vanished, setting the diagonal of $\bar{K}$, such that the equal row sum condition is fulfilled, i.e., $K\mathbf{e} = \bar{K}\mathbf{e}$.

The global stiffness matrix reads as $K = \sum_{e \in \mathcal{T}_h} K_e$, where K_e is the current element stiffness matrix. The following important geometric interpretation of K_e holds (see, e.g., in [3])

$$K_e = \frac{a_e}{6} \begin{bmatrix} \sum\limits_{1 \neq i < j} l_{ij} \cot\theta_{ij} & -l_{34}\cot\theta_{34} & -l_{24}\cot\theta_{24} & -l_{23}\cot\theta_{23} \\ -l_{34}\cot\theta_{34} & \sum\limits_{2 \neq i < j \neq 2} l_{ij}\cot\theta_{ij} & -l_{14}\cot\theta_{14} & -l_{13}\cot\theta_{13} \\ -l_{24}\cot\theta_{24} & -l_{14}\cot\theta_{14} & \sum\limits_{3 \neq i < j \neq 3} l_{ij}\cot\theta_{ij} & -l_{12}\cot\theta_{12} \\ -l_{23}\cot\theta_{23} & -l_{13}\cot\theta_{13} & -l_{12}\cot\theta_{12} & \sum\limits_{i < j \neq 4} l_{ij}\cot\theta_{ij} \end{bmatrix}, \tag{6}$$

where l_{ij} denotes the length of the edge connecting vertices v_i and v_j of the tetrahedron e, and θ_{ij} stands for the dihedral angle along that edge. This interpretation shows that each positive offdiagonal entry in the element stiffness matrix corresponds to an obtuse dihedral angle in the tetrahedron e. The related positive entry tends to infinity when the dihedral angle tends to $180\,^\circ$. Now, let us turn on to the case of Crouzeix-Raviart nonconforming finite elements. It is easily seen that $K_e^{(nc)} = 9K_e^{(c)}$, where $K_e^{(c)}$ and $K_e^{(nc)}$ stand for the element stiffness matrices corresponding to linear conforming and nonconforming finite elements, associated with the element e. One direct conclusion is the applicability of the geometric interpretation (6) to the case of nonconforming linear tetrahedral elements.

Since the MIC(0) factorization is applied to the auxiliary matrix $\bar{K}$, the convergence rate of the MIC(0) PCG solver strongly deteriorates with the raise of dihedral angles in the FEM mesh.

When the Crank-Nicholson scheme is implemented solving the parabolic problem (2) we have to get a preconditioner for the matrix $M + \frac{\tau}{2}K$. Then, the diagonal compensation for K in combination with lumping the mass for M, which are applied

before the MIC(0) factorization. At this point, an advantage of the nonconforming Crouzeix-Raviart elements is, that the related mass matrix is always M-matrix, i.e., lumping the mass is not required.
We investigate the following three grid generators: NETGEN, TetGen and Gmsh. The presented qualitative analysis is based on the range of the dihedral angles of the triangulation of a given domain. It is well known that very small and very large angles directly affect the accuracy of the FEM approximation. Such kind of strong mesh anisotropy deteriorates also the condition number of the related stiffness matrix, and as will be shown later on, the convergence rate of the implemented iterative solution methods.
The domain we chose for the presented comparison is

$$\Omega = \{(x, y, z) \mid 0.1 \leq x^2 + y^2 + z^2 \leq 1, x, y, z \geq 0\} \ . \tag{7}$$

Different parameters of the grid generators may affect the quality of the resulting meshes. Some generated meshes are shown bellow

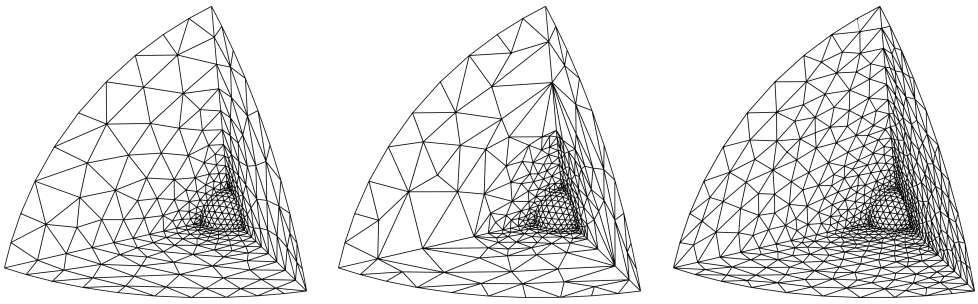

NETGEN TetGen Gmsh

The obtained results show that NETGEN generally achieves better dihedral angles than TetGen. Similar dihedral angles are obtained with Gmsh, but due to the considerably larger number of elements/nodes in Gmsh, NETGEN is preffered.
The presented numerical tests illustrate the MIC(0)–PCG convergence rate. A relative PCG stopping criteria in the form $\mathbf{r}_k^T C^{-1} \mathbf{r}_k \leq \varepsilon^2 \mathbf{r}_0^T C^{-1} \mathbf{r}_0$ is employed. Here $\mathbf{r}_k$ is the residual vector at the k-th iteration and C is the MIC(0) preconditioner. We compare the obtained results in the cases of linear conforming and nonconforming finite elements.
Both the (1) and (2) are solved on both structured (unit cube) and unstructured grids. The obtained iteration counts are presented in graphical form bellow

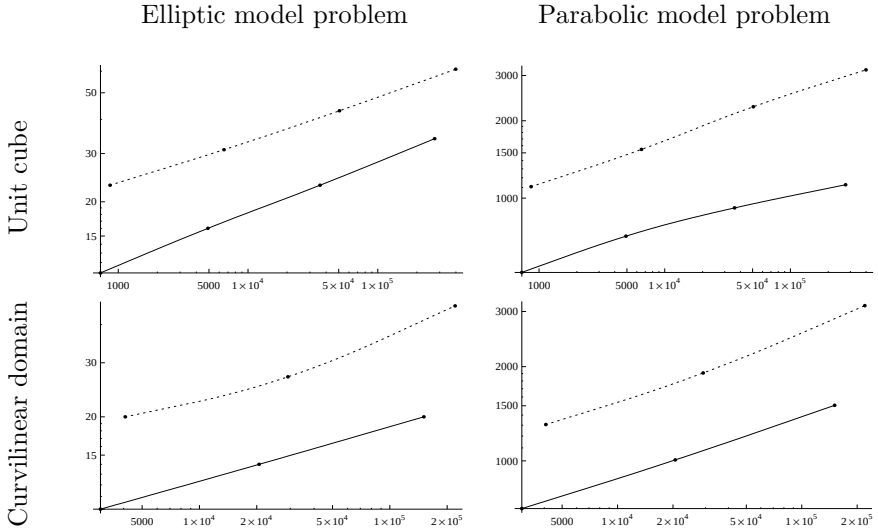

When parabolic problems are considered, the iteration count is the total number for all time steps. The solid and dashed lines correspond to the cases of conforming and nonconforming finite elements. The logarithmic scale more transparently illustrates the asymptotic behavior of the number of iterations.

The rigorous theory of MIC(0) preconditioning is directly applicable only to the model elliptic problem in the unit cube when discretized by standard linear conforming finite elements. The reported number of iterations, in this case, fully confirms the estimate $n_{it} = O(N^{1/6})$. The same asymptotic behaviour of the PCG iterations for all remaining problems is observed, including the case of Crouzeix-Raviart nonconforming finite elements. As we see, the considered algorithms have a well expressed stable behavior for the unstructured meshes. The next general conclusion is that the iteration count is smaller for the conforming FEM problems when compared to the results for nonconforming FEM systems of the same size. However, the stable convergence rate of the MIC(0)–PCG solver for Crouzeix-Raviart FEM systems is of a particular importance, due to the special robustness properties of these nonconforming elements.

References

[1] O. Axelsson: *Iterative solution methods*, Cambridge University Press, Cambridge, MA, 1994.

[2] I. Gustafsson: *An incomplete factorization preconditioning method based on modification of element matrices*, BIT **36:1** (1996), 86–100.

[3] J. Shewchuk: *What Is a Good Linear Finite Element? - Interpolation, Conditioning, Anisotropy, and Quality Measures*, Eleventh International Meshing Roundtable (2002), 115–126.

On the Local Attainability of a Closed Set

Mikhail Krastanov

The problem of local attainability with respect to the trajectories of a differential inclusion is a basic problem of the contemporary control theory. This problem can not be reduced to the problem of small-time local attainability at every point of the set. So, it needs a specific study. The problem has been partially studied using mainly zero order and first order approach (cf. [1, 3, 6, 7, 9, 10, 11]). To state the problem of small-time local attainability, let us consider the following control system:

$$\dot{x}(t) \ \in \ F(x(t)), \tag{1}$$

where $F : R^n \Rightarrow R^n$ is a multifunction with compact and convex values. An absolutely continuous function $x(\cdot)$, satisfying (1) for almost every t from $[0, T]$, is called a trajectory of (1) defined on $[0, T]$. For a fixed point x and for $T > 0$, the attainable set $\mathcal{A}(x, T)$ of (1) from x at time $T > 0$ is defined as the set of all points that can be reached in time T from x by means of trajectories of (1).

Definition 1. *Let S be a closed subset of R^n. It is said that S is small-time locally attainable (STLA) with respect to the control system (1) iff for any $T > 0$ there exists a neighbourhood Ω of S such that for every point $x \in \Omega$ there exists an admissible trajectory of the control system (1) starting from the point x and reaching the set S in time not greater than T, i.e. $\mathcal{A}(x, t) \cap S \neq \emptyset$ for some $t \in [0, T]$.*

One of the most common conditions to ensure local attainability of a closed set is the so called Petrov condition (cf. [8]). Roughly speaking, this condition states that at every point of a neighbourhood of the target there exists an admissible velocity that "points" toward the target in a special way. To formulate this condition in a rigorous way, we follow the notations from the paper [3]: Let S be a compact subset of R^n. We set

$$S_r \ := \ \{y \in R^n | \ \mathrm{d}_S(y, S) \ \leq r\},$$

where

$$\mathrm{d}_S(y) \ := \ \inf \{\|y - s\| \mid s \in S\}.$$

If x is an arbitrary point from $S_r \setminus S$, we set

$$\pi(x) \ := \ \{y \in S | \ \|y - x\| = \mathrm{d}_S(x)\},$$

i.e. $\pi(x)$ is the set of all metric projections of the point x on the set S.
Let us consider the control system (1) under the assumption that F is continuous of modulus ω near S, i.e.

$$H(F(x), F(y)) \ \leq \ \omega(\|x - y\|), \quad \text{for all } x, y \quad \text{near } S,$$

where $H(\cdot,\cdot)$ denotes the Hausdorff metric and $\omega : [0,\infty) \to [0,\infty)$ is a nondecreasing continuous function with $\omega(0) = 0$. Let y belong to the boundary ∂S of the set S. A vector $\xi \in R^n$ is called a proximal normal to S at y provided there exists $r > 0$ so that the point $y + r\xi$ has y as the closest point. The set of all proximal normals at a point y is a cone. This cone is denoted by $N_S^p(y)$ (for a detailed treatment of proximal analysis and some of its applications, see for example the books [2] and [4]. Using these notations, the results of the papers [3, 10] and [11] can be formulated as follows:

Theorem 1. *Suppose that S is a nonempty and compact subset of R^n, and $F : R^n \Rightarrow R^n$ is a continuous multifunction of modulus ω with compact convex values. Suppose that there exists $\delta > 0$ so that, whenever $y \in S$ and $\xi \in N_S^p(y)$, there exists $v \in F(y)$ for which*

$$< \xi, v > \leq \ -\delta\|\xi\|. \tag{2}$$

Then S is STLA with respect to (1).

Unfortunately, if the inequality (2) is violated at some boundary point y of S (for example, when all admissible velocities are "tangent" to the closed set S at y), we can not apply Theorem 2. There are simple examples (cf. [6]) that demonstrates this phenomenon.
The so called "high-order conditions" for attainability of a closed set are also known. Usually the "high-order" term is used for conditions involving Lie brackets of the original vector fields (generating the corresponding control system) to verify a condition of the type (2) instead to use admissible velocities. Such kind of conditions ensure local attainability of a closed set and imply Hölder continuity of the minimal-time function (cf., for example, [1] for the case of attainability of a point, and [5] and [6] in the general case).
Recently, a sufficient condition of first order for attainability of a closed set with respect to the trajectories of a smooth nonlinear system is proved in [7]. The proof of this condition uses control variation of zero and first order and is based on an additional assumption for regularity of the target. In this condition the positive number δ in the Petrov's condition (2) is replaced by a suitable continuous nondecreasing function $\mu(\cdot)$ with $\mu(\rho) > 0$ for $\rho > 0$.
In the present talk we extend the result of [7] in two directions. First, we do not impose any regularity assumptions for the set S, and second we use high-order control variations. For our knowledge, high-order control variations suitable for studying of the problem of local attainability of a set are defined in [5].

References

[1] A. Bacciotti, G. Stefani, *Self-accessibility of a set with respect to a multivalued field*, Journal of Optimization Theory and Applications **48** (1980), 535–552.

[2] F. Clarke, *Optimization and nonsmooth analysis,* Canadian Mathematical Society Series of Monographs and Advanced Texts. A Wiley-Interscience Publication. New York: John Wiley & Sons, Inc. XIII, 308 p. (1983).

[3] F. Clarke, P. Wolenski, *Control of systems to sets and their interiors*, Journal of Optimization Theory and Applications **88** (1996), 3–23.

[4] F. Clarke, Y. Ledyaev, R. Stern and P. Wolenski, "Nonsmooth Analysis and Control Theory," Springer-Verlag, New York, 1998.

[5] M. I. Krastanov, M. Quincampoix, *Local small-time controllability and attainability of a set for nonlinear control system*, ESAIM: Control Optim. Calc. Var. **6** (2001), 499-516.

[6] M. I. Krastanov, A sufficient condition for small-time local attainability of a set, Control and Cybernetics **31** (2002), 739–750.

[7] A. Marigonda, Second order conditions for the controllability of nonlinear systems with drift, Commun. Pure Appl. Anal. **5** (2006), no. 4, 861–885.

[8] N. N. Petrov, *Local controllability*, Differ. Equations **12** (1976), 1545-1550.

[9] P. Soravia, *Hölder continuity of the minimal-time function for C^1-manifold targets*, Journal of Optimization Theory and Applications, **75** (1978), 790–802.

[10] V. M. Veliov, *Attractiveness and invariance: The case of uncertain measurement*, in Modeling techniques for uncertain systems, Prog. Syst. Control Theory. **18** (1994), 277–288.

[11] V. M. Veliov, *On the Lipschitz continuity of the value function in optimal control*, Journal of Optimization Theory and Applications **94** (1997), 335–361.

Polynomial Lotka-Volterra CNN Model: Dynamics and Complexity

Angela Slavova, Maya Markova

In this paper we shall study the following Lotka-Volterra system which models the community of three interacting populations:

$$\left|\begin{array}{l} \frac{dx_1}{dt} = x_1(r_1 - a_{11}x_1 - a_{12}x_2 + a_{13}x_3) \\ \frac{dx_2}{dt} = x_2(r_2 - a_{21}x_1 - a_{22}x_2 + a_{23}x_3) \\ \frac{dx_3}{dt} = x_3(r_3 + a_{31}x_1 + a_{32}x_2 - a_{33}x_3), \end{array}\right. \tag{1}$$

where x_i, $i = 1, 2, 3$ is the density of the i-th population, r_i, a_{ij}, $i, j = 1, 2, 3$ are positive real coefficients; r_i is the intrinsic growth rate of the ith population and the coefficient a_{ij} describes the influence of the jth population upon the ith population [7]. The signs of a_{ij} and a_{ji} determine the nature of the interaction between the populations i and j.

We will apply Cellular Neural Networks (CNN) with the translation invariant polynomial feedback functions for studying Lotka-Volterra system (1). In a recently proposed VLSI development [12] a first CNN based hardware implementation with polynomial weight functions has been presented.

The theory of local activity provides a definitive answer to the fundamental question: What are the values of the cell parameter for which the interconnected system may exhibit complexity? The answer is given in [5,6] - the necessary condition for a non-conservative system to exhibit complexity is to have its cell locally active. The theory which will be presented below and which follows [6] offers a constructive analytical method for uncovering local activity. In particular, for PCNN model, one can determine the domain of the cell parameters in order for the cells to be locally active, and thus potentially capable of exhibiting complexity. This precisely defined parameter domain is called the edge of chaos [6].

We apply the following constructive algorithm:

1. Map Lotka-Volterra system (1)into the following associated discrete- space version which we shall call Lotka-Volterra CNN model:

$$\begin{array}{rcl} \frac{dx_i^1}{dt} & = & f^1(x_i^1, x_i^2, x_i^3) + r^1 x_i^1 = F^1 \\ \frac{dx_i^2}{dt} & = & f^2(x_i^1, x_i^2, x_i^3) + r^2 x_i^2 = F^2 \\ \frac{dx_i^3}{dt} & = & f^3(x_i^1, x_i^2, x_i^3) + r^3 x_i^3 = F^3, \end{array} \tag{2}$$

where f^1, f^2 and f^3 are Taylor series expansions of the functions f_1, f_2 and f_3 respectively. In order to model a Lotka-Volterra system represented by the solutions of (1) using PCNN model (5) the coefficients $b_{ll'}^{(k)}$ have to be determined in a optimization process [12].

2. Find the equilibrium points of (5). For the Lotka-Volterra CNN model (5), the equilibrium points are defined as follows. Let us rewrite (5) in the vector form:

$$\frac{dX}{dt} = X(R - AX) = F \tag{3}$$

where $X = col(x_i^1, x_i^2, x_i^3)$, $R = (r^1, r^2, r^3)$, $A = \begin{pmatrix} a_{11} & a_{12} & a_{13} \\ a_{21} & a_{22} & a_{23} \\ a_{31} & a_{32} & a_{33} \end{pmatrix}$. Then the equilibrium points X_e are such that

$$X_e(R - AX_e) = 0. \tag{4}$$

There are at least two equilibrium points: $X_e^1 = (0, 0, 0)$ and $X_e^2 = RA^{-1}$ if A^{-1} exists.

3. Calculate now the cell coefficients of the Jacobian matrix of (7) about each system equilibrium point $X_e^j, j = 1, 2$:

$$J = \left[\begin{array}{ccc} \frac{\partial f^1}{\partial x^1} & \frac{\partial f^1}{\partial x^2} & \frac{\partial f^1}{\partial x^3} \\ \frac{\partial f^2}{\partial x^1} & \frac{\partial f^2}{\partial x^2} & \frac{\partial f^2}{\partial x^3} \\ \frac{\partial f^3}{\partial x^1} & \frac{\partial f^3}{\partial x^2} & \frac{\partial f^3}{\partial x^3} \end{array} \right] |_{(x^1,x^2,x^3)=X_e^j, j=1,2} \tag{5}$$

$$= \left[\begin{array}{ccc} f_e^{11} & f_e^{12} & f_e^{13} \\ f_e^{21} & f_e^{22} & f_e^{23} \\ f_e^{31} & f_e^{32} & f_e^{33} \end{array} \right].$$

4. Calculate the trace $Tr(X_e^j)$ and the determinant $\Delta(X_e^j)$ of the Jacobian matrix (8) for each equilibrium point:

$$\begin{aligned} Tr(X_e^j) &= f_e^{11} + f_e^{22} + f_e^{33} \\ \Delta(X_e^j) &= f_e^{11} f_e^{22} f_e^{33} + f_e^{12} f_e^{23} f_e^{31} + \\ &+ f_e^{13} f_e^{21} f_e^{31} - f_e^{13} f_e^{22} f_e^{31} - \\ &- f_e^{11} f_e^{23} f_e^{32} - f_e^{12} f_e^{21} f_e^{33}. \end{aligned} \tag{6}$$

Definition 1 *Stable and Locally Active Region $SLAR(X_e^j)$ at the equilibrium point X_e^j for Lotka-Volterra CNN model (5) is such that $Tr < 0$ and $\Delta > 0$.*

We shall consider the equilibrium point $X_e = (1, 1, 1)$ [9]. In this case the above condition can be written as follows:

$$\begin{aligned} Tr(X_e = (1, 1, 1)) = r^1 - 2a_{11} + r^2 - \\ -2a_{22} + r^3 - 2a_{33} < 0, \end{aligned} \tag{7}$$

$$\Delta(X_e = (1,1,1)) = (r^1 - 2a_{11})(r^2 - 2a_{22})$$
$$(r^3 - 2a_{33}) - -a_{12}a_{23}a_{31} - a_{13}a_{21}a_{32} -$$
$$-(r^1 - 2a_{11})23a_{32} - (r^2 - 2a_{22})a_{13}a_{32} -$$
$$-(r^3 - 2a_{33})a_{12}a_{21} > 0$$

6. Edge of chaos.

In the literature [6] the so called edge of chaos (EC) means a region in the parameter space of a dynamical system where complex phenomena and information processing can emerge. We shall try to define more precisely this phenomena till know known only via empirical examples. Moreover, we shall present an algorithm for determining the edge of chaos for reaction-diffusion CNN models as the Lotka-Volterra CNN model (5). Let us set $R = 0$ in equilibrium equations (7),i.e.:

$$\begin{aligned} f^1(x_e^1, x_e^2, x_e^3) &= 0 \\ f^2(x_e^1, x_e^2, x_e^3) &= 0 \\ f^3(x_e^1, x_e^2, x_e^3) &= 0 \end{aligned} \tag{8}$$

For the Lotka-Volterra CNN model (4) we shall consider the equilibrium point $X_e = (1,1,1)$ [9]. Our next step is to calculate the local cell coefficients $f_e^{11}, f_e^{12}, f_e^{13}$, $f_e^{21}, f_e^{22}, f_e^{23}, f_e^{31}, f_e^{32}, f_e^{33}$ from (8) about the equilibrium point X_e. We determine Local Activity Region and Stable Local Activity Region for the point in the cell parameter space by (10). We shall identify the edge of chaos domain EC in the cell parameter space by using the following definition [6]:

Definition 2 *A Lotka-Volterra CNN model is said to be operating on the edge of chaos EC iff there is at least one equilibrium point X_e which is both locally active and stable at X_e when A^{-1} exists and $R = 0$.*

The following theorem then hold:

Theorem 1 *PCNN model of Lotka-Volterra system (1) is operating in the edge of chaos regime iff (i) A^{-1} exists and (ii) $2(a_{11}a_{23}a_{32} + a_{22}a_{13}a_{32} + a_{33}a_{12}a_{21}) > (a_{11}a_{22}a_{33} + a_{12}a_{23}a_{31} + a_{13}a_{21}a_{32})$. For this parameter values there is at least one equilibrium point which is both locally active and stable.*

REFERENCES

[1] Bomze I., Lotka-Volterra equations and replicator dynamics:A two dimensional classification, Biol.Cybern. 48, pp. 201-211, 1983.

[2] Britton N.F., Reaction-Diffusion Equations and Their Applications to Biology, New York: Academic, 1986.

[3]Chua L.O., Yang L., Cellular Neural Network: Theory and Applications, IEEE Trans. CAS, vol. 35, pp. 1257-1290, Oct. 1988.

[4] Chua L.O., Hasler M., Moschytz G.S., Neirynsk J., Autonomous cellular neural networks: a unified paradigm for pattern formation and active wave propagation, IEEE Trans. CAS-I, vol. 42, N 10, pp. 559-577, Oct. 1995.

[5] Chua L.O., CNN:A Paradigm for Complexity, World Scientific Series on Nonlinear Science, Series A - Vol. 31, World Scientific, 1998.
[6] Chua L.O., Local activity is the origin of complexity, Int.J. of Bifurcations and Chaos, Nov. 2005.
[7] Hofbauer J., Sigmund K., The theory of evolution and dynamical systems, Mathematical Aspectes of Selection, in: London Math.Soc. Student Texts, vol. 7, Cambridghe Univ.Press, 1988.
[8] Liang X., Juang J., The dynamical behavior of type-K competitive Kolmogorov systems and its applicatuions to 3-dimensional type-K competitive Lotka-Volterra systems, Nonlinearity, 16, pp. 785-801, 2003.
[9] Roska T., Chua L.O., Wolf D., Kozek T., Tetzlaff R., Puffer F., Simulating nonlinear waves and partial differential equations via CNN- Part I: Basic techniques, IEEE Trans. CAS-I, vol. 42, N 10, pp. 807-815, Oct. 1995.
[10]Slavova A., Applications of some mathematical methods in the analysis of Cellular Neural Networks, J.Comp.Appl.Math., 114, pp. 387-404, 2000.
[11] R. Tetzlaff, F. Gollas, Modeling complex systems by reaction-diffusion Cellular Nonlinear Networks with polynomial Weight-Functions, *Proc. IEEE CNNA2005*, 2005.

Neural Networks for Solving Sudoku Problems

Valeri Mladenov

1. Introduction. In 1979 the first Sudoku puzzle was introduced by the architect Howard Garns under the name Number Place [1]. Since neural networks are constructed in such a way that only binary or bipolar outputs are accepted, Sudoku puzzles have to be transformed to another representation. Chosen representation is given in the following subsection. In next subsection the constraints of the Sudoku puzzle are transformed to the neural representation. For every number k which can be places at a location in the puzzle (i, j) a neuron exists. Now neurons are denoted by $V(i, j, k)$, where i the row number, j the column number and k the number to be placed. From the size of the puzzle it follows that i, j and k can take values in the range from 1 to 9. The output of the neurons can be interpreted as: if the neuron fires, the output of $V(i, j, k)$ is 1, then the number k should be placed at location (i, j). In order to have a good representation of the neurons in Matlab, the neurons have to be arranged in a vector form. This is chosen in the following way:

$$V_m(l) = V(i, j, k)\,, \tag{1}$$

where $l = 92(l-1) + 9(j-1) + k$. The total number of neurons is: $\max(l) = l = 92(9-1) + 9(9-1) + 9 = 729$. In Sudoku puzzles exactly one number has to be placed at every position, having constraints that every number (1-9) can only be placed once in every: row; column; non-overlapping square subregion of size 3×3. To simplify notations we will continue with the name subregion for the non-overlapping square subregions of size 3. The constraints in neuron form are given by the following equations:

$$\sum_{i=1}^{9} V(i, j, k) = 1, \forall j, k \tag{2}$$

$$\sum_{j=1}^{9} V(i, j, k) = 1, \forall i, k \tag{3}$$

$$\sum_{k=1}^{9} V(i, j, k) = 1, \forall i, j \tag{4}$$

$$\sum_{i \in i', j \in j'}^{9} V(i, j, k) = 1, \forall j, k \tag{5}$$

Equations (2) and (3) make sure that every number k is only placed once in every column j and row i. Equation (4) has to ensure that only one number k is placed at a location (i, j). Constraint 3 is taken care of by equation (5) which sums over subregions, which are defined above. Every number is placed only once in every subregion. By combining all equations, all constraints of the Sudoku puzzle are given in a neural form. The total number of constraints is $9 \cdot 9 \cdot 4 = 324$.

1.1. Hopfield network. A continuous Hopfield network is chosen with binary outputs. The continuous Hopfield network is a single layer network which contains integrators, binary sigmoid functions and multipliers. In this section the network is initialized. First the size and architecture of the network is given and finally weights are calculated. A Hopfield network contains simple neuron models which have a binary or bipolar output value and the input to output relation of the activation function is a logsig function, which is described by:

$$V_i = g_i(x) = \frac{1}{1 + \exp(-u_i)} \tag{6}$$

Designed Hopfield network contains 729 neurons as described above. These neurons are connected in such a way that constraints are not violated. The network also contains an input Θ, which has a certain value for the neurons which were already supposed on by the given puzzle. Last part of the network is biases. These can also be added to the neurons if it is desirable. A simple Hopfield network is shown in figure 1.

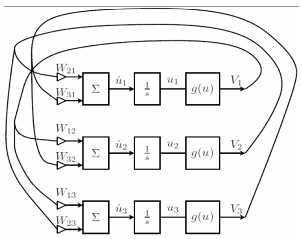

Fig.1. Architecture of a Hopfield network

This Hopfield network consists of 3 neuron models which are connected to the other neurons and not connected to themselves. The differential equation of given neuron model can be described by:

$$w_i = \frac{du_i}{dt} = \sum_{j=1}^{n} W_{ij} V_j + \Theta_i,\ i = 1, 2, 3 \tag{7}$$

with W the interconnection matrix and Θ the input vector. A fixed Hopfield network with no self-connections, $W_{ii} = 0$, and symmetric weights, $W_{ij} = W_{ji}$, has the Lyapunov function:

$$E = -\frac{1}{2} \sum_{i,j} W_{ij} V_i V_j - \sum_i \Theta_i V_i \tag{8}$$

With help of the gradient an expression for du/dt can be given as function of the Lyapunov function $E(t)$:

$$\frac{du_i}{dt} = -\frac{\partial E}{\partial V_i} \tag{9}$$

The Lyapunov function can be used as a cost function which has to be minimized. By rewriting the Sudoku problem in neural form to a Lyapunov function, the initial weights of the Hopfield network are obtained. The chosen Lyapunov function in equation (10) is used to maximize the number of neurons which fire, given the constraints of the Sudoku puzzle.

$$E = -\sum_{i,j,k} V(i,j,k) + \alpha \sum_{i,j,k,i',j',k'} V(i,j,k).V(i',j',k') \tag{10}$$

By combining (9) and (10), the following equation for weighting filters can be obtained

$$w_i = I + \alpha.V_i(i',j',k') \tag{11}$$

Now the weighting filters are determined for the constraints, only the first part of formula (10) has to be implemented in a weighting filter. As can be seen from (11) the weighting consists of only bias terms. So a weighting filter of size [729×1] has to be created with all constant positive bias terms. When the neural network is implemented an optimization for best performance has to be made for values of α, bias weighting and input weighting with respect to the logsig function. If the performance of this network is not sufficient, then a coprocessor can be used to improve performance.

1.2. Coprocessor. Proposed coprocessor is used to give a probability that a certain number can be placed at a certain location. With help of this information the Hopfield network can be initialized to find the right solution. If the Hopfield network still fails, it is possible to use the coprocessor again, to find new initial inputs for the Hopfield network. The coprocessor tries to solve Sudoku puzzles as linear programming problem. A simple example on linear programming with inequality constraints is given by equation (12).

$$\begin{gathered} \max f(x) = 3x_1 + x_2 + 2x_3 \quad s.t. \\ r_1(\mathbf{x}) = 3x_1 - 2x_2 + 4x_3 - 8 \geq 0;\ r_2(\mathbf{x}) = -x_1 - 2x_2 - x_3 + 9 \geq 0; \\ r_3(\mathbf{x}) = -2x_1 - 2x_2 - x_3 + 9 \geq 0;\ x_1 \geq 0;\ x_2 \geq 0;\ x_3 \geq 0 \end{gathered} \tag{12}$$

The neural network used to find the answer to this problem is a recurrent network with two layers. A first layer neuron consists of a bias, N multipliers and a *poslin*-function, for which holds:

$$S_m = poslin(r_m) = \begin{cases} r_m & \text{for } r_m > 0 \\ 0 & \text{for } r_m \leq 0 \end{cases}$$

A second layer neuron consists of a bias, M multipliers, an integrator and also a poslin-function. The differential equation for the integrator is given by:

$$\frac{dx_j}{dt} = \mu_j \left(b_j - \sum_{m=1}^{M} S_m a_{mj} \right) \tag{13}$$

where μ a growing rate, b_j the bias, S_m the output of a first layer poslin-function and a_{mj} the weighting for the j-th variable and the m-th constraint. For the given

example the differential equations become:

$$\frac{dx_1}{dt} = \mu\,(3 - k(3S_1 - S_2 - 2S_3))\,;\ \frac{dx_2}{dt} = \mu\,(1 - k(-2S_1 - 2S_2 - S_3))\,;$$
$$\frac{dx_3}{dt} = \mu\,(2 - k(4S_1 - S_2))\,;$$

with k the amount of penalty for constraint violations. An alternative with the same architecture is obtained by replacing the poslin-function with a threshold-function. The output of this function can be written as:

$$S_m = threshold(x_m) = \begin{cases} 0 & \text{for } x_m \leq 0 \\ 1 & \text{for } x_m > 0 \end{cases} \tag{14}$$

Advantage of this approach is that the value of k is not needed to be very large. A drawback of this method is that the output in simulation becomes very nervous if the value for μ is too large. Previous section showed how a linear programming problem can be solved using a neural network. This neural network can also be developed for Sudoku puzzles if in the constraints, given by equations (2) to (5), the equal sign '=' is replaced by a '$\leq$'-sign and an optimization function like $maxf(x) = \sum x(l)$ is chosen, where $x(l)$ is the probability that neuron $V(l)$ has to fire. With this approach of solving Sudoku puzzles, the network consists of 729 V neurons which represent the probability of placing a certain integer at a certain position and 324 constraint neurons which give a positive value if representing constraint is violated. Every constraint neuron sums over 9 V neurons, in such a way that every constraint neuron represents one constraint. For the constraint neurons a weighting matrix R can be constructed which contains all a_{mj} elements from the differential equation as shown in (13). This weighting matrix can be used to check whether a constraint is violated. Then the differential equation for the coprocessor becomes

$$\frac{dx_j}{dt} = \mu\,(b - k.R(j,:).S)$$

Above suggested neural network can be used as coprocessor for the Hopfield network. Several choices have to be made to let the Hopfield network and the coprocessor work together.

References

[1] http://www.maa.org/editorial/mathgames/mathgames 09 05 05.html.

[2] http://arxiv.org/vc/q-bio/papaers/0609/0609006.pdf.

[3] D. W. Tank and J.J. Hopfield. Simple optimization networks: an a/d converter and a linear programming circuit. IEEE Circuits and Systems, (CAS-33):533541, 1986.

Modified Product Cubature Formulae

Geno Nikolov, Vesselin Gushev

In the univariate case, there is a well-developed theory on the error estimation of the quadrature formulae for integrands from the Sobolev classes of functions. It is based on the Peano kernel representation of linear functionals, which yields sharp error bounds for the quadrature remainder. Namely, if a quadrature formula Q,

$$Q[g] = \sum_{\nu=1}^{n} a_\nu f(x_\nu),\ a \le x_1 < \cdots < x_n \le b,$$

designed to approximate the definite integral

$$\ell[g] := \int_a^b g(x)\,dx,$$

is exact for all the algebraic polynomials of degree not exceeding r, then for its remainder $R[Q;g] := \ell[g] - Q[g]$ one has the sharp estimate

$$|R[Q[g]| \le c_{r,p}(Q).\|g^{(r)}\|_{L_p[a,b]},$$

provided that $g^{(r)}$ belongs to $L_p[a,b]$ $(1 \le p \le \infty)$. Here, the constant $c_{r,p}(Q)$ is the $L_q[a,b]$-norm $(p^{-1}+q^{-1}=1)$ of $K_r(Q;t)$, the r-th Peano kernel of Q. Another useful property of quadratures is the definiteness. If Q is positive or negative definite of order r (which is the case exactly when $K_r(Q;t) \ge 0$ or $K_r(Q;t) \le 0$ on (a,b)), then $Q[g]$ furnishes one-sided approximation to $\ell[g]$ whenever $g^{(r)}$ does not change its sign in (a,b).

When we consider the problem of calculation of a double integral over the rectangular region $\Delta = \{(x,y) \in \mathbb{R}^2 : a \le x \le b,\ c \le y \le d\}$,

$$I[f] := \iint_\Delta f(x,y)\,dxdy,$$

a natural way for approximation of $I[f]$ is by a product cubature formula $C[f]$,

$$C[f] = C(Q_1,Q_2)[f] := \sum_{i=1}^{n_1}\sum_{j=1}^{n_2} c_i d_j f(t_i,\tau_j), \tag{1}$$

where $Q_1[g] = \sum_{i=1}^{n_1} c_i g(t_i)$ and $Q_2[g] = \sum_{j=1}^{n_2} d_j g(\tau_j)$ are quadrature formulae approximating $\ell_1[g] := \int_a^b g(x)\,dx$ and $\ell_2[g] := \int_c^d g(x)\,dx$, respectively.

Some natural questions arise about the magnitude of the error

$$E[C;f] := I[f] - C[f].$$

How small is $|E[C;f]|$? Is it possible, as in the univariate case, to estimate $|E[C;f]|$ by a certain norm of a single derivative of the integrand, say, of $D^{r,s}f := \dfrac{\partial^{r+s}f}{\partial x^r \partial y^s}$?
Can we build definite cubature formulae of order (r,s) ?
The answer of the second question is in the negative. Indeed, an estimate of the form $|E[C;f]| \leq c_{r,s}(C)\|D^{r,s}f\|$ would mean that the cubature formula C is exact for all functions from $B^{r,s}(\Delta)$. Here, $B^{r,s}(\Delta)$ is the class of blending functions

$$B^{r,s}(\Delta) := \{f \in C^{r,s}(\Delta) : \ D^{r,s}f = 0\},$$

where

$$C^{r,s}(\Delta) := \{f : \Delta \to \mathbb{R} : D^{i,j}f \ \text{ continuous }, \ 0 \leq i \leq r, \ 0 \leq j \leq s\}.$$

Hence, while in the univariate case we deal with *algebraic degree of precision*, in the bivariate case we have to deal with the notion of *blending degree of precision*. And, in contrast to the univariate case, the linear space of blending functions $B^{r,s}(\Delta)$ is of infinite dimension. Therefore, no cubature formula exists, which uses only finite number of point evaluations and is exact for all $f \in B^{r,s}(\Delta)$.
We show that error estimation of the above mentioned type is still possible, if we allow our cubature formulae to involve, in addition to the standard data of point evaluations, some line integrals. For the construction of our cubature formulae we need some facts about *blending interpolation*.
Given two sets $\mathbf{X} = \{x_1, x_2, \ldots, x_m\}$ and $\mathbf{Y} = \{y_1, y_2, \ldots, y_n\}$, such that $a \leq x_1 < x_2 < \cdots < x_m \leq b$ and $c \leq y_1 < y_2 < \cdots < y_n \leq d$, we define a *blending grid* $G = G(\mathbf{X}, \mathbf{Y})$ by

$$G(\mathbf{X}, \mathbf{Y}) := \{(x,y) \in \Delta : \ \prod_{\mu=1}^{m}(x - x_\mu) \prod_{\nu=1}^{n}(y - y_\nu) = 0\}.$$

For any bivariate function f defined on Δ there exists a unique *Lagrange blending interpolant* $Bf = B_G f \in B^{m,n}(\Delta)$, which satisfies $Bf_{|G(X,Y)} = f_{|G(X,Y)}$. It is given explicitly by

$$Bf = \mathcal{L}_x f + \mathcal{L}_y f - \mathcal{L}_x \mathcal{L}_y f,$$

where $\mathcal{L}_x$ and $\mathcal{L}_y$ are the Lagrange interpolation operators with respect to variables x and y, defined by the interpolation points $\mathbf{X}$ and $\mathbf{Y}$, respectively. Let $\{l_\mu\}_{\mu=1}^m$ and $\{\bar{l}_\nu\}_{\nu=1}^n$ be the Lagrange fundamental polynomials, defined by $l_\mu(x_j) = \delta_{\mu j}$ $(j = 1, \ldots, m)$ and $\bar{l}_\nu(y_k) = \delta_{\nu k}$ $(k = 1, \ldots, n)$, respectively, with δ_{ij} being the Kronecker symbol. Then

$$Bf(x,y) = \sum_{\mu=1}^{m} l_\mu(x) f(x_\mu, y) + \sum_{\nu=1}^{n} \bar{l}_\nu(y) f(x, y_\nu) - \sum_{\mu=1}^{n}\sum_{\nu=1}^{n} l_\mu(x)\bar{l}_\nu(y) f(x_\mu, y_\nu).$$

The construction of our cubature formulae is realized through the following scheme.

We approximate $I[f - Bf]$ by $C[f - Bf]$, where C is a product cubature formula of the customary type, i.e., which involves only point evaluations of the integrand. This results in a cubature formula $S[f]$ for approximate calculation of $I[f]$,

$$I[f] \approx S[f], \quad S[f] := C[f] + I[Bf] - C[Bf]. \tag{2}$$

We call the cubature formulae S obtained through (2) *modified product cubature formulae* (in short, MPCF). Among the components of S, it is $I[Bf]$ the one that looks differently from the conventional cubature formulae. Indeed, by the explicit form of $Bf(x, y)$ we obtain

$$\begin{aligned} I[Bf] = &\sum_{\mu=1}^{m} b_\mu \ell_2[f(x_\mu, \cdot)] + \sum_{\nu=1}^{n} \overline{b}_\nu \ell_1[f(\cdot, y_\nu)] \\ &- \sum_{\mu=1}^{m} \sum_{\nu=1}^{n} b_\mu \overline{b}_\nu f(x_\mu, y_\nu). \end{aligned} \tag{3}$$

Here, $Q'[g] = \sum_{\mu=1}^{m} b_\mu g(x_\mu)$ is the interpolatory quadrature formula for $\ell_1[g] = \int_a^b g(x)\,dx$, generated by $\mathcal{L}_x$, and $Q''[g] = \sum_{\nu=1}^{n} \overline{b}_\nu g(y_\nu)$ is the interpolatory quadrature formula for $\ell_2[g] = \int_c^d g(y)\,dy$, generated by $\mathcal{L}_y$.

It turns out that the modified product cubature formulae possess all the useful features of the quadrature formulae we mentioned above. In particular, their error can be bounded by the norm of a single partial derivative of the integrand. Not surprisingly, the Peano kernel of a MPCF S is expressed in terms of the Peano kernels of the two pairs of quadrature formulae involved in the construction of S: (Q', Q''), which determines the blending interpolation operator B, and (Q_1, Q_2), which defines the product cubature formula Q. This connection provides some sufficient conditions (criteria) for the definiteness of a MPCF. Also, some classes of integrands are specified, for which a product cubature formula C is inferior to its modified counterpart S.

As it was mentioned above, it is not possible to obtain an error bound for a product cubature formula C in terms of a certain norm of a single partial derivative of the integrand. On using the connection between C and S we show that three partial derivatives of the integrand do the job.

Optimal Order FEM for Coupled Eigenvalue Problems on Overlapping Domains*

Andrey Andreev, Milena Racheva

We present a new finite element approach applied to a nonstandard second order elliptic eigenvalue problem, defined on two overlapping domains. The purpose is to derive optimal order error estimates as distinct from [1], where they are suboptimal. Let Ω_1 and Ω_2 be overlapping rectangles and Ω be two-component rectangular domain, i.e. $\overline{\Omega} = \overline{\Omega}_1 \cup \overline{\Omega}_2$ (see Figure 1). Let also $H^m(\Omega_i)$ be the usual $m-$th order Sobolev space on $\Omega_i,\ i = 1, 2$ with a norm $\|\cdot\|_{m,\Omega_i}$.
Consider the following second-order two-dimensional elliptic operators:

$$L^{(i)} \equiv -\sum_{k,m=1}^{2} \frac{\partial}{\partial x_k}\left(a_{km}^{(i)} \frac{\partial}{\partial x_m}\right) + a_0^{(i)}, \quad i = 1, 2,$$

where $a_{km}^{(i)}(x) > 0$ and $a_0^{(i)}(x) \geq 0$ are bounded functions on $\Omega_i,\ i = 1, 2$.
The eigenvalue problem is defined by: find $(\lambda, u_1, u_2) \in \mathbf{R} \times H^2(\Omega_1) \times H^2(\Omega_2)$ which obey the differential equations

$$L^{(i)} u_i + (-1)^i \chi_{\Omega_1 \cap \Omega_2} K = \lambda u_i \quad \text{in} \ \ \Omega_i,\ i = 1, 2, \tag{1}$$

and the classical Robin/Neumann and Dirichlet boundary conditions

$$\frac{\partial u_i}{\partial \nu} + \sigma^{(i)} u_i = 0 \ \ \text{on} \ \ \Gamma_i', \ \ u_i = 0 \ \ \text{on} \ \ \Gamma_i,\ i = 1, 2, \tag{2}$$

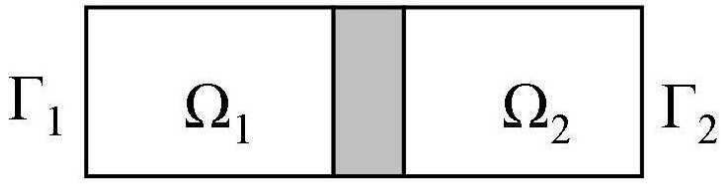

Figure 1: Overlapping rectangular domains

as well as the following nonlocal *coupling condition*

$$\int_{\Omega_1 \cap \Omega_2} [u_1(x) - u_2(x)]\, dx = 0, \tag{3}$$

*This work is supported by the Bulgarian Ministry of Science under grant VU-MI 202/2006.

where $\sigma^{(i)} \geq 0$, $\chi_{\Omega_1 \cap \Omega_2}$ denotes the characteristic function of $\Omega_1 \cap \Omega_2$ and $\Gamma_i' = \partial\Omega_i \backslash \Gamma_i$. We introduce the spaces $V_i = \left\{ v_i \in H^1(\Omega_i) : \ v_i = 0 \ \text{ on } \ \Gamma_i \right\}$, $i = 1, 2$, $\widetilde{V} = V_1 \times V_2$ and thus the closed subspace of $\widetilde{V}$ which incorporates the condition (3) is:

$$V = \left\{ v \in \widetilde{V} : \ \int_{\Omega_1 \cap \Omega_2} [v_1(x) - v_2(x)] \, dx = 0 \right\}.$$

Consider the variational eigenvalue problem:find $(\lambda, u) \in \mathbf{R} \times V$ such that

$$a(u, v) = \lambda(u, v), \quad \forall v \in V, \tag{4}$$

$$a(u, v) = \sum_{i=1}^{2} \left[\int_{\Omega_i} \left(\sum_{k,m=1}^{2} a_{km}^{(i)} \frac{\partial u_i}{\partial x_k} \frac{\partial v_i}{\partial x_m} + a_0^{(i)} u_i v_i \right) dx + \int_{\Gamma_i'} \sigma^{(i)} u_i v_i \, ds \right].$$

According to the properties of coefficient functions, it is easy to see that $a(\cdot, \cdot)$ is bounded, symmetric and strongly coersive on $V \times V$ and V is a closed subspace of $H^1(\Omega_1) \times H^1(\Omega_2)$.
Thus, the problem (4) could be refer to the theory of abstract elliptic eigenvalue problems in Hilbert space [2] and the following result (see [1], Theorem 6) is valid:

Theorem 1 *The problems (1) – (3) and (4) are formally equivalent. Both problems have a countable infinite set of eigenvalues λ_l, all being strictly positive and having finite multiplicity, without a finite accumulation point. The corresponding eigenfunctions u_l can be chosen to be a Hilbert basis of V, orthonormal with respect to $(\cdot, \cdot)$.*

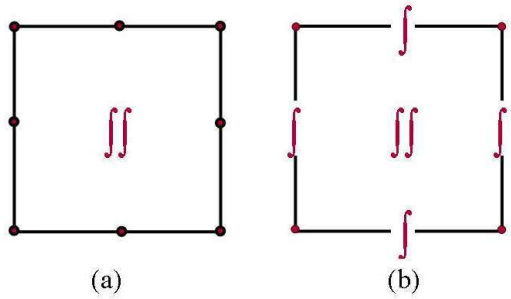

Figure 2: (a) - integral value on T; (b) - vertex-edge conditions.

Let $\tau_{h_i}^{(i)}$ be families of regular finite element partitions of Ω_i, $i = 1, 2$, which fulfill standard assumptions. Herein h_i, $i = 1, 2$ are mesh parameters. The partitions $\tau_{h_i}^{(i)}$ consist of rectangles $T_j^{(i)}$.

We introduce the FE spaces related to the partitions $\tau_{h_i}^{(i)}$: for $i = 1, 2$

$$X_{h_i}^{(i)} = \left\{ v_i \in C(\overline{\Omega}_i) : \ v_{i|_{T^{(i)}}} \in Q_2(T^{(i)}) \ \forall T^{(i)} \in \tau_{h_i}^{(i)} \right\}, \ X_h = X_{h_1}^{(1)} \times X_{h_2}^{(2)},$$

$$X_{h,0} = \left\{ v = (v_1, v_2) \in X_h : \ v_{i|_{\Gamma_i}} = 0, \ i = 1, 2 \right\},$$

Then, the FE space related to the nonlocal boundary condition (3) is:

$$V_h = \left\{ v \in X_{h,0} : \ \int_{\Omega_1 \cap \Omega_2} [v_1(x) - v_2(x)] \, dx = 0 \right\}, \quad V_h \subset V.$$

In order to derive optimal error estimates we introduce suitable modified degrees of freedom and corresponding interpolation operator (cf. [4]). Let the vertices and edges of any element T be noted by M_k and l_k, $k = 1, \ldots, 4$, respectively. For T we choose its degrees of freedom in such a way that every polynomial $p(x) \in Q_2(T)$ is determined by: the values at M_k; the integral value $\int_T p(x, y) \, dx \, dy$; the values at the midpoints of l_k for Case (a) and the integral values $\int_{l_k} p(s) \, ds$ for Case (b), respectively.

According to the degrees of freedom we have chose, we define the interpolation operator $\pi_h : C(\Omega_1) \times C(\Omega_2) \to X_{h,0}$ on the analogy (in a sense) with the usual Lagrange interpolation operator Π_h.

Estimating the difference between both interpolants Π_h and π_h and using the fact, that the order of $\|v - \Pi_h v\|_{m,\Omega}$ is an optimal one, we formulate and prove the following results:

Theorem 2 *Let the function $v = (v_1, v_2)$ belong to $V \cap H^3(\Omega)$, $\overline{\Omega} = \overline{\Omega}_1 \cup \overline{\Omega}_2$. Then there exists a constant $C = C(\Omega) > 0$, independent of h, such that*

$$\|v - \pi_h v\|_{m,\Omega} \leq C h^{3-m} \|v\|_{3,\Omega}, \quad m = 0, 1.$$

Proposition 1 *The finite element space $V_h \subset V$ satisfies the following approximation property:*

$$\inf_{v_h \in V_h} \{\|v - v_h\|_{0,\Omega} + h|v - v_h|_{1,\Omega}\} \leq C h^3 \|v\|_{3,\Omega},$$

$$\|v - \mathcal{R}_h v\|_{1,\Omega} \leq C h^3 \|v\|_{3,\Omega}, \quad \forall v \in V \cap H^3(\Omega),$$

where $\mathcal{R}_h : \ V \to V_h$ is the elliptic projection operator.

Finally, we consider finite element approximation of the eigenvalue problem: find $(\lambda_h, u_h) \in \mathbf{R} \times V_h$ such that

$$a(u_h, v_h) = \lambda_h (u_h, v_h) \quad \forall v_h \in V_h. \tag{5}$$

Using biquadratic finite elements to solve (5), we get optimal order error estimate:

$$\|u - u_h\|_{1,\Omega} \leq C h^2 \|u\|_{3,\Omega},$$

$$|\lambda - \lambda_h| \leq C h^4 \|u\|_{3,\Omega}^2,$$

where $C = C(\Omega)$ is independent of the mesh parameters.

References

[1] De Shepper, H.: Finite element analysis of a coupling eigenvalue problem on overlapping domains. JCAM, **132** (2001) 141–153

[2] Raviart, P.A., Thomas, J.M.: Introduction a l'Analyse Numerique des Equations aux Derivees Partielles. Masson Paris (1983)

[3] Ciarlet, P.G.: The Finite Element Method for Elliptic Problems. North-Holland Amsterdam New York Oxford (1978)

[4] Andreev, A.B., Racheva, M.R.: Optimal Order Finite Element Method for a Coupled Eigenvalue Problem on Overlapping Domains, Proceedings of LSSC'07, to appear as Springer LNCS 4818.

On Chamley's Problem of Optimal Taxation

Mikhail Krastanov, Rossen Rozenov

In an influential article Chamley [1] introduced the problem of optimal taxation in a dynamic general equilibrium framework. He showed that if the utility function is separable in consumption and labour, the optimal tax on capital income is zero in the long run. Frankel [3] considered the case of a general utility function and claimed that the capital income tax may be positive or negative depending on whether the sum of the elasticities of marginal utility with respect to consumption and labour is increasing or decreasing over time (Theorem 1). In the process of derivation of their results both Chamley and Frankel used informal arguments about the sign of the one of the co-state variables.

In this paper we take the Chamley problem to a specific example of utility function and show that the assumption about the sign of the co-state variable for the private assets equation in the government's problem is not true in general. Moreover, following the approach in [3], which is based on necessary conditions only, we demonstrate that the problem of the agent may not have a solution.

The setup in the general case as presented in [3] is as follows. There is one representative consumer which maximizes a utility functional subject to a differential equation describing the dynamics of the private assets. Formally, the consumer solves:

$$I = \int_0^\infty e^{-\rho t} u(c(t), l(t)) dt \to \max \tag{1}$$

$$\dot{a}(t) = r^*(t)a(t) + w^*(t)l(t) - c(t) \tag{2}$$

$$a(0) = a_0 \tag{3}$$

$$\lim_{t\to\infty} e^{-\int_0^t r^*(s)ds} a(t) \geq 0 \tag{4}$$

Here the controls are the consumption c and the labour input (hours of work). The functions $r^*(t)$ and $w^*(t)$ represent the after tax returns on assets and labour, respectively, and the consumer takes these functions as given by the government. Private assets consist of capital k and government bonds b, i.e. $a = k + b$. The instantaneous utility $u(c, l)$ is assumed concave with $u'_c > 0$ and $u'_l < 0$ and ρ is the time preference parameter. Condition (4) is an additional constraint which is typically imposed by economists to ensure that the private assets tend to a non-negative quantity as time goes to infinity. In other words, the agent is not allowed to end up with debt.

The government solves the following problem:

$$I = \int_0^\infty e^{-\rho t} u(c^*(t), l^*(t)) dt \to \max \tag{5}$$

subject to

$$\dot{a}(t) = r(t)a(t) + w(t)l^*(t) - c^*(t) \tag{6}$$

$$\dot{k}(t) = f(k(t), l^*(t)) - c^*(t) - g(t) \tag{7}$$

$$k(0) = k_0 \tag{8}$$

$$a(0) = a_0. \tag{9}$$

The government has control over r and w and takes c^* and l^* as given by the solution of the consumer's problem. Since the two optimization problems are interrelated, we are in a situation of a dynamic game and in order to find the solution we have to adopt an appropriate equilibrium concept. Following the literature, we shall look for a Stackelberg equilibrium [2]. This means that in addition to (6) – (9) we add as an additional constraint the co-state equation for the consumer's problem:

$$\dot{\pi}(t) = \pi(t)(\rho - r^*(t)), \tag{10}$$

Proposition 1. The following assertions hold true:

(i) Let $\xi > 0$ be an arbitrary real number, c^* and l^* be optimal controls, and a^* be the corresponding optimal trajectory for the problem (1)–(4). Then c^* and l^* are optimal controls, and $a^*(t) + e^{\int_0^t r^*(s)ds}\xi$ is the corresponding optimal trajectory for the problem (1)–(4), where the equality (3) is replaced by $a(0) = a_0 + \xi$;

(ii) Let $A > 0$ be an arbitrary real number, c and l be admissible controls, and a be the corresponding trajectory for the problem (1)–(4) such that

$$\lim_{t\to\infty} \left(e^{-\int_0^t r^*(s)ds} a(t) \right) = A > 0. \tag{11}$$

If $\displaystyle\int_0^t r^*(s)ds \geq \rho t$ for each $t > 0$, then the controls c and l, and the trajectory a are not optimal for the problem (1)–(4).

Next, we investigate Chamley's problem for a concrete example. Let the utility function be $u(c, l) = \ln c - \dfrac{l^2}{2}$ and the production function be $f(k, l) = \gamma_1 k + \gamma_2 l$ for some $\gamma_1 > 0$ and $\gamma_2 > 0$. Using the necessary conditions for the consumer's problem we can write the Hamiltonian for the government's problem in terms of the co-state variable π as follows:

$$\begin{aligned} H_2(r, w, a, k, \pi, \lambda, \mu, \xi) = \quad & -\ln \pi - \frac{\pi^2 w^2}{2} + \lambda \left(ar + w^2 \pi - \frac{1}{\pi} \right) \\ & + \mu \left(\gamma_1 k + \gamma_2 w \pi - \frac{1}{\pi} - g \right) + \xi \pi (\rho - r) \end{aligned}$$

¿From the necessary conditions we obtain that $\mu(t) = \pi(t)$ and applying Michel's result [4], which provides a relationship between the Hamiltonian function and the criterion when controls are optimal, we find that

$$w^2\pi_0^2 = \frac{(\rho\pi_0 a_0 - 1)(\rho - 2\gamma_1)}{\rho} \tag{12}$$

Since in order for the integral (1) to be convergent it is necessary that $\rho < 2\gamma_1$, the last expression implies that $\rho\pi_0 a_0 - 1 < 0$. Finally, noting that the value of the Hamiltonian for the agent's problem is equal to the one for the government's problem, we obtain for $t = 0$ that

$$\lambda_0 = \frac{\rho\pi_0^2(\gamma_1(a_0 - k_0) + g_0)}{2\gamma_1(\rho\pi_0 a_0 - 1)}. \tag{13}$$

Thus, the sign of λ_0 will depend on the sign of $\gamma_1(a_0 - k_0) + g_0$. If the government starts with sufficient savings the latter expression could be negative and so λ_0 will be positive in contrast with the assertions of Chamley and Frankel.

References

[1] Chamley, C.: Optimal Taxation of Capital Income in General Equilibrium with Infinite Lives, *Econometrica* **54** (1986), No.3, 607-622.

[2] Dockner, E., Jorgensen, S., Van Long, N., Sorger, G.: Differential Games in Economics and Management Science, Cambridge University Press, 2000.

[3] Frankel, D.: Transitional Dynamics of Optimal Capital Taxation, *Macroeconomic Dynamics* **2** (1998), 492-503.

[4] Michel, Ph.: On the Transversality Condition in Infinite Horizon Optimal Problems, *Econometrica* **50** (1982), Issue 4, 975-986.

Applications of Cellular Neural Networks for Image Processing

Angela Slavova, Victoria Ivanova

One of the most interesting aspects of the world is that it can be considered to be made up of patterns. It is characterized by the order of the elements of which it is made rather than by the intrinsic nature of these elements.

Norbert Wiener

Many phenomena with complex patterns and structures are widely observed in the nature. For instance, how does the leopard get its spots, or how does the zebra get its stripes, or how does the fingerprint get its patterns? These phenomena are some manifestations of a multidisciplinary paradigm called emergence or complexity. They share a common unifying principle of dynamic arrays, namely, interconnections of a sufficiently large number of simple dynamic units can exibit extremely complex and self-organizing behaviors.

The invention, called cellular neural network (CNN), is due to L.Chua and L.Yang in 1988. Many complex computational problems can be formulated as well-defined tasks where the signal values are placed on a regular geometric 2-D or 3-D grid, and the direct interactions between signal values are limited within a finite local neighborhood. CNN is an analog dynamic processor array which reflects just this property: the processing elements interact directly within a finite local neighborhood. The concept of CNN is based on some aspects of neurobiology and adapted to integrated circuits. For example, in the brain, the active medium is provided by a sheet-like array of massively interconnected excitable neurons whose energy comes from the burning of glucose with oxygen.In cellular neural networks the active medium is provided by the local interconnections of active cells, whose building blocks include active nonlinear devices (e.g., CMOS transistors) powered by dc batteries.

Cellular Neural Networks have very impressive and promising applications in image processing and pattern recognition. For such applications CNN functions as a two-dimensional filter. However, unlike the conventional two-dimensional digital filters, our cellular neural network uses parallel processing of the input image space and delivers its output in continuous time. This remarkable feature makes it possible to process a large-size image in real time. Moreover, the nearest neighbourhood interactive property of CNN makes them much more amenable to VLSI implementation.

Chip implementation of Cellular Neural Networks differ by their size and by their degree of functionality. Some have a fixed template, and 256 cells, whereas others are limited to about 30 cells, but are electrically controllable. A programmable chip of 1024 cells is currently implemented. The programmability and the rapidity of the chip makes the CNN attractive, the nonlinearity, as we will see, allows to obtain a nonlinear signal processing, but these advanteges are counterbalanced by the need of a large silicon area per cell and a quite large power consumption.

Stimulating applications of CNNs have in fact been developed into a wide range of disciplines, ranging from classical and sophisticated image filtering, to biological signal processing solution of nonlinear partial differential equations, physical systems and nonlinear phenomena modelling, generation of nonlinear and chaotic dynamics, associative memories, neurophysiology, robotics, etc. Recently new spatio-temporal based processing strategies able to mimic processing in the retina have been constructed. Similarly to a retina, the cellular processor array consists of a large number of identical analog processing elements. Like in the retina, these elements have local (usually nearest neighbour) interconnections, to make the implementation feasible. The interconnection weight pattern in space invariance means that the network has only a few free parameters. The processor can process either grayscale or binary valued images. Based on the structure and funcionality of the processing elements, and the interconnection and weighting, a large number of various cellular network types can be implemented.
Due to the fact that CNNs can constitute analog primitives to represent complex dynamics in space-time a number of mechatronic structures were developed. Their locomation was driven by CNN based circuits, like those able to drive bioinspired walking machines, endowed with a large number of joints.
After the introduction of the CNN paradigm, CNN Technology got a boost when the analogic cellular computer architecture, the CNN Universal Machine has been invented. The most successful chips embedded in a computational infrastucture provided the framework for analogic cellular software development. The industrial applications rely on the available **Aladdin** system, for which more information can be found on the web site:
www.analogic-computers.com.

REFERENCES

[1]Chua L.O., Yang L., Cellular Neural Network: Theory and Applications, IEEE Trans. CAS, vol. 35, pp. 1257-1290, Oct. 1988.
[2] Chua L.O., Hasler M., Moschytz G.S., Neirynsk J., Autonomous cellular neural networks: a unified paradigm for pattern formation and active wave propagation, IEEE Trans. CAS-I, vol. 42, N 10, pp. 559-577, Oct. 1995.
[3] Chua L.O., CNN:A Paradigm for Complexity, World Scientific Series on Nonlinear Science, Series A - Vol. 31, World Scientific, 1998.
[4] Roska T., Chua L.O., Wolf D., Kozek T., Tetzlaff R., Puffer F., Simulating nonlinear waves and partial differential equations via CNN- Part I: Basic techniques, IEEE Trans. CAS-I, vol. 42, N 10, pp. 807-815, Oct. 1995.
[5]Slavova A., Applications of some mathematical methods in the analysis of Cellular Neural Networks, J.Comp.Appl.Math., 114, pp. 387-404, 2000.
[6] Slavova A., Cellular Neural Networks: Dynamics and Modeling, Kluwer Academic Publishers, 2003.

Price Dynamics in a Strategic Model of Trade between Two Regions

Iordan Iordanov, Stoyan Stoyanov, Andrey Vassilev

The present work develops a model of trade between two regions in which, depending on the relation among output, financial resources and transportation costs, the adjustment of prices towards a steady state is studied. We assume that there is one type of traded good and local producers can supply only a fixed amount of this traded good, which cannot be stored for future consumption. As usual, prices change to balance supply and demand. In the chosen setup, the evolution of prices according to an exogenous rule is studied, starting from pre-specified initial conditions. More specifically, whenever there are unsold quantities left, the price is decreased proportionally and when there are local financial resources unspent, the price is increased proportionally. This allows us to abstract away from producer behaviour and focus exclusively on consumers' decisions. The representative consumers in the two regions seek to maximize their per-period utility in a strategic situation arising from the need to compete for scarce resources. We utilize the concept of Nash equilibrium to characterize optimal behaviour in the game theoretic interaction.

We consider the consumption decisions of two economic agents occupying distinct spatial locations, called region I and II, respectively. The consumer in region I (or, shortly, consumer I) exogenously receives money income $Y_1 > 0$ in each period. Similarly, the consumer in region II (consumer II) receives money income $Y_2 > 0$. For each period t, in region i, $i = 1, 2$, a fixed quantity $q_i > 0$ of a certain good is supplied at a price $p_{i,t}$. The consumers place orders for the desired quantities in each region, observing their budget constraints and incurring symmetric transportation costs $\rho > 0$ per unit of shipment from the "foreign" region. Each consumer attempts to maximize their total consumption for the current period. Consumers can be considered myopic in that they do not optimize their consumption over a specified time horizon but their decisions are confined only to the current period.

In cases when total orders for the respective region exceed the quantity available, the following distribution rule is applied: first, the order of the local consumer is executed to the extent possible and then the remaining quantity, if any, is allocated to the consumer from the other region. It is clear then that the choice of orders to be placed has a strategic element to it, since the actual quantity received by the consumer depends on the choices made by the counterpart in the other region. The agents are assumed to have complete knowledge of all the relevant aspects of the situation under discussion.

More formally, for each period t we model the above situation as a static noncooperative game of complete information. Denote by α and β the orders placed by consumer I in region I and II, respectively. In an analogous manner, γ and δ stand for the orders of consumer II in regions I and II, all orders obviously being nonnegative quantities. In period t consumer I's strategy space S_1 is determined by the budget

constraint and the nonnegativity restrictions on the orders:

$$S_1 = \{(\alpha, \beta) \in \mathbb{R}^2 | \alpha p_{1,t} + \beta(p_{2,t} + \rho) \leq Y_1, \quad \alpha,\ \beta \geq 0\}. \tag{1}$$

Consumer II's strategy space in period t is

$$S_2 = \{(\gamma, \delta) \in \mathbb{R}^2 | \gamma(p_{1,t} + \rho) + \delta p_{2,t} \leq Y_2, \quad \gamma,\ \delta \geq 0\}. \tag{2}$$

We adopt the shorthand $p'_{1,t} := p_{1,t} + \rho$ and $p'_{2,t} := p_{2,t} + \rho$. We also omit the subscript t whenever it is evident from the context or irrelevant.
The payoff function for consumer I is given by

$$\begin{aligned} P_1(\alpha, \beta, \gamma, \delta) &= \min(\alpha,\ q_1) + \min(\beta,\ q_2 - \min(\delta,\ q_2)) \equiv \\ &\equiv \min(\alpha,\ q_1) + \min(\beta,\ \max(0,\ q_2 - \delta)) \end{aligned} \tag{3}$$

and that for consumer II by

$$\begin{aligned} P_2(\alpha, \beta, \gamma, \delta) &= \min(\gamma,\ q_1 - \min(\alpha,\ q_1)) + \min(\delta,\ q_2) \equiv \\ &\equiv \min(\delta,\ q_2) + \min(\gamma,\ \max(0,\ q_1 - \alpha)). \end{aligned} \tag{4}$$

Any unspent fraction of the current-period income is assumed to perish and consequently the accumulation of stocks of savings is not allowed in the model. Similarly, the goods available each period cannot be stored for future consumption. Let q_i^{cons} denote the total amount consumed in region i and Y_i^{res} stand for the part of the region i's income not spent in the other region. In other words, $q_1^{cons} := \alpha_0 + \gamma_0$, $q_2^{cons} := \beta_0 + \delta_0$, $Y_{1,t}^{res} := Y_1 - p'_{2,t}\beta_0$ and $Y_{2,t}^{res} := Y_2 - p'_{1,t}\gamma_0$.
There are two mutually exclusive situations leading to an adjustment in prices. First, if the quantity available in the respective region has not been entirely consumed, prices are adjusted downwards. In discrete time this is captured by the equation

$$\frac{p_{i,t} - p_{i,t+1}}{p_{i,t}} = \frac{q_i - q_{i,t}^{cons}}{q_i} \text{ or } p_{i,t+1} q_i = p_{i,t} q_{i,t}^{cons}. \tag{5}$$

Clearly, if $q_i^{cons} = 0$, then $p_{i,t+1} = 0$. Second, if Y_i^{res} is not entirely exhausted in absorbing local supply, which can be expressed in value terms as $p_i q_i$, then the price $p_{i,t}$ is adjusted upwards to $p_{i,t+1}$ to ensure residual income exhaustion:

$$\frac{p_{i,t+1} - p_{i,t}}{p_{i,t}} = \frac{Y_{i,t}^{res} - p_{i,t} q_i}{p_{i,t} q_i} \text{ or } p_{i,t+1} q_i = Y_{i,t}^{res}. \tag{6}$$

The counterparts of the above price adjustment rules are also specified in continuous time. We formally prove the claim that the two situations leading to price adjustment cannot occur simultaneously. As usual, we consider prices in a steady state (price equilibrium) if the rules given by equations (5) and (6) do not lead to a change in prices.
We show that there exists a Nash equilibrium for the basic static game. Moreover, the Nash equilibria for the different parameterizations of the model are computed

explicitly by finding the best-reply correspondences for the two players, forming a system of equations and solving it for the respective Nash equilibrium. Because of the presence of many parameters the analysis decomposes into the study of a number of separate cases. The best-reply correspondences have a fairly complex structure and different cases have to be considered to obtain the Nash equilibria. Economically justifiable supplementary rules are introduced to select Nash equilibria whenever these are not unique and to ensure existence in cases when a price is zero.
The paper provides a complete classification of the various types of Nash equilibria occurring and the corresponding dynamics of prices. The different cases arising in the computation of the Nash equilibria lead to a natural partition of the set of possible incomes into zones, which is useful for analyzing the discrete-time case. The types of Nash equilibria are unique for each zone up to a relationship between prices and transportation costs. As prices change the partition changes, leading to different Nash equilibria. The resulting price dynamics in discrete time can be very different depending on the zone.
For instance, in zone III, defined as

$$\frac{Y_1}{q_1} \geq p_{1,0}, \ \frac{Y_2}{q_2} \geq p_{2,0} \tag{7}$$

there is a unique Nash equilibrium given by $(q_1, 0, 0, q_2)$ and after at most one (upward) price adjustment an equilibrium point with positive prices is reached.
As an example of a more complicated situation, in Zone II-2, defined as

$$\begin{cases} Y_1 < p_{1,0}q_1, \ p_{2,0}q_2 \leq Y_2, \\ q_2 > \frac{1}{p_{2,0}} \left[Y_2 - p'_{1,0} \left(q_1 - \frac{Y_1}{p_{1,0}} \right) \right] \\ \frac{Y_1}{p_{1,0}} + \frac{Y_2}{p'_{1,0}} \geq q_1, \end{cases} \tag{8}$$

we find several types of Nash equilibria. The corresponding price adjustment processes can lead to regular or degenerate (with one price equal to zero) price equilibria. The dynamics of prices in zone II-2 are quite diverse, in some cases with only one adjustment step needed to reach equilibrium, in other cases with an infinite adjustment process under which prices tend to a limit equilibrium point, and in yet others with a finite number of adjustment steps in one regime, after which a switch to a different regime takes place.
Thus, depending on the parameters of the model, the types of price dynamics can range from simple to quite complex. Complex price dynamics are usually obtained when transportation costs are "important" as compared to prices and incomes. In some cases degenerate equilibria with a zero price arise.
In the continuous-time case, the phase space is partitioned in a way analogous to the discrete-time case. The equilibrium points of the price system lie on two hyperbolae and are shown to be only Lyapunov stable. No degenerate equilibria arise for dynamics in continuous time.

On a Local Semirefinement Multigrid Algorithm for Convection-Diffusion Problems

Daniela Vasileva

A multigrid (MG) algorithm with local semirefinement (LSR) is presented for the solution of convection-diffusion problems. The method is based on the discontinuous Galerkin (DG) discretisation, which can conveniently handle grid adaptation. Rectangular finite elements are used and during the process of adaptation they may be refined in the x, y or in both (x and y) directions. The algorithm is presented here for 2D problems, but it can be generalized for 3D. In order to achieve optimal efficiency, the recursive mesh adaptation is combined with a MG solver.

DG discretisation. We consider the linear boundary value problem:

$$-\varepsilon\Delta u + \boldsymbol{\nabla}\cdot(\mathbf{b}u) + cu \;=\; f \;\text{ in }\; \Omega\subset\mathbb{R}^2, \quad u(x,y) \;=\; u_0(x,y) \;\text{ on }\; \Gamma=\partial\Omega, \quad (1)$$

where $\varepsilon > 0$ is a parameter, the coefficients $\mathbf{b}(x,y) = (b_1(x,y), b_2(x,y)) \in (C^1(\Omega))^2$, $c(x,y) \geq 0$, $c(x,y) \in L_\infty(\Omega)$ and the right-hand side $f(x,y) \in L_2(\Omega)$. We assume that Ω allows a regular partitioning $\Omega_h = \{\Omega_e \mid \cup_e \Omega_e = \Omega,\ \Omega_i \cap \Omega_j = \emptyset,\ i \neq j\}$, into equally sized rectangular cells Ω_e. As weak form for (1) we use Baumann-Oden's [1, 2] DG formulation and the space $S_h = \{\sum_e \phi_e,\ \phi_e \in \mathcal{P}_3(\Omega_e),\ \Omega_e \in \Omega_h\}$ of piecevise cubic polynomials on the partitioning Ω_h is used in the discretisation (for more details see [3, 4, 5, 6]). The discretisation yields a linear system $L_h u_h = f_h$, where the matrix L_h has a diagonal block structure with blocks of size 16×16. We order the basic functions *point-wise* (for details see [3, 4, 5]) and the obtained linear system is iterated using the block Jacobi method with underrelaxation ($\omega = 0.5$).

MG algorithm. A detailed description of a "standard" MG approach and the corresponding smoothing analysis in the case of DG methods with constant coefficients may be found in [3, 4, 5]. Here we combine the DG discretisation with a *semicoarsening MG technique* (see [7] and references therein). The Sawtooth MG and full approximation storage (FAS) algorithms [8, 9] are implemented. Sawtooth MG iteration ensures path-independent restrictions (see [7] for details) and FAS provides a way for local refinement (LR). The grid structure consists of the finest grid Ω_{mn} and all coarser (with $k \leq m$ and $l \leq n$) semicoarsened grids Ω_{kl} (see Fig.1). The number of cells on the finest grid is $2^m \times 2^n$, and the total number of cells on all grids is $(2^{m+1}-1) \times (2^{n+1}-1) \approx 4 \times 2^m \times 2^n$, i.e., 3 times more than in the standard MG. A description of one semicoarsening MG iteration for the discrete system $L_{kl}u_{kl} = f_{kl}$ on the grid Ω_{kl} with $level = k + l$ is given below:

1. $r_{kl} = f_{kl} - L_{kl}u_{kl}, \quad \tilde{f}_{kl} = f_{kl};$

2. Repeat
  for all $k+l=level$
    if $k>0$ then $r_{k-1,l}=\bar{R}_{kl}^{k-1,l}r_{kl}$, $u_{k-1,l}=R_{kl}^{k-1,l}u_{kl}$, $\bar{u}_{k-1,l}=u_{k-1,l}$,
      $\tilde{f}_{k-1,l}=L_{k-1,l}\bar{u}_{k-1,l}+r_{k-1,l}$;
    if $l>0$ then $r_{k,l-1}=\bar{R}_{kl}^{k,l-1}r_{kl}$, $u_{k,l-1}=R_{kl}^{k,l-1}u_{kl}$, $\bar{u}_{k,l-1}=u_{k,l-1}$,
      $\tilde{f}_{k,l-1}=L_{k,l-1}\bar{u}_{k,l-1}+r_{k,l-1}$;
  $level--$;
  until $level=0$;
3. Solve $L_{00}u_{00}=\tilde{f}_{00}$; $c_{00}=u_{00}-\bar{u}_{00}$;
4. Repeat
  $level++$;
  for all $k+l=level$
    if $k>0$ then $c_{kl}=P_{kl}^{k-1,l}c_{k-1,l}$;
      else $c_{kl}=0$;
    if $l>0$ then $c_{kl}+=P_{kl}^{k,l-1}c_{k,l-1}$;
    if $k,l>0$ then $c_{kl}-=P_{kl}^{k-1,l-1}c_{k-1,l-1}$;
    $u_{kl}+=c_{kl}$;
    Perform ν relaxations on $L_{kl}u_{kl}=\tilde{f}_{kl}$;
    $c_{kl}=u_{kl}-\bar{u}_{kl}$;
  until $level=m+n$;

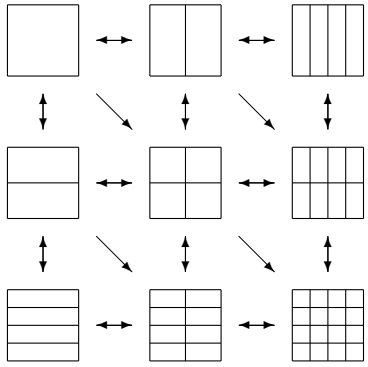

Figure 1: Grid structure

Restrictions and prolongations are defined according to [3, 4, 5]: Let S_{kl} be the space of piecewise cubic polynomials on Ω_{kl}. Then the natural prolongation $P_{k+1,l}^{kl}: S_{kl}\to S_{k+1,l}$ on $\Omega_{k+1,l}$ preserves the coarse grid functions on the fine grid. The restriction operator *for the residues*, $\bar{R}_{k+1,l}^{kl}: S_{k+1,l}\to S_{kl}$ is the adjoint of $P_{k+1,l}^{kl}$ and the Galerkin relation exists between the discretisation on the coarse and fine grid $L_{kl}=\bar{R}_{k+1,l}^{kl}\ L_{k+1,l}\ P_{k+1,l}^{kl}$. Another restriction $R_{k+1,l}^{kl}$ is used *for the solution*, which preserves the function values and the derivatives at the coarse cell vertices. It is a left-inverse of the prolongation, i.e., $R_{k+1,l}^{kl}\ P_{k+1,l}^{kl}=I_{kl}$.

The LSR-MG algorithm is a generalization of a LR-MG algorithm [10, 11, 12]. On the first stage the equation is discretised and solved on the global coarsest grid Ω_{00}. In later stages, some unrefined cells on existing grids are selected for x, y or xy-refinement and divided into smaller cells. The solution in the new cells is interpolated from the previous grids and several relaxation sweeps (MG Sawtooth cycles) are performed. The restrictions are performed where both children cells really exist. Outside the refined region on $\Omega_{k+1,l}$ we may define a *virtual solution* $u_{k+1,l}=P_{k+1,l}^{kl}\ u_{kl}$, and as $r_{kl}=\bar{R}_{k+1,l}^{kl}\left(f_{k+1,l}-L_{k+1,l}\ P_{k+1,l}^{kl}\ u_{kl}\right)=\bar{R}_{k+1,l}^{kl}\ f_{k+1,l}-L_{kl}\ u_{kl}$, then $\tilde{f}_{kl}=L_{kl}\ u_{kl}+r_{kl}=\bar{R}_{k+1,l}^{kl}\ f_{k+1,l}\approx f_{kl}$, i.e., the right-hand side $\tilde{f}_{kl}$ on the coarser grid Ω_{kl} may be defined as in the standard LR-MG algorithm.

The internal boundaries. A cell on $\Omega_{k+1,l}$ may have no neighbours on the same grid at some of its faces, although these faces are not on the boundary $\partial\Omega$. Thus for the discretisation on $\Omega_{k+1,l}$ *auxiliary cells* are used at the internal boundaries.

The solution values are derived by interpolation from coarser grids. But, unlike the standard LR-MG, some coarse cells, used in this interpolation, may have children on another finer grid, i.e., the solution there may be further improved.
An example of a locally semirefined grid and the corresponding grid structure for MG semicoarsening is given in Fig.2. The finest cells are marked with "•", the *fathers*, used in MG sweeps, are marked with "o", and the auxiliary cells are marked with "+".

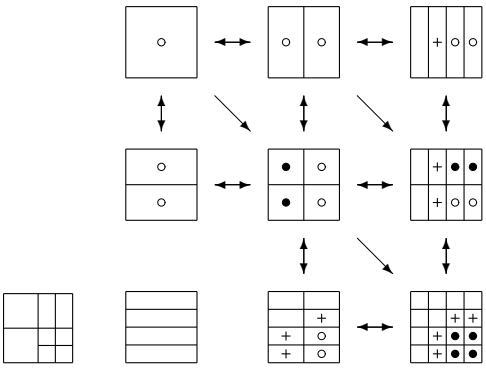

Figure 2: A semirefined grid and the LSR-MG structure

Examples. In the examples $\Omega = [0,1]^2$ and the initial grid has 1 cell. 7 stages of x, y or xy LSR are done. In each stage 10 MG sweeps with 2 post-smoothing iterations are performed.

Example 1. We consider the 2D equation $\varepsilon\Delta u+(x-0.5)u_x+(y-0.5)u_y = 0$, $\varepsilon = 0.0002$, with Dirichlet boundary conditions, corresponding to an exact 1D solution $u(x,y) = \mathrm{erf}((x-0.5)/\sqrt{2\varepsilon})$. The solution and the finest grids in the cases of standard LR and of LSR are plotted in Fig.3. The C-norm of the error is one and the same in both cases, but the number of cells N on the finest grid and the number NN of all cells in the MG structure is much less for the LSR-MG case.

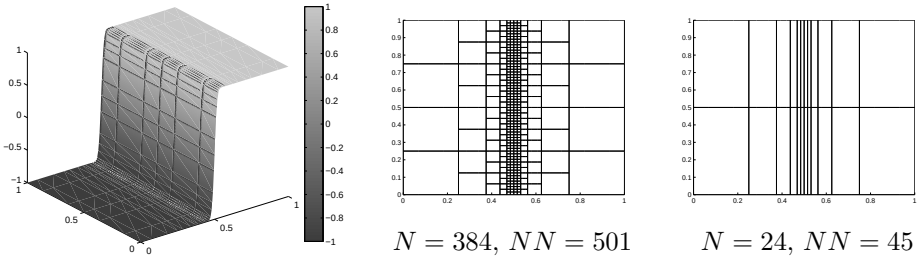

$N = 384$, $NN = 501$ $\qquad$ $N = 24$, $NN = 45$

Figure 3: The solution, standard LR and LSR for Example 1

Example 2. The following problem is considered $\varepsilon\Delta u - xu_x - yu_y - 2u = f(x,y)$, $\varepsilon = 0.01$, where $f(x,y)$ and the Dirichlet boundary conditions correspond to the exact solution $u(x,y) = -xy(1-\exp((x-1)/\varepsilon)(1-\exp((y-1)/\varepsilon)$. The solution and the finest grids in the cases of LR and LSR are plotted in Fig.4. The C-norm of the error is one and the same in both cases, the computing resources (memory and CPU time) are less in the LSR-MG case. Also, the solution converges faster (i.e., less MG sweeps may be performed) and some computations (especially restrictions and prolongations) are cheaper for LSR-MG.

Conclusions. LSR-MG may be successfully used for resolution of boundary and interior layers. The comparison with standard LR-MG shows that significantly less

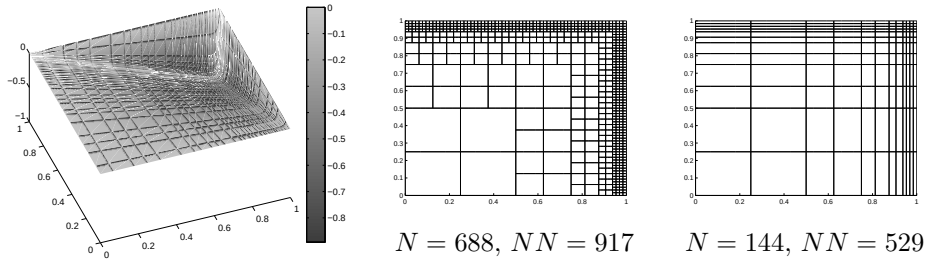

Figure 4: The solution, LR and LSR for Example 2

resources may be used for layers, (almost) parallel to the x or y axis. But in the "worst" cases (layers diagonal to the axes) approximately three times more computations may be performed.

Notes about a possible adaptation criterion. We plan to use an adaptation criterion, based on the comparison of the discrete solution on the finest grid and its restrictions to the next (in the x and y directions) grids (details for LR-MG may be found in [6]). In the LSR-MG case, the grid adaptation may be performed as:
1. All cells of Ω_{00} are refined in the x and y direction at least once;
2. Let $\Omega_e \in \Omega_{kl},\ k+l > 1,$ be an unrefined cell and $F^x(\Omega_e)$ and $F^y(\Omega_e)$ be its x and y fathers. Let $r^x_{kl} := \|u_{kl} - R^{k-1,l}_{kl}\, u_{kl}\|_{C(F^x(\Omega_e))},\ r^y_{kl} := \|u_{kl} - R^{k,l-1}_{kl}\, u_{kl}\|_{C(F^y(\Omega_e))},$ $Q = q(1+q)/(1-q)^2,$ where q depends on the local regularity of the solution (for details see [6]), and tol be a desired tolerance. If $q \geq 1$ the cell is always refined in both directions. Otherwise if $r^x_{kl}\ Q > tol$, the cell is refined in the x direction. Correspondingly, if $r^y_{kl}\ Q > tol$, the cell is refined in the y direction.

Acknowledgments. D. Vasileva thanks Prof. P.W. Hemker (CWI) for proposing the idea for LSR development and for the many fruitful discussions about MG for DG.

References

[1] Baumann, C.E., Oden, J.T.: Comput. Meth. Appl. Mech. Engrg., **175** (1999)
[2] Baumann, C.E.: PhD thesis, University of Texas at Austin (1997)
[3] Hemker, P.W., Hoffmann, W., van Raalte, M.H.: SIAM J. Sci. Comp., **25** (2004)
[4] Hemker, P.W., van Raalte, M.H.: Comp. Vis. Sci., **7** (2004)
[5] Van Raalte, M.H., Hemker, P.W.: Num. Lin. Alg. Appl., **12** (2005)
[6] Vasileva, D., Kuut, A., Hemker, P.W.: Lect. Notes Comp. Sci., **3743** (2006)
[7] De Zeeuw, P.M.: Appl. Numer. Math., **19** (1996)
[8] Hackbusch, W.: Multi-Grid Methods and Applications. Springer, Berlin (1985)
[9] Wesseling, P.: An Introduction to Multigrid Methods. Wiley, New York (1991)
[10] Brandt, A.: Math. Comp., **31** (1977)
[11] Hemker, P.W.: BIT, **20** (1980)
[12] McCormick, S.F.: Multilevel Adaptive Methods for Partial Differential Equations. SIAM, Philadelphia (1989)

On the Numerical Integration of Systems with Deterministic Uncertainties*

Vladimir M. Veliov

The framework of deterministic (set-membership) uncertainties is a complementary tool to the stochastic one, which is useful when no reliable statistical information for the uncertainties is available, while reasonable bounds for the magnitude of the uncertainties are known. In the latter case the deterministic approach has the advantage to give guaranteed results, although some times rather conservative.
A basic tool for deterministic modeling of uncertain processes is the Aumann integral of a set-valued mapping $F : [0, T] \Rightarrow \mathbf{R}^n$:

$$\int_0^T F(t)\,\mathrm{d}t = \left\{ \int_0^T f(t)\,\mathrm{d}t : \ f \in L_1(0,T),\ f(t) \in F(t) \right\}.$$

The approximation of such integrals by quadrature formulae is an issue to which a lot of investigations are devoted, and which is troubled by the following facts (excluding "non-generic cases"): (i) no reasonable Tailor expansions for set-valued maps exist; (ii) the usual way of estimating the global error of linear quadrature formulae with step h by summing the local errors does not give a better error estimate than $O(h)$, no matter what quadrature formula is used and how "nice" is the set valued map.
The author has established in a series of papers the so-called "non-accumulation effect", which in the case of an Aumann integral can be formulated as follows: for linear composite quadrature formulae with step h, that are exact for linear functions, the global error estimate is of order $O(h^2)$ under rather general conditions for F, although the local error at every integration step may also be of order $O(h^2)$. That is, the local errors do not "accumulate".
Extensions of the non-accumulation effect to more general cases include the so-called affine multi-systems (affine control systems, or systems with affine uncertainties):

$$\dot{x} = f_0(x) + G(x)u(t), \quad x(0) = x_0, \qquad x(t) \in \mathbf{R}^n, \quad u(t) \in U \subset \mathbf{R}^r,$$

where U is a convex and compact set. The reachable set of this multi-system, $R(T)$, is defined as the set of all points in $\mathbf{R}^n$ which are reached by a trajectory of the above equation corresponding to some measurable function u with values in U.
Let us consider a single-step discretization scheme with a step length $h = T/N$ for the above equation, where u is assumed to have the constant value $u_k \in U$ in the k-th interval of discretization $[t_k, t_{k+1}]$:

$$x_{k+1} = \mathcal{F}_h(x_k, u_k), \quad k = 0, \ldots N-1.$$

Similarly as above one can define the reachable set $R_N(T) = \{x_N\}$ for the last discrete time inclusion, letting u_k take all possible values in U.

*This research was supported by the Austrian Science Foundation (FWF) under grant P18161.

Under natural differentiability and growth conditions for f_0 and $G = [g_1 \dots g_r]$, and under the more restrictive condition that $[g_i, g_j] := \frac{\partial g_i}{\partial x} g_j - \frac{\partial g_j}{\partial x} g_i = 0, \quad i, j = 1, \dots, r$, the theorem (roughly) formulated below holds.

Theorem 3 *(Veliov, 1997) Assume that the discretization scheme has a third order local error when applied to equations with sufficiently smooth right-hand sides. Then there exists a constant C such that for every differentiable function $l : \mathbf{R}^n \mapsto \mathbf{R}$ with locally bounded (by M_l) and Lipschitz continuous (with a constant L_l) derivative it holds that*

$$\left| \inf_{x \in R(T)} l(x) - \inf_{x_N \in R_N(T)} l(x_N) \right| \leq C(M_l + L_l)h^2.$$

This theorem also exhibits the non-accumulation effect, since one can see in trivial examples that the local error of the discretization scheme applied to the underlying set-dynamics $X_{k+1} = \mathcal{F}_h(X_k, U), \quad k = 0, \dots N-1$, is of order $O(h^2)$ – the same as the global one, expressed in the terms of all functionals l satisfying the assumptions of the theorem.

A number of applications of the non-accumulation effect are known, most of them for numerical approximations of control systems, but also some qualitative ones. Below we present some ongoing work on time-discretization of *switched systems*, which are in the focus of many recent investigations due to their applications in control of electric circuits and other technical systems with various modes of operation, but also in economics.

The simplest nontrivial problem that arises for switched systems in the context of reachability is formulated below.

Let two $n \times n$ matrices A_1, A_2 be given, and let the following dynamics be considered:

$$\dot{x} = A_1 x, \quad \text{or} \quad \dot{x} = A_2 x, \qquad x(0) = x_0.$$

A trajectory, $x(t)$, is an absolutely continuous function satisfying for a.e t either the first or the second linear differential equation. The reachable set by $k-1$ switches is

$$R(T; k) = \{e^{A_{i_k} \tau_k} \dots e^{A_{i_2} \tau_2} e^{A_{i_1} \tau_1} x^0 : \ \tau_s > 0, \ \sum_{s=1}^{k} \tau_s = T\},$$

and the (limit) reachable set is

$$R(T) = \text{cl} \cup_k R(T; k).$$

In 2007 Margaliot showed by an example with matrices A_1 and A_2 of dimension 4 and order of nilpotency equal to 3 that $R(T; k) \neq R(T)$ for every k (contrary to a conjecture formulated by Gurvits in 1995). Thus no finite number of switchings is enough to cover the whole reachable set. This fact implies the following problem for practical implementation of the considered switched system.

Let a time-step $h = T/N$ be given, let the reachable set $R^h(T)$ be defined similarly as $R(T; N)$, but with switches allowed only at moments $t_i = ih$, $i = 1, \dots, N-1$.

If the claim that $R(T;k) = R(T)$ were true for a finite k, than it would have been easy to prove the following estimation for the Hausdorff distance between $R(T)$ and $R^h(T) \subset R(T)$:

$$H(R^h(T), R(T)) \leq Ckh.$$

However, this is not the case as the example of Margaliot has shown. In general, one can prove using a result of Gramel (2003) that

$$H(R^h(T), R(T)) \leq C\sqrt{h}$$

where C depends only on $\|A_i\|$.

Conjecture 1: For every two matrices A_1 and A_2 it holds that

$$H(R^h(T), R(T)) \leq Ch,$$

where C depends only on A_1 and A_2.
The switching system considered above allows the following control formulation:

$$\dot{x} = (1 - u(t))A_1x + u(t)A_2x, \quad x(0) = x_0, \qquad u(t) \in \{0, 1\}.$$

The reachable set, $R(T)$ of this system is the same as the one defined above. It also coincides with the reachable set of the *relaxed system*

$$\dot{x} = (1 - u(t))A_1x + u(t)A_2x, \quad x(0) = x_0, \qquad u(t) \in [0, 1],$$

where the control function $u(t)$ can take all values in $[0, 1]$, in contrast to the switched system, where $u(t) \in \{0, 1\}$.
Following a Sharon and Margaliot (2007), we consider the reachable set, $\hat{R}(T;k)$, of the relaxed system, generated by using only piece-wise constant $u(t)$ with no more than $k - 1$ jumps. Sharon and Margaliot (2007) showed that $\hat{R}(T;5) = R(T)$ holds for matrices with an order of nilpotency not exceeding 3. If $\hat{R}(T;k) = R(T)$ for some k it is easy to prove that

$$H(\hat{R}^h(T)), \hat{R}(T)) \leq Ckh^2,$$

where C depends only on A_1 and A_2. However, Margaliot (2007) gave an example (using the Fuller phenomenon) with $n = 7$ and order of nilpotency equal to 5, in which $\hat{R}(T;k)) \neq \hat{R}(T)$ for any k.
It is easy to show that in the general case the estimation

$$H(\hat{R}^h(T)), \hat{R}(T)) \leq Ch$$

holds true with C depending only on A_1 and A_2. However, it seems that the approximation is of higher order:
Conjecture 2:

$$H(\hat{R}^h(T), R(T)) \leq Ch^{1.25},$$

where C depends only on $\|A_i\|$.
There is a good reason to believe that the above two conjectures are true, namely, that we have proofs, which however, need to be carefully checked before stating the conjectures as theorems. However, we have no reasons to claim that the latter estimation is exact. The proofs use the results and ideas presented in the first part above. We stress that both "conjectures" present further manifestations of the effect of non-accumulation of errors, since in both cases the summation of the local errors gives lower order estimations than the ones that actually hold.
The error analysis of the above switching system may be of interest for ensuring consistency of the time-discretization steps in cases where the system is incorporated in a more complex structure. However, the main value of these results is delivered by the proofs, which give hints for efficient numerical approximations.

References

[1] G. Gramel (2003). Towards fully discretized differential inclusions. *Set-Valued Analysis*, **11**(1):1-8.

[2] L. Gurvitz (1995). Stability of discrete linear inclusions. *Linear Algebra Appl.*, **231**:47–85.

[3] M. Margaliot (2007). A counterexample to a conjecture of Gurvits on switched systems. *IEEE Trans. Automat. Control*, **52**(6):1123–1126.

[4] Y. Sharon and M. Margaliot (2007). Third-order nilpotency, finite switchings and asymptotic stability. *J. Diff. Eqns.*, **233**:135–150.

[5] V.M. Veliov (1997). On the time-discretization of control systems. *SIAM J. Control Optim.*, **35**(5):1470–1486.

Formulation, Analysis and Numerical Solution of Parabolic Interface Problems on Disjoint Intervals

Boško S. Jovanović, Lubin G. Vulkov, etc.

Interface problems appear in variety of applications. Here we discuss the following initial boundary-value problem (IBVP): find functions $u_1(x,t),\ u_2(x,t)$, that satisfy the parabolic equations, [7]

$$\frac{\partial u_1}{\partial t} - \frac{\partial}{\partial x}\left(p_1(x)\frac{\partial u_1}{\partial x}\right) + q_1(x)u_1 = f_1(x,t),\ \ x \in \Omega_1 \equiv (a,b),\ \ t>0, \tag{1}$$

$$\frac{\partial u_2}{\partial t} - \frac{\partial}{\partial x}\left(p_2(x)\frac{\partial u_2}{\partial x}\right) + q_2(x)u_2 = f_2(x,t),\ \ x \in \Omega_2 \equiv (c,d),\ \ t>0, \tag{2}$$

where $-\infty < a < b < c < d < +\infty$, and the internal boundary (or nonlocal interface jump) conditions

$$p_1(b)\frac{\partial u_1(b,t)}{\partial x} = -\alpha_1 u_1(b,t) + \beta_1 u_2(c,t) + \gamma_1(t), \tag{3}$$

$$-p_2(c)\frac{\partial u_2(c,t)}{\partial x} = -\alpha_2 u_2(c,t) + \beta_2 u_1(b,t) + \gamma_2(t). \tag{4}$$

These two conditions have the form of Dirichlet-Robin (DR) mixed boundary conditions, see [1], [5] and the review of Givoli [3]. DR conditions have been incorporated in a finite element formulation in order to eliminate an infinite domain [3], a singular domain [3], or a substructure [3] from computational domain. Finally, in order to complete the IBVP we pose simplest external boundary conditions and initial conditions

$$u_1(a,t) = 0, \quad u_2(c,t) = 0;\ \ u_1(x,0) = u_{10}(x), \quad u_2(x,0) = u_{20}(x). \tag{5}$$

Throughout the paper we assume that, for $i = 1, 2$, the data satisfy the usual regularity and ellipticity conditions

$$p_i(x),\ q_i(x) \in L_\infty(\Omega_i);\ \ 0 < p_{0i} \le p_i(x),\ \ 0 \le q_i(x)\ \text{ a.e. in }\ \Omega_i,\ \ i = 1,2. \tag{6}$$

Consider the product space $L = L_2(\Omega_1) \times L_2(\Omega_2)$, endowed with the inner product and associated norm

$$(u,v)_L = \beta_2(u_1,v_1)_{L_2(\Omega_1)} + \beta_1(u_2,v_2)_{L_2(\Omega_2)}, \quad \|v\|_L = (v,v)_L^{1/2},$$

We also introduce the product space endowed with the inner product

$$\begin{aligned}(u,v)_{H^1} \quad &= \beta_2\left[(u_1,v_1)_{L_2(\Omega_1)} + \left(\tfrac{du_1}{dx},\tfrac{dv_1}{dx}\right)_{L_2(\Omega_1)}\right] \\ &+\beta_1\left[(u_2,v_2)_{L_2(\Omega_2)} + \left(\tfrac{du_2}{dx},\tfrac{dv_2}{dx}\right)_{L_2(\Omega_2)}\right]\end{aligned}$$

and associated norm. We also use the energy inner product and norm

$$[u,v]=\beta_2[u_1,v_1]_1+\beta_1[u_2,v_2]_2,\quad [u_i,v_i]_i=\int_{\Omega_i}\Big(p_i\,\frac{du_i}{dx}\,\frac{dv_i}{dx}+q_iu_iv_i\Big)\,dx,\quad i=1,2.,$$

Let us introduce the cylinders $Q_{iT}=\{(x,t)|\in\Omega_i,0<t<T\}$, $i=1,2$ and the bilinear form

$$A(v,w)\equiv[v,w]\beta_2\alpha_1v_1(b)w_1(b)+\beta_1\alpha_2v_2(c)w_2(c)-\beta_1\beta_2\big[v_1(b)w_2(c)+v_2(c)w_1(b)\big].$$

Theorem 1 *Assume $f=(f_1,f_2)\in L_2(0,T;L)$, $u_0=(u_{10},u_{20})\in L$ and that assume that*

$$\alpha_i>0,\quad \beta_i>0,\quad i=1,2\ \ and\ \ \beta_1\beta_2\le\alpha_1\alpha_2. \tag{7}$$

Then the IBVp has a unique solution $u=(u_1,u_2)\in H^{1,0}\equiv L_2(0,T;H^1)$ which satisfies the following weak formulation:

$$-\beta_2\int_{Q_{1T}}u_1\frac{\partial v_1}{\partial t}dxdt-\beta_1\int_{Q_{2T}}u_2\frac{\partial v_2}{\partial t}dxdt+\int_0^T A(u(\cdot,t),v(\cdot,t))dt$$

$$=\beta_2\int_{\Omega_1}u_{10}(x)v_1(x,0)dx+\beta_1\int_{\Omega_2}u_{20}(x)v_2(x,0)dx+\beta_2\int_{Q_{1T}}f_1(x,t)v_1dxdt$$

$$+\beta_1\int_{Q_{2T}}f_2(x,t)v_2dxdt+\beta_2\int_0^T\gamma_1(t)v_1(b,t)dt+\beta_1\int_0^T\gamma_2(t)v_2(c,t)dt,$$

$$\forall\ v=(v_1,v_2)\in H^{1,1}\equiv L_2(0,T;H^1)\cap H^1(0,T;L),\ \ v_i(x,T)=0\ \ a.e.\ in\ \Omega_i.$$

Considering the heat conduction problem, the temperature of a body can not be negative if the temperature was nonnegative in the initial state and the boundary of the body. This property is called nonnegativity preservation (NP). In this section we analyze the NP for problem (1)-(8). For some $T>0$ let us consider the inequalities

$$\partial u_i/\partial t-L_iu_i\ge 0\quad \text{in } Q_{i_T},\quad i=1,2.,\ \text{and} \tag{8}$$

$$l_1(u_1,u_2)\ge 0,\quad l_2(u_1,u_2)\ge 0,\quad 0<t<T. \tag{9}$$

On the base of the general theory [2] we proved (NP) in [7] .

Theorem 2 *Let $u_i(x,t)$, $i=1,2$, be in Holder class and satisfy (8) and (9) weakly. If $u_i(x,0)\ge 0$ then $u_i(x,t)\ge 0$ a.e. in Q_{iT}.*

Theorem 3. *Let the assumptions (6), (7) hold and $u_{i0}\in L_2(\Omega_i)$, f_{i0}, $f_{i1}\in L_2(Q_i)$, $f_{i2}\in L_2(R_i)$, $\gamma_i\in H^{-1/4}(0,T)$, $i=1,2$. Then the IBVP (1)-(7) has a unique weak solution $u=(u_1,u_2)\in H^{1,1/2}$ and a priori estimate holds*

$$\begin{aligned}\|u\|^2_{H^{1,1/2}}\ &\le C\sum_{i=1}^2\beta_{3-i}\Big(\|u_{i0}\|^2_{L_2(\Omega_i)}+\|f_{i0}\|^2_{L_2(Q_i)}\\ &+\|f_{i1}\|^2_{L_2(Q_i)}+\|f_{i2}\|^2_{L_2(R_i)}+\|\gamma_i\|^2_{H^{-1/4}(0,T)}\Big)\end{aligned}$$

Let $\bar{\omega}_{1,h_1}$ be an uniform mesh in $\bar{\Omega}_1$ with the step-size $h_1 = (b_1 - a_1)/n_1$, $\omega_{1,h_1} = \bar{\omega}_{1,h_1} \cap \Omega_1$, $\omega^-_{1,h_1} = \omega_{1,h_1} \cup \{a_1\}$, $\omega^+_{1,h_1} = \omega_{1,h_1} \cup \{b_1\}$. Analogously we define uniform mesh $\bar{\omega}_{2,h_2}$ in $\bar{\Omega}_2$ with the step-size $h_2 = (b_2 - a_2)/n_2$ and its submeshes $\omega_{2,h_2} = \bar{\omega}_{2,h_2} \cap \Omega_2$, $\omega^-_{2,h_2} = \omega_{2,h_2} \cup \{a_2\}$, $\omega^+_{2,h_2} = \omega_{2,h_2} \cup \{b_2\}$. Finally, we introduce uniform mesh $\bar{\omega}_\tau$ in $[0,T]$ with the step-size $\tau = T/n$ and set $\omega_\tau = \bar{\omega}_\tau \cap (0,T)$, $\omega^-_\tau = \omega_\tau \cup \{0\}$, $\omega^+_\tau = \omega_\tau \cup \{T\}$. From now on, we will assume that u_i belongs to $H^{3,3/2}(Q_i)$, while $p_i \in H^2(\Omega_i)$ and $q_i \in H^1(\Omega_i)$. Consequently, $f_i \in H^{1,1/2}(Q_i)$ and may be discontinuous function. That is way we approximate IBVP (1)-(6) with the following implicit FDS with averaged input data:

$$v_{1,\bar{t}} - (\bar{p}_1 v_{1,\bar{x}})_x + \bar{q}_1 v_1 = \bar{f}_1, \qquad x \in \omega_{1,h_1}, \quad t \in \omega^+_\tau, \tag{10}$$

$$\begin{aligned} v_{1,\bar{t}}(b_1,t) + \frac{2}{h_1}\Big[\bar{p}_1(b_1) v_{1,\bar{x}}(b_1,t) + \alpha_1 v_1(b_1,t) - \beta_1 v_2(a_2,t)\Big] \\ + \bar{q}_1(b_1) v_1(b_1,t) = \bar{f}_1(b_1,t) + \frac{2}{h_1}\,\bar{\gamma}_1(t), \qquad t \in \omega^+_\tau, \end{aligned} \tag{11}$$

$$v_{2,\bar{t}} - (\bar{p}_2 v_{2,\bar{x}})_x + \bar{q}_2 v_2 = \bar{f}_2, \qquad x \in \omega_{2,h_2}, \quad t \in \omega^+_\tau, \tag{12}$$

$$\begin{aligned} v_{2,\bar{t}}(a_2,t) - \frac{2}{h_2}\Big[\bar{p}_2(a_2+h_2) v_{2,x}(a_2,t) - \alpha_2 v_2(a_2,t) + \beta_2 v_1(b_1,t)\Big] \\ + \bar{q}_2(a_2) v_2(a_2,t) = \bar{f}_2(a_2,t) - \frac{2}{h_2}\,\bar{\gamma}_2(t), \qquad t \in \omega^+_\tau, \end{aligned} \tag{13}$$

$$v_1(a_1,t) = 0, \qquad v_2(b_2,t) = 0, \qquad t \in \omega^+_\tau, \tag{14}$$

$$v_i(x,0) = u_{i0}(x), \qquad x \in \bar{\omega}_{i,h_i}, \tag{15}$$

where

$$\bar{p}_i(x) = \frac{1}{2}\left[p_i(x) + p_i(x-h_i)\right], \quad \bar{q}_i(x) = T_x^2 q_i(x), \quad x \in \omega_{i,h_i}, \quad i = 1,2,$$

$$\bar{q}_1(b_1) = T_x^{2-} q_1(b_1), \quad \bar{q}_2(a_2) = T_x^{2+} q_2(a_2), \bar{f}_i(x,t) = T_x^2 T_t^- f_i(x,t),\ t \in \omega^+_\tau,\ i = 1,2,$$
$$\bar{f}_1(b_1,t) = T_x^{2-} T_t^- f_1(b_1,t), \quad \bar{f}_2(a_2,t) = T_x^{2+} T_t^- f_2(a_2,t), \quad \bar{\gamma}_i(t) = \gamma_i(t),$$

Finally, the next theorem is the main result of [8].

Theorem 4. *Let $p_i \in H^2(\Omega_i)$, $q_i \in H^1(\Omega_i)$, $\gamma_i \in H^1(0,T)$, $i = 1,2$, and let assumptions (6) and (7) hold. Let also the solution of IBVP (1)-(7) belongs to the space $H^{3,3/2}$. Then the solution v of FDS (10)-(15) converges to the solution u of IBVP (1)-(7) in $H^{1,1/2}_{h,\tau}$ and the following convergence rate estimate holds true:*

$$\begin{aligned} \|u - v\|_{H^{1,1/2}_{h,\tau}} \le C(h^2\sqrt{\log 1/\tau} + \tau)\Big(1 + \max_i \|p_i\|_{H^2} + \max_i \|q_i\|_{H^1}\Big) \\ \times \Big(\|u\|_{H^{3,3/2}} + \|\gamma\|_{H^1(0,T)}\Big). \end{aligned}$$

Remark 1. For $u \in H^{s,s/2}$, $1.5 < s < 3$, using Bramble-Hilbert lemma and technique similar to those in [4], [6] , one can obtain convergence rate $O(h^{s-1}\sqrt{\log 1/h})$ assuming $\tau \asymp h^2$.

Linear and nonlinear elliptic problems on disjoint domains are discussed in [8], [9] .

References

[1] L. Caffarelli, *A monotonicity formula for heat functions in disjoint domains*, in: B. V. Problems for PDEs and Appls., RMA Res. Notes Appl. Math. 29, 53-60, Masson, Paris, 1993.

[2] D. Gilbarg, N. Truddinger, *Elliptic partial differential equations of second order*, 3rd edition, Springer, 2001.

[3] D. Givoli, *Finite Element Modeling of Thin Layers*, CMES 5, 6, 2004, 497-531.

[4] B. Jovanovich, L. Vulkov. On the Convergence of Finite Difference Schemes for Parabolic Problems with Concentrated Capacity. Numer. Math, 89, 2001, 715-734.

[5] B. S. Jovanovic, L. G. Vulkov, *Energy stability for a class of two-dimensional interface linear parabolic problems*, J. Math. Anal. Appl. 311 (2005), 120-138.

[6] B. S. Jovanovic, L. G. Vulkov, On the convergence of finite difference schemes for parabolic problems with concentrated data, Int. J. Numer. Anal. and Modelling, v.5, N3 (2008), 386-407

[7] B. S. Jovanovic, L. G. Vulkov, *Formulation and analysis of parabolic interface problems on disjoint intervals* (submitted).

[8] B. S. Jovanovic, L. G. Vulkov, *Numerical solution of a parabolic transsmision problem* (submitted).

[9] M. Koleva, *Finite element solutions of 1D boundary value linear and nonlinear problems with nonlocal jump conditions*, in: M. Todorov (Ed.), Amer. Inst. of Phys. Conf. Proceed. Series 964 (2007), 163-170.

[10] L. G. Vulkov, *Well posedness and a monotone iterative method for a nonlinear interface problem on disjoint intervals*, in: M. Todorov (Ed.), Amer. Inst. of Phys. Conf. Proceed. Series 964 (2007), 188-195.

Parallel PCG Algorithms for Voxel Elasticity Problems*

Svetozar Margenov, Yavor Vutov

Two parallel iterative solvers for large-scale linear systems related to μFEM simulation are presented. The problems solved represent the strongly heterogeneous structure of real bone specimens or a geocomposite material. The voxel data are obtained by a high resolution computer tomography.

We consider the weak formulation of the linear elasticity problem in the form: find $\mathbf{u} \in [H^1_E(\Omega)]^3 = \{\mathbf{v} \in [H^1(\Omega)]^3 : \mathbf{v}_{\Gamma_D} = \mathbf{u}_S\}$ such that

$$\int_\Omega [2\mu\varepsilon(\mathbf{u}) : \varepsilon(\mathbf{v}) + \lambda \operatorname{div}\mathbf{u} \operatorname{div}\mathbf{v}]d\Omega = \int_\Omega \mathbf{f}^t\mathbf{v}d\Omega + \int_{\Gamma_N} \mathbf{g}^t\mathbf{v}d\Gamma, \tag{1}$$

$\forall \mathbf{v} \in [H^1_0(\Omega)]^3 = \{\mathbf{v} = [H^1(\Omega)]^3 : \mathbf{v}_{\Gamma_D} = 0\}$, with the positive constants λ and μ of Lamé, the symmetric strains

$$\varepsilon(\mathbf{u}) := 0.5(\nabla\mathbf{u} + (\nabla\mathbf{u})^t),$$

the volume forces $\mathbf{f}$, and the boundary tractions $\mathbf{g}$, $\Gamma_N \cup \Gamma_D = \partial\Omega$, $|\Gamma_D| \neq \emptyset$. The Lamé coefficients are given by $\lambda = \dfrac{\nu E}{(1+\nu)(1-2\nu)}$, $\mu = \dfrac{E}{2(1+\nu)}$, where E stands for the modulus of elasticity, and $\nu \in (0, \frac{1}{2})$ is the Poisson ratio.

To obtain a stable saddle-point system one usually uses a mixed formulation for $\mathbf{u}$ and $\operatorname{div}\mathbf{u}$. By the choice of piece-wise constant finite elements for the dual variable, it can be eliminated at the macroelement level, and thereafter we get a symmetric positive definite FEM system in primal unknowns (displacement). This approach is known as *reduced and selective integration* (RSI) technique, see [2]. The discretization of (1) using nonconforming rotated trilinear elements of Rannacher-Turek [4] leads to the coupled system of linear equations

$$\begin{bmatrix} K_{11} & K_{12} & K_{13} \\ K_{21} & K_{22} & K_{23} \\ K_{31} & K_{32} & K_{33} \end{bmatrix} \begin{bmatrix} \mathbf{u}_h^1 \\ \mathbf{u}_h^2 \\ \mathbf{u}_h^3 \end{bmatrix} = \begin{bmatrix} \mathbf{f}_h^1 \\ \mathbf{f}_h^2 \\ \mathbf{f}_h^3 \end{bmatrix}. \tag{2}$$

Here the stiffness matrix K is written in block form corresponding to a separate displacements components ordering of the vector of nodal unknowns. Since K is sparse, symmetric and positive definite, we use the PCG algorithm to solve the system (2). Crucial for its performance is the preconditioning technique used. Here we focus on two preconditioners based on the isotropic variant of the displacement decomposition (DD)[5]. We write the DD auxiliary matrix in the form

$$C_{DD} = \begin{bmatrix} A & & \\ & A & \\ & & A \end{bmatrix} \tag{3}$$

*This work is partly supported by the Bulgarian Ministry of Science under grant VU-MI 202/2006.

where A is the stiffness matrix corresponding to the bilinear form

$$a(u^h, v^h) = \sum_{e \in \Omega^h} \int_e E \left(\sum_{i=1}^{3} \frac{\partial u^h}{\partial x_i} \frac{\partial v^h}{\partial x_i} \right) de. \tag{4}$$

Such approach is motivated by the second Korn's inequality, which holds for the RSI FEM discretization under consideration. This means that the estimate

$$\kappa(C_{DD}^{-1} K) = O((1 - 2\nu)^{-1})$$

holds uniformly with respect to the mesh size parameter in the FEM discretization. The first of the studied preconditioners is obtained by parallel MIC(0) factorization of the blocks in (3). As an alternative, inner PCG iterations with BoomerAMG preconditioner for A are used to approximate the DD block-diagonal matrix (3). BoomerAMG is a parallel algebraic multigrid implementation from the package Hypre, developed in LLNL, Livermore. For a description of the algorithms used and their settings, see [3] and the references therein.
Table 1 presents the time T in seconds, the number of iterations It (the outer ones for the AMG code), varying the preconditioners, the problem sizes and the platforms for a model problem representing vertically loaded brick. The computer platforms C1, C2 and C3 are described in [3].

Table 1: Parallel Tests I

			C1				C2				C3			
			MIC(0)		AMG		MIC(0)		AMG		MIC(0)		AMG	
n	N	p	$T[s]$	It	$T[s]$	It	$T[s]$	It	$T[s]$	It	$T[s]$	It	$T[s]$	It
64	2 396 160	1	136.6	115	150.1	9	83.7	115	84.0	9	83.9	115	115.1	9
128	19 021 824	8	202.0	163	195.6	10	172.1	163	229.8	10	127.8	163	152.6	10
256	151 584 768	64	355.6	230	261.4	10	464.1	230	430.0	10	328.2	230	307.1	10

In a good agreement with the theory, the number of iterations for MIC(0) increases as $O(\sqrt{n})$, while the AMG iterations stay about the same. For the smallest problem (N=2 396 160) MIC(0) clearly outperforms the AMG code. For the medium size (N= 19 021 824) the times are rather similar. However, for the largest problem (N=151 584 768) the advantage of AMG is well expressed.
The bone microstructure is a typical example of strongly heterogeneous media. In the presented tests, the computational domain is a composition of solid and fluid phases. The CT image is extracted from the dataset [1]. The voxel size is 37μm. Each voxel corresponds to a macroelement from the RSI FEM discretization. The bone specimen is placed between two plates (see Fig. 1). The thickness of the plates is 1 voxel. The position of the bottom plate is fixed (homogeneous Dirichlet boundary conditions), and a force of $||g|| = 1$ is uniformly distributed on the top one. This setting simulates a vertically loaded bone specimen.

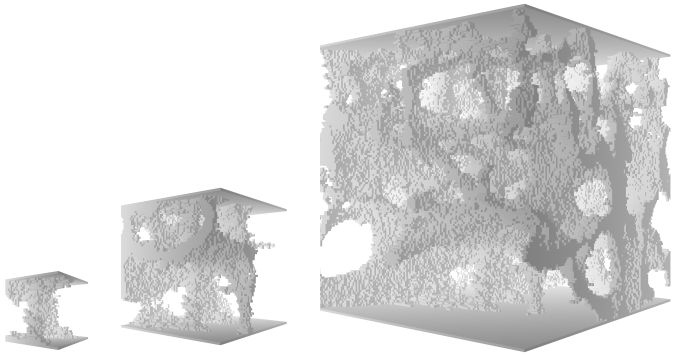

Figure 1: Structure of the solid phase: $32 \times 32 \times 32$ - left, $64 \times 64 \times 64$ - middle, and $128 \times 128 \times 128$ - right.

The considered test problems are given by the following parameters: $E_p = 10$, $E_s = 1$, $E_f = \zeta \in \{0.1, 0.01, 0.001\}$, $\nu = 0.3$. Here, E_p is the elasticity modulus of the two plates, E_s stands for a scaled elasticity modulus of the solid phase, while E_f introduces varying coefficient jumps between solid and fluid phases.
The results are presented in Table 2.

Table 2: Parallel Tests II

		$\zeta = 0.1$				$\zeta = 0.01$				$\zeta = 0.001$			
		MIC(0)		AMG		MIC(0)		AMG		MIC(0)		AMG	
n	p	$T[s]$	It	$T[s]$	It	$T[s]$	It	$T[s]$	It	$T[s]$	It	$T[s]$	It
64	1	239.3	330	374.9	27	348.3	505	757.9	57	588.6	823	1040.5	78
128	8	833.2	708	681.0	25	975.5	830	1501.3	60	2166.7	1850	2908.9	107
256	64	2393.8	1237	945.4	25	3495.7	1831	2114.4	57	6025.8	3150	5520.1	114

The considered algorithms were successfully applied to another test problem. The voxel data represents a coal-polyurethane geocomposite (see Fig. 2 left). The domain is cubic – 75x75x75mm, but the scan is non-uniform in all directions – 35x110x110 voxels. The mechanical properties used were: Coal – $\nu = 0.25$, $E = 4000$MPa; Polyurethane – $\nu \in [0.1, 0.25]$, $E \in [200, 2100]$MPa. The setting used was the same – vertically loaded specimen. On the right on Fig. 2 are shown vertical displacements.

The general conclusion is that the studied codes provide a stable toolkit for computer simulation of the bone microstructure. Both approaches have their advantages depending on the size of the FEM systems and the level of heterogeneity of the bone specimens. The achieved parallel scalability well corresponds to the connectivity of the considered problems.

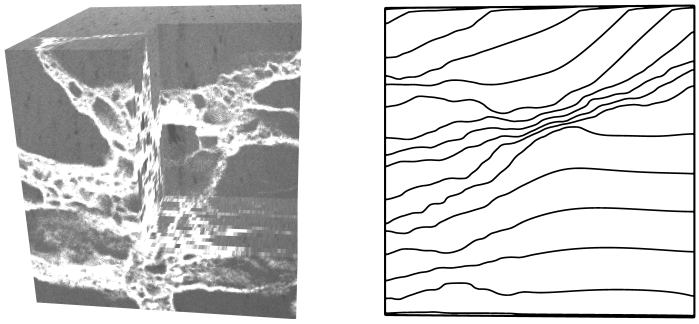

Figure 2: Left: coal-polyurethane geocomposite brick; right: vertical displacements.

References

[1] Gisela Beller, Markus Burkhart, Dieter Felsenberg, Wolfgang Gowin, Hans-Christian Hege, Bruno Koller, Steffen Prohaska, Peter I. Saparin and Jesper S. Thomsen: Vertebral Body Data Set ESA29-99-L3, http://bone3d.zib.de/data/2005/ESA29-99-L3/

[2] D. Malkus, T. Hughes. Mixed finite element methods. Reduced and selective integration techniques: an uniform concepts. *Comp. Meth. Appl. Mech. Eng.,*15: 63-81, 1978.

[3] Svetozar Margenov, Yavor Vutov, Parallel PCG Algorithms for Voxel FEM Elasticity Systems, Proceedings of the International Multiconference on Computer Science and Information Technology, 2007, pp. 517-526

[4] R. Rannacher, S. Turek: *Simple nonconforming quadrilateral Stokes Element*, Numer. Methods Partial Differential Equations 8(2), 1992, 97-112.

[5] R. Blaheta: *Displacement Decomposition - incomplete factorization preconditioning techniques for linear elasticity problems*, Numer. Lin. Alg. Appl., **1** (1994), 107–126

Part D

List of Participants